ANTIOXIDATIVE FUNCTION OF LIVER FATTY ACID BINDING PROTEIN

Jing Yan

A Thesis Submitted to the Faculty of Graduated Studies

In Partial Fulfillment of the Requirements for the

Degree of Doctor of Philosophy

Faculty of Pharmacy

University of Manitoba

Winnipeg, Manitoba

ABSTRACT

Liver fatty acid binding protein (L-FABP) binds and translocates many lipophilic substrates within the cytoplasm including long chain fatty acids. Moreover it was reported that L-FABP possesses antioxidative properties within hepatocytes. However, the mechanism of L-FABP's antioxidative activity remains to be determined.

Peroxisome proliferator activated receptor (PPAR) agonists and antagonists can regulate L-FABP levels. However, it needs to be investigated how PPAR agonists and antagonists regulate L-FABP expression. And whether the altered expression of L-FABP by these agents will affect its antioxidative properties within hepatocytes remains unclear. In this thesis we employed clofibrate (PPARα agonist), MK886 (PPARα antagonist), and GW9662 (PPARγ antagonist) to elucidate the mechanism whereby PPAR regulate L-FABP expression and what effect such expression has on the antioxidant activity of L-FABP in CRL-1548 hepatoma cells. Clofibrate served to upregulate L-FABP expression while MK886 and GW9662 were employed to inhibit L-FABP expression. The principal findings revealed that clofibrate treatment enhanced L-FABP mRNA stability and transcription, which resulted in increased L-FABP levels, while MK866 and GW9662 reduced these levels. We also demonstrated that increases in L-FABP levels were associated with reduced cytosolic reactive oxygen species (ROS), while L-FABP siRNA knockdown resulted in a decrease in L-FABP expression and an associated increase in ROS levels.

Abstract

The antioxidant mechanism of recombinant rat L-FABP in the presence of a hydrophilic (AAPH) and lipophilic (AMVN) free radical generators was also evaluated. Recombinant rat L-FABP was produced in *E. coli* and its amino acid sequence was confirmed by MALDI QqTOF MS. Antioxidant activity was assayed using the thiobarbituric acid method. Ascorbic acid served as a positive control for the AAPH reaction while α-tocopherol was used as a positive control for the AMVN reaction. The antioxidant activity of recombinant L-FABP was greater when free radicals were generated with AAPH than AMVN. Oxidative modification of L-FABP included up to five methionine oxidative peptides with a total of 80 Da mass shift compared to native L-FABP. These findings suggest that the mechanism of L-FABP's antioxidant activity involved the reaction of methionine with free radicals.

In conclusion, L-FABP expression is regulated by PPAR agonists and antagonists through transcription and mRNA stability. Moreover, methionine residues appear to play an important role in the antioxidative activity of L-FABP.

ACKNOWLEDGEMENTS

I would like to express my deepest gratitude and appreciation to my esteemed supervisors, Dr Frank J Burczynski and Dr. Yuewen Gong for their valuable suggestions and enthusiastic guidance. They gave me great support and constant encouragement in both my academic work and life in general. I will never forget the patience they gave me throughout my work. I consider myself fortunate to have had the chance to learn from such excellent mentors.

I would like to thank Dr Chris Siow for serving as my committee member and providing me with valuable constructive comments during my program. I would like to extend my thanks to the members of Dr.Gong's lab for their various technical supports throughout the duration of my research. I have benefited a lot from their rich experience and knowledge. My appreciation goes to Dr Yiming She, University of Queens, for his valuable contribution to the MALDI-TOF MS studies. My sincere thanks go to all of my friends for their support and friendship.

My special thanks and deepest love go to my parents and my brother for their love and constant encouragement throughout my life. I am extremely grateful for the support of my husband, Jian Wang for his love and patience and my mother-in law and father-in law for their love and great support.

I am grateful to the University of Manitoba for an International Graduate Student Fellowship (UMISGF) and University of Manitoba Graduate Travel Award during my studies.

TABLE OF CONTENTS

ABSTRACT i

ACKNOWLEDGEMENTS iii

TABLE OF CONTENTS iv

LIST OF TABLES x

LIST OF FIGURES xii

ABBREVIATIONS xvi

I. INTRODUCTION

A. Liver Fatty Acid Binding Protein

1. General introduction of fatty acid binding proteins 1

1.1 Evolution and classification of fatty acid binding proteins 1

1.2 Physiological functions of fatty acid binding proteins 4

2. Liver fatty acid binding protein 7

2.1 Gene organization of L-FABP 7

2.2 Conformational structure of L-FABP 10

B. Oxidative Stress

1. Production of Oxidative stress 15

1.1 Reactive oxygen species or reactive nitrogen species 15

1.2 Lipid Peroxidaion 16

1.2.1 Oxidative modification of lipid 16

1.2.2 Consequences of lipid peroxidation 18

1.3 Oxidation of DNA 19

1.3.1 Oxidative modification of DNA 19

1.3.2 Consequences of DNA oxidation 20

1.4 Oxidation of protein 21

1.4.1 Oxidative modification of protein 21

1.4.2 Consequences of protein oxidation 23

C. Hepatocellular Oxidative Status

1. General aspects 23
2. Pathogenesis 24
3. The signalling pathway that involved in ROS induced liver diseases 27

D. Antioxidants

1. Antioxidant system 29
2. Hydrophilic antioxidants 31
3. Lipophilic antioxidants 34
4. Interaction of hydrophilic and lipophilic antioxidants 35
5 Antioxidant function of L-FABP 38

II. HYPOTHESIS AND OBJECTIVES 41

III. METERIALS AND METHODS 42

A. Materials 42

B. Methods 43

1. Cell line and culture condition 44
2. RNA isolation 44
3. Reverse transcription polymerase chain reaction (RT-PCR) 45

4. Protein sample preparation from cell culture 48

5. Western blot analysis 48

6. Northern blot analysis 49

6.1 RNA sample preparation 49

6.2 Random primer DNA labelling 50

6.3 Northern blot 51

7. Nuclear run-off assay 52

7.1 Nuclear isolation 52

7.2 Preparation of ^{32}P-labeled nascent nuclear RNA 52

7.3 Immobilization of cDNA on nitrocellulose membranes 53

7.4 Hybridization of labelled transcript with cDNA 53

8. siRNA transfection 54

9. Measurement of antioxidant activity in vivo 55

10. Measurement of antioxidant enzyme 56

10.1 Superoxide dismutase (SOD) 56

10.2 Glutathione peroxidise (GPx) 58

10.3 Catalase 60

11. Recombinant L-FABP protein construction

11.1 Rat L-FABP cloning 62

11.2 Transformation of expression plasmid pGEX-6p-2 with competent *E.coli* 63

11.3 Plasmid DNA isolation 66

11.4 Restriction enzyme digestion 67

11.5 Agrose gel electrophoresis 68

11.6 DNA extraction from agrose gel 69

11.7 Construction of recombinant plasmid L-FABP/ pGEX-6p-2 70

11.8 Recombinant L-FABP protein expression 72

11.9 Recombinant L-FABP protein purification 73

12. Measurement of antioxidant activity in vitro 74

13. Isolation of lipoprotein 74

14. Lipid peroxidation induction 75

15. Thiobarbituric acid reactive substances (TBARS) assay 75

16. MALDI-QgTOF mass spectrometry 77

17. Purification of [^{3}H]-palmitate 78

18. Determination of L-FABP binding affinity 79

19. Statistical Analyses 80

IV. RESULTS AND DISCUSSION

1. Regulation of L-FABP gene expression by PPAR 82

1.1 Introduction 82

1.2 Results 83

1.2.1 Regulation of L-FABP expression 83

1.2.2 L-FABP mRNA stability 89

1.2.3 L-FABP mRNA transcription 91

1.2.4 L-FABP antioxidant activity 93

1.3 Discussion 100

2. Recombinant Rat L-FABP protein construction using

Glutathione-S-transferase (GST) fusion system 104

2.1 Introduction 104

2.2 Results 105

2.2.1 Expression of recombinant GST/L-FABP from E. coli 105

2.2.2 Rapid Purification of recombinant GST/L-FABP from E. coli 108

2.2.3 Expression of the recombinant L-FABP 108

2.2.4 MALDI QqTOF mass spectrometry of recombinant L-FABP 111

2.2.5 Antioxidant activity of recombinant L-FABP 118

2.3 Discussion 120

3. L-FABP antioxidant defence mechanism 126

3.1 Introduction 126

3.2 Results 127

3.2.1 Lipid peroxidation in the presence of AAPH and AMVN in vitro 127

3.2.2 Protection of ascorbic acid and α-tocopherol against lipid peroxidation induced by AAPH and AMVN 129

3.2.3 Protection against lipid peroxidation of L-FABP in AAPH and AMVN 131

3.2.4 Antioxidant effect of L-FABP upon binding of palmitate or α-bromo-palmitate 133

3.2.5 The binding affinity of L-FABP with palmitate upon oxidization by H_2O_2 135

3.2.6 MALDI QqTOF mass to identify the modified recombinant L-FABP by AAPH or AMPH 137

3.2.7 MALDI QqTOF mass to identify the oxidized methionine residues oxidized by AAPH or AMVN 139

3.2.8 MALDI QqTOF mass to identify the oxidized methionine residues oxidized by H_2O_2 142

3.3 Discussion 144

V CONCLUSION 150

VI REFERENCES 153

LIST OF TABLES

Table 1 Characteristics of the mammalian intracellular lipid-binding proteins 3

Table 2 Putative L-FABP isoforms 14

Table 3 Amino acids most susceptible to oxidation 22

Table 4 List of hydrophilic antioxidants and lipophilic antioxidants 30

Table 5 Materials used in experiments 42

Table 6 PCR reaction components 47

Table 7 Volume of each solution for sample, blank 1, 2 and 3 57

Table 8 Volume of glutathione peroxidase reaction scheme 59

Table 9 Dilitions for Preparation of the Hydrogen Peroxide Standard Curve 61

Table 10 Catalase Colorimetric Enzymatic Reaction Scheme 61

Table 11 Restriction enzyme digestion reaction 67

Table 12 Components for L-FABP DNA ligation reaction 71

Table 13 Clofibrate did not alter SOD, GPx and catalase activities in CRL-1548 hepatoma cells 99

Table 14 L-FABP protein sequence identification by MALDI QqTOF mass spectrometry 112

Table 15 [^{3}H]-palmitate heptane-to-buffer partition ratio and calculated the unbound [^{3}H]-palmitate fraction (α) 136

Table 16 MALDI MS analyses of the methionine-containing peptides in the Glu-C digests of FABPs 141

LIST OF FIGURES

Figure 1 The transduction pathway of ligands to the nucleus regulated by FABP 5

Figure 2 L-FABP gene in human, mouse and rat 8

Figure 3 Rat L-FABP transcript structure from Ensembl website 8

Figure 4 5'-flanking region of rat L-FABP 10

Figure 5 Amino acid sequence of rat L-FABP 11

Figure 6 Crystal structure of L-FABP 13

Figure 7 Schematic diagram of lipid peroxidation chain reactions 17

Figure 8 Effect of oxidative stress on liver injury 26

Figure 9 Factors involved in ROS induced liver diseases 28

Figure 10 ROS and hydrophilic antioxidants defence systems 32

Figure 11 A scheme of the plasma membrane redox system 37

Figure 12 The oxidation and reduction of catalytic reaction for methionine residues 39

Figure 13 Cysteine residues of protein participate as S-thiolation/dethiolation reduction cycle 40

Figure 14 Map of expression vector pGEX-6P-2 65

Figure 15 Thiobarbituric acid reaction 76

Figure 16 Western blot analyses of L-FABP levels from control and clofibrate (500μM) treated CRL-1548 hepatoma cells 85

Figure 17 Western blot of L-FABP levels from control, clofibrate (500 μM) and PPARα antagonist MK-886 (1, 10, 20 μM), or clofibrate (500 μM) and PPARγ antagonist GW-9662 (1, 10, 20 μM) treated cells 86

Figure 18 Western blot analyses of L-FABP levels from control (no drug treatment), clofibrate (500 μM), and PPARα antagonist MK-886 (20 μM), PPARγ antagonist GW-9662 (20 μM), co-treated with clofibrate (500 μM) and MK-886 (20 μM, CLO+MK), clofibrate (500 μM) and GW-9662 (20 μM, CLO+GW) treated cells 87

Figure 19 RT-PCR analysis of L-FABP mRNA expression in control (no drug treatment), clofibrate (500 μM), and cells co-treated with the PPARα antagonist MK-886 (20 μM) and clofibrate (500 μM) (CLO+MK) and PPARγ antagonist GW-9662 (20 μM) and clofibrate (500 μM) (CLO+GW) on day 4 88

Figure 20 Northern Blot analysis of L-FABP mRNA stability in 1548 cells 90

Figure 21 Nuclear run-off analysis of nascent L-FABP RNA transcription rate in control and treated CRL-1548 cells 92

Figure 22 Intracellular ROS levels induced by H_2O_2 treatment in CRL-1548 hepatoma cells 94

Figure 23 Western blot analysis of L-FABP levels from control (no drug treatment); clofibrate (500 μM) treated cells with/without negative siRNA or L-FABP siRNA transfection 97

Figure 24 Intracellular ROS levels induced by H_2O_2 treatment in CRL-1548 hepatoma cells after using RNA interference (siRNA) to silence the expression of L-FABP 98

Figure 25 Analysis of recombinant pGEX-6P-2/L-FABP by restriction enzyme digestion 106

Figure 26 Schematic representation of the pGEX-6p-2-L-FABP expression vector employed for biosynthesis of rat L-FABP in *E. coli* 107

Figure 27A Expression and purification of GST/L-FABP fusion protein and L-FABP using *E. coli* DH5α cells and the GST fusion system 109

Figure 27B Identification of recombinant L-FABP and L-FABP purified from rat 1548 hepatoma cytosol by SDS-PAGE 109

Figure 27C Identification purified rat L-FABP and cytosolic proteins from rat 1548 hepatoma cells by Western blot with antibody raised against rat L-FABP 109

Figure 28 MALDI-TOF MS spectrum of recombinant L-FABP 113

Figure 29 MALDI-TOF MS spectrum of the endoproteinase Glu-C digests of recombinant L-FABP 114

Figure 30 MS/MS spectrum of a Glu-C digested peptide at m/z 1526.70 115

Figure 31 MS/MS spectrum of a trypsin digested peptide at m/z 1379.71 116

Figure 32 MS/MS spectrum of a trypsin digested peptide at m/z 2941.31 117

Figure 33 Reactive oxygen species (ROS) levels versus recombinant L-FABP concentration 119

Figure 34 MDA formation as a function of incubation of LDL with varying concentrations of two different azo-compounds 128

Figure 35 A comparison of the effect of ascorbic acid, α-tocopherol and L-FABP on AAPH and AMVN induced MDA production in LDL 130

Figure 36 The effect of L-FABP on AAPH and AMVN induced MDA production in LDL 132

Figure 37 A comparison of the effect of recombinant L-FABP after binding with palmitate or α-bromo-palmitate on AAPH or AMVN induced MDA production in LDL 134

Figure 38 MALDI-TOF MS spectrum of recombinant L-FABP (A), L-FABP incubated with 40mM AAPH (B) or 10mM AMVN (C) 138

Figure 39 MALDI-TOF MS spectrum of the Glu-C digest of recombinant L-FABP containing peptide 140

Figure 40 MALDI-TOF MS spectrum of the Glu-C digests of recombinant L-FABP incubated with H_2O_2 containing peptide 143

ABBREVIATIONS

°C	degree Celsius
%	percent
µCi	microcurie
µl	microliter
µg	microgram
aa	amino acid
AP-1	activator protein-1
bp	basepair(s)
BSA	Bovine Serum Albumin
cDNA	complementary DNA
CLO	clofibrate
CO_2	carbon dioxide
CoQ	coenzyme Q
DCF	dichlorofluorescein
DCFH	dichlorofluorescien
DMEM	dulbecco's modified eagle's medium
DNA	deoxyribonuclieic acid
DNase	deoxyribonuclease
dNTP	deoxyribonucleotide triphosphate
EB	ethidium bromide
ECM	extracellular matrix

E.coli	*Escherichia coli*
EDTA	ethylene diaminetetracetic acid
EGFR	epidermal growth factor receptor
ERK	extracellular signal-regulated kinases
FABP	fatty acid binding protein
FBS	fetal bovine serum
HNE	4-hydroxy-2-nonenal
HSC	hepatic stellate cells
IL-6	interleukin 6
g	gram
GAPDH	glyceraldehydes 3-phosphate dehydrogenase
GPx	glutathione peroxidise
GSH	glutathione
GSHR	glutathione reductase
GSSG	glutathione disulfide
HCl	hydrochloric acid
H_2O	water
H_2O_2	hydrogen peroxide
KCl	potasium chloride
JNK	c-Jun N-terminal kinases
kDa	kilo Daltons
LB	luria-betani
LCFA	long chain fatty acids

L-FABP	liver fatty acid binding protein
LOOH	lipid hydroperoxide
M	molar
MAPKs	mitogen-activated protein kinases
MDA	malondialdehyde
Met	methionine
MetSO	methionine sulfoxide
$MgCl_2$	magnesium chloride
mM	millimolar
min	minute(s)
ml	millilitre
mRNA	messenger RNA
MSR	methionine sulfoxide reductase
NaCl	sodium chloride
NADPH	nicotinamide adenine dinucleotide phosphate
NaOH	sodium acetate
NF-κb	nuclear factor kappa B
NQO1	NAD(P)H quinone oxidoreductase 1
OD	optical density
ONE	4-oxo-2-nonenal
PA	palmitate
PAGE	polyacrylamide gel electrophoresis
PBS	phosphate buffered saline

PCR	polymerase chain reaction
PDGFR	platelet-derived growth factor
Rpm	rotations per minute
RNA	ribonucleic acid
RNase	ribonuclease
ROS	reactive oxygen species
RT-PCR	reverse transcriptase PCR
SDS	sodium dodecyl sulfate
SOD	superoxide dismutase
TBS	Tris buffered saline
TBS-T	Tris buffered saline with 0.1% Tween 20
TE	Tris-EDTA
TEMED	N,N,N',N-tetramethylethylenediamine
TGF-β	transforming growth factor
ThR	thioredoxin reductase
TNF- α	tumor necrosis factor-α
Tris	tris (hydroxymethyl) amino methane
Tween-20	polyxyethylene-sorbitan monolaurate
UV	ultraviolet
v	voltage
VEGFR	vascular endothelial growth factor receptor

I. INTRODUCTION

A. Liver fatty acid binding protein (L-FABP)

1. General introduction of fatty acids binding proteins

1.1 Evolution and classification of fatty acids binding proteins

In 1969, a low-molecular-weight binding protein fraction from rat liver was identified (Levi, Gatmaitan et al. 1969) and designated as Z protein. Ockner (Ockner, Manning et al. 1972) discovered the presence of a similar protein in both the small intestine and liver which bound bromosulphophthalein and long-chain fatty acids. Because this protein was found to bind fatty acids, it was named "fatty acid binding protein" (FABP). Subsequently, FABPs have been identified in various tissues of many organisms. Their main function was thought to be intracellular transportation of long-chain fatty acids and other lipophilic ligands.

FABPs are present in both vertebrates and invertebrates. It is believed that individual genes of this ubiquitous gene family arose from an ancestral FABPs gene through gene duplication and diversification. A common ancestral FABP gene likely evolved from fungi and plants. Duplication of the first gene occurred approximately 900 million years ago with current intracellular FABPs being widely distributed throughout the animal kingdom. Major gene duplications gave rise to four major subfamilies of mammalian proteins (Table 1). These families have been categorized based on sequence homology and ligand binding characteristics (Hanhoff, Lucke et al. 2002).

Vertebrate FABP subfamily I can be subdivided into the cellular retinoic acid binding protein (CRABP-I and II) and the cellular retinol-binding protein (CRBP-I, II, III, and IV). Subfamily II contains intestinal bile acid-binding protein (I-BABP) and the liver fatty acid binding protein (L-FABP). I-BABP and L-FABP are closely related based on sequence homology and characteristics with their binding site that allows for the binding of larger ligands such as bile acids and eicosanoids. L-FABP is found in the liver of birds, fish, reptiles, and amphibians. I-FABP (intestinal) is the only member of subfamily III while the remaining proteins H (heart), A (adipocyte), E (epidermal), M (yelin), T (testis), and B (brain) FABP belong to subfamily IV. Most FABPs are not confined to a single tissue and some tissues express more than one type as seen in Table 1. For example, L-FABP is found in abundance in hepatocytes, accounting for approximately 3-5% of the total cellular protein content but is also found in intestine, kidney, lung, and pancreas.

Table 1: Characteristics of the mammalian intracellular lipid-binding proteins

FABPs type	Expression	Ligands	Human gene	Mouse gene	Chromosome region in rat	Chromosome region in human	Protein length
Subfamily I							
CRBP I	Ovary	Retinol	RBP1	Rbp1		3q23	134
CRBP II	Intestine	Retinol	RBP2	Rbp2		3q23	133
CRBP III	Kidney	Retinol				12p–p13.31	134
CRBP IV	Heart	Retinol	RBP7	Rbp7			133
CRABP I	Testis	Retinoic acid	RBP5	Rbp5		15q24	136
CRABP II	Skin	Retinoic acid	RBP6	Rbp6		1q21.3	137
Subfamily II							
L-FABP	Liver, intestine, kidney, lung, pancreas	LCFA, cholesterol, heme, acyl-CoAs, bile acids	FABP1	Fabpl	4q33	2p11	127
I-BABP	Ileal enterocytes	Bile acids	FABP6	Ilbp		5q23–q35	127
Lb-FABP	Fish and bird liver	LCFA					
Subfamily III							
I-FABP	Intestine, liver	LCFA	FABP2	Fabpi	2q42	4q28–q31	131
Subfamily IV							
H-FABP	Heart, skeletal muscle, brain, kidney, lung, mammary, placenta	LCFA	FABP3	Fabph	5q36	1p32–p33	132
B-FABP	Brain, glia cells, retina	LCFA,	FABP7	Fabpb	20q11	6q22–q23	131
A-FABP	adipose tissue, macrophages liver	LCFA, retinoic acid	FABP4	Fabpa/Ap2/Albp	2q23	8q21	131
M-FABP	Schwann cells, brain	LCFA, retinoids	FABP8	Fabpm	-	8q21–q22	131
T-FABP	Testis	LCFA	FABP9		2q23	-	131
E-FABP	Skin, adipose tissue, lung, brain, heart, skeletal muscle, testis, retina	LCFA, eicosanoids	FABP5	Fabpe	-	8q21.13	134

All human, mouse and rat gene locations have been retrieves from the human genome database (GDB), mouse & rat genome database.

1.2 Physiological functions of fatty acid binding proteins

FABPs are involved in a variety of biological activities. They have been implicated in the uptake and intracellular transport of long-chain fatty acids as well as other lipophilic ligands; the maintenance of cellular long-chain fatty acid levels; regulation of long-chain fatty acids metabolic activity; and the modulation of cell growth and differentiation.

FABPs modulate metabolic reactions by transporting lipophilic ligands through the cytosol (Hsu and Storch 1996; Storch and Thumser 2000). Cellular uptake of ligands such as long-chain fatty acids can be divided into several steps (Figure 1): (1) adsorption – binding of the ligand to the outer leaflet of the plasma membrane; (2) crossing the membrane – hydrophobic ligands can be transported through the membrane by membrane transport proteins, such as $FABP_{pm}$, FATP and FAT/CD36; and (3) desorption – leaving the cytosolic leaflet of the plasma membrane. Transfer of these ligands from membranes to L-FABP is thought to occur by a diffusive process; i.e., the ligand first dissociates and diffuses from the membrane site to L-FABP. While transfer of these ligands from membranes to I-FABP is thought to occur by a direct collision interaction (Thumser and Storch 2000).

FABPs transport long chain fatty acids and other lipophilic ligands to various intracellular organelles including the nucleus, where they are transferred to their respective nuclear receptor. These nuclear receptors could be specific subtypes of peroxisome proliferator-activated receptors (PPAR) and/or retinoid X receptor (RXR) (Hsu and Storch 1996). Once the nuclear receptors bind the delivered ligands they will then interact with the corresponding responsive elements to activate gene transcription.

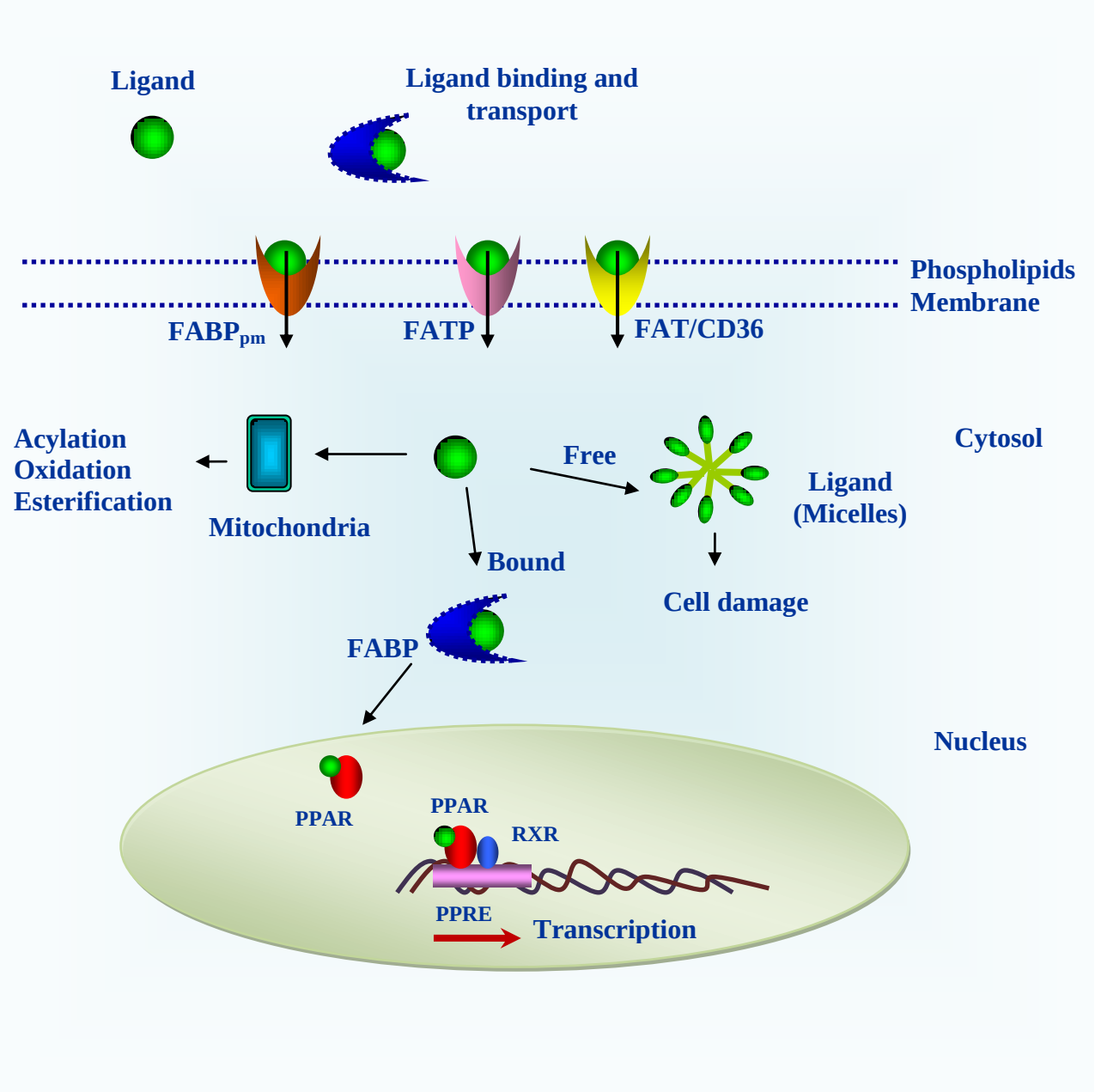

Figure 1: The transduction pathway of ligands to the nucleus regulated by FABP.

There are multiple isoforms of PPAR in mice (α, γ, and δ) (Kliewer, Forman et al. 1994), *Xenopus laevis* (α, β, and γ) (Dreyer, Krey et al. 1992), and humans (α, γ, and δ) (Semple, Chatterjee et al. 2006). The different PPARs bind cooperatively to peroxisome-proliferator response elements (PPREs) of the DR-1 class (TGA/TCCT) as a heterodimer with the RXRα. A-FABP and E-FABP selectively interact with PPARβ and PPARγ, respectively (Tan, Shaw et al. 2002) while L-FABP interacts with both PPARα and PPARγ (Wolfrum, Borrmann et al. 2001). L-FABP may readily pass through nuclear pores or enter the nuclei by a specific recognized signal of nuclear compartment (Lawrence, Kroll et al. 2000). L-FABP is present in nuclei at concentrations similar to those in the cytoplasm (Huang, Starodub et al. 2004). Immunolabelling techniques allow the detection and localization of L-FABP in hepatocytes (Bordewick, Heese et al. 1989). It appears that translocation of L-FABP into the nucleus is a regulative process in response to ligand binding and gene regulation (Huang, Starodub et al. 2002).

Expression of FABPs such as those in hepatocytes, adipocytes, and cardiac myocytes is taken as a reflection of the lipid-metabolizing capacity of those tissues, particularly where fatty acids are the prominent substrates for lipid biosynthesis, storage, or breakdown. Certain FABPs also seem to be involved in modulation of cell growth and proliferation either through their binding of mitogens or carcinogens (Sorof 1994; Lawrie, Dundas et al. 2004), or through direct interactions with other cellular components (Spitsberg, Matitashvili et al. 1995). L-FABP promotes mitogenesis of hepatocytes (Khan and Sorof 1994), while H-FABP stimulates cardiomyocyte growth and differentiation (Tang, Kindler et al. 2004).

2. Liver Fatty Acid Binding Protein (L-FABP)

2.1 Gene organization of L-FABP

Restriction fragment length polymorphism has been used to determine the chromosome locations of the L-FABP gene in different species. Human L-FABP gene resides in the p12 region and is 5.07kb on human chromosome 2 (Chen, Van Tuinen et al. 1986). Rat L-FABP gene is located in the q33 region and spans 3.78kb on chromosome 4, while mouse L-FABP gene is 5.14kb in length on mouse chromosome 6 (Sweetser, Birkenmeier et al. 1987). The L-FABP gene contains four exons interrupted by three introns in human, rat and mouse species (Figure 2). The first exon includes a short 5'-UTR (untranslated region) and coding exons. The last exon includes a short 3'-UTR (Figure 2). The coding region contains exons and the entire open reading frame.

Human, mouse, and rat L-FABP cDNA sequences were found in Genbank database as the sequence of 497 bp (Genbank accession no BC032801), 492 bp (Genbank accession no BC086947), and 518 bp (Genbank accession no BC086947), respectively. Computational analyses and sequence comparisons reveal human and mouse L-FABP are both highly homologous to rat L-FABP. The transcription unit of rat L-FABP spans 3780 nucleotides (Figure 3) and contains four exons (115, 173, 93, and 121 base pairs) interrupted by three introns (1454, 1224, and 610 base pairs). There are no other abundant mRNAs that appear to be transcribed from sequences located within 4 kilobases (5') of this gene. After transcription, the sequence contains the entire open reading frame coding for a protein of 127 amino acids. This part of the review will focus on the rat L-FABP gene expression and regulation.

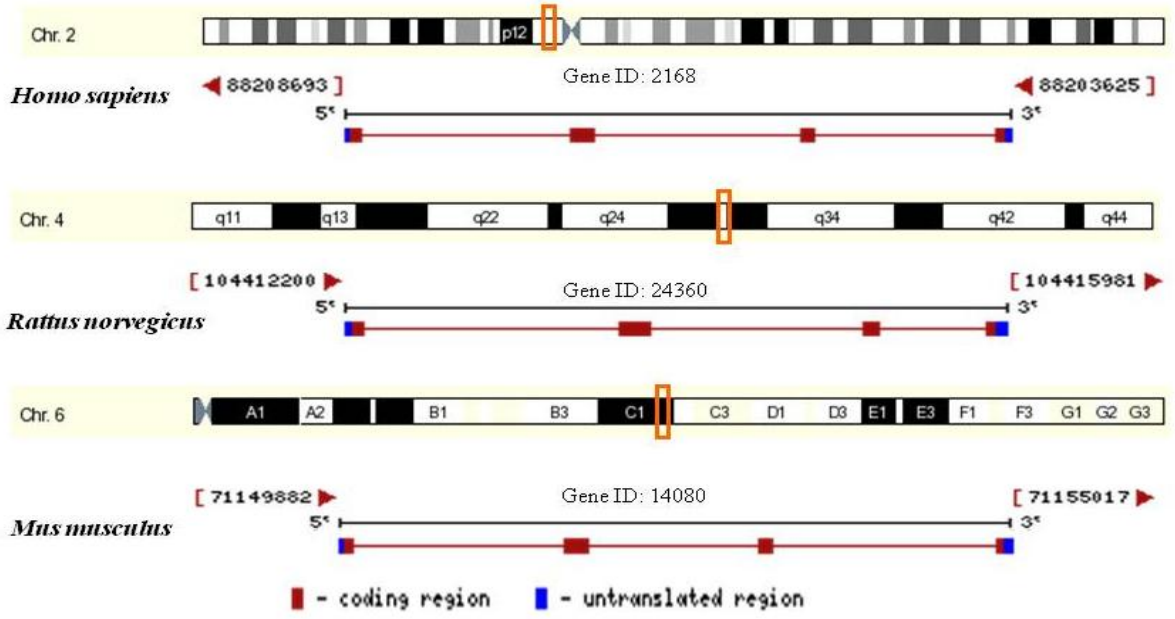

Figure 2: L-FABP gene in human, rat, and mouse. L-FABP gene, located on chromosome 2 (human), 4 (rat), and 6 (mouse), contains 4 exons interrupted by 3 introns. http://www.ncbi.nlm.nih.gov/sites/entrez?db=gene&cmd=search&term=L-FABP.

Transcript structure

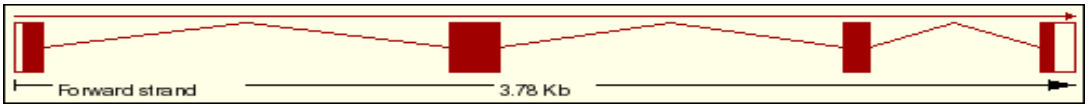

Figure 3: Rat L-FABP transcript structure from Ensembl website.

Red box: Untranslated regions of the transcript; Cream colour box: Translated regions of the transcript.

Four kilobases of the 5'-flanking region of the rat L-FABP gene (Figure 4) are sufficient to correctly direct expression of a reporter gene in hepatocytes. The rat L-FABP gene contains the canonical TATA box, 5'-TATAAAA-3', which is located approximately 23–30 nucleotides upstream of the position corresponding to the 5' end of the mRNA and is believed to be the transcription start site. Another sequence, CGACAATCA, which is located at position 77, has homology to the so-called "CCAAT". L-FABP contains three upstream regulatory elements CCAAT/enhancer binding protein alpha (C/EBPα) binding sites located at −402 to −385, −356 to −345, and −306 to −275 bp. The C/EBPα binding sites are able to protect nucleotides from DNase I digestion (Bernlohr, Simpson et al. 1997; Tang, Jiang et al. 1999). The L-FABP potential functional domains include two hepatic nuclear factor 1α (HNF1α) binding sites between nucleotides -343 and -328, and between nucleotides -115 and -102 relative to the transcriptional start site (Sweetser, Lowe et al. 1986). A putative "GATA" binding site is present at nucleotides -245 to -240 of rat L-FABP and lies adjacent to the HNF-1α site. GATA factors interact with hepatic nuclear factor (HNF)-1α to activate the L-FABP gene (Divine, Staloch et al. 2004). Transcription of the L-FABP gene is also regulated through a 22bp peroxisome proliferate response element (PPRE) present at L-FABP promoter which is located at −75 to −66 bp (5"TGACCTATGGCCT-3') (Simon, Roth et al. 1993). PPRE is bound by the peroxisome proliferator activated receptor (PPAR) allowing responsiveness to peroxisome proliferators through PPAR (Issemann, Prince et al. 1992; Simon, Roth et al. 1993).

5'-flanking region of rat L-FABP

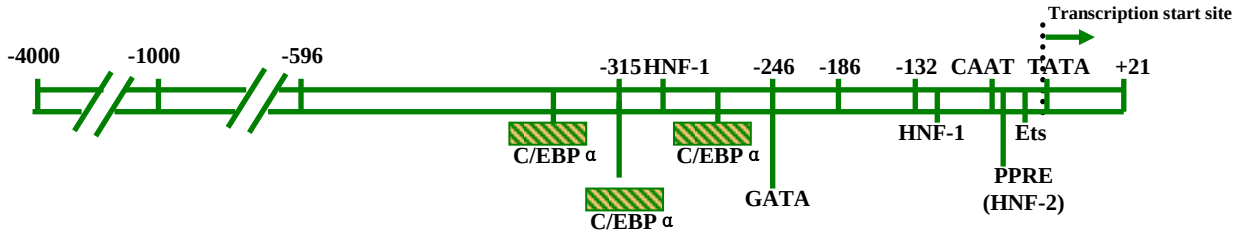

Figure 4: 5'-Flanking region of rat L-FABP. Upstream regulatory elements are relative to the start of transcription of rat L-FABP. Arrows indicate transcription initiation position.

2.2 Conformational structure of L-FABP

L-FABP belongs to a family of low molecular weight (14-15 kDa) proteins with 127 amino acids (Chan, Wei et al. 1985) (Figure 5). Successful expression of L-FABP in *E. coli* resulted in substantial quantities of recombinant protein being available for structural biologists to gain deeper insights into its structure and binding properties. L-FABP shares a similar tertiary structure with other member of FABPs as revealed by crystallography (Sacchettini, Gordon et al. 1989; Xu, Bernlohr et al. 1992; Zanotti, Scapin et al. 1992; Cowan, Newcomer et al. 1993; Thompson, Winter et al. 1997; Hohoff, Borchers et al. 1999; Balendiran, Schnutgen et al. 2000) and nuclear magnetic resonance (NMR) (Lassen, Lucke et al. 1995; Hodsdon, Ponder et al. 1996; Lucke, Zhang et al. 1996; Lucke, Zhang et al. 2000; Lucke, Rademacher et al. 2001). The tertiary structure of L-FABP is comprised of ten antiparallel β strands (βA-βJ), consisting of two orthogonal antiparallel 5-stranded sheets that form the "clam"-shaped binding cavity (Banaszak, Winter et al. 1994). Figure 6 demonstrates the typical "β-clam" structure of L-FABP.

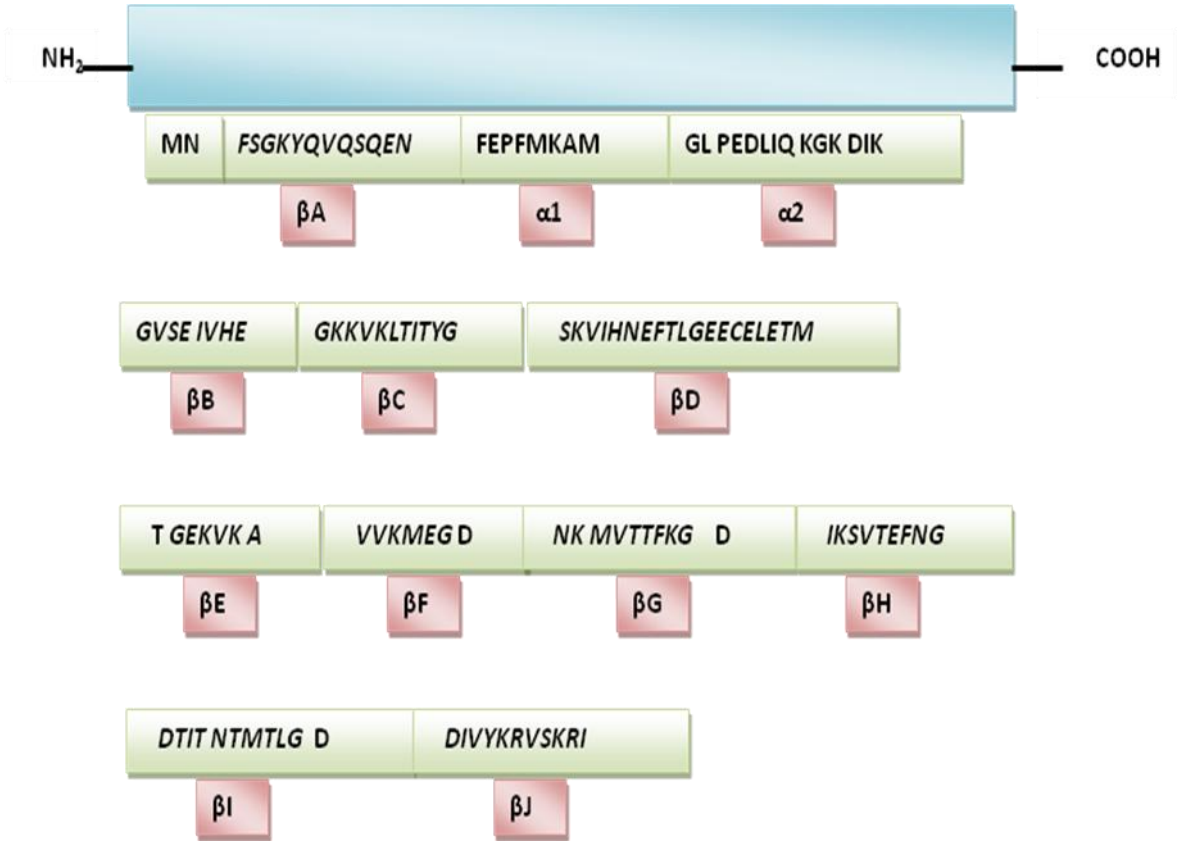

Figure 5: Amino acid sequence of rat L-FABP. One cysteine residue is located at position 69. Seven methionine residues located at positions 1, 19, 22, 74, 85, 91 and 113.

L-FABP exhibits high binding affinity for endogenous and exogenous lipophilic ligands. Computer aided predictions revealed the presence of a relatively high content of both α-helical and β-stranded structures forming an alternating pattern of hydrophobic and hydrophilic domains (Takahashi, Odani et al. 1983). This pattern provides L-FABP with a hydrophilic surface for solubilization in the aqueous cytoplasm and a distinct hydrophobic domain for ligand binding (Paulussen and Veerkamp 1990). The bound ligand (e.g. a long-chain fatty acid, cholesterol, or retinoid) is located in its internal water-filled cavity (Paulussen and Veerkamp 1990). For example, the carboxylate site of a long chain fatty acid binds to amino acid side chains in the binding pocket of L-FABP that is lined with polar and hydrophobic amino acids (Zimmerman and Veerkamp 2002; Chmurzynska 2006). The binding pocket of L-FABP is considerably larger than that of other FABPs, allowing the binding of two ligands simultaneously via two different binding sites with high and low affinities (Rolf, Oudenampsen-Kruger et al. 1995). L-FABP is able to bind and translocate many lipophilic substrates throughout the cytosol. Some of these substrates include long chain fatty acids (Thumser and Storch 2000; Norris and Spector 2002; Schroeder, Petrescu et al. 2008), bile acids (Martin, Atshaves et al. 2005), eicosanoids (Raza, Pongubala et al. 1989), and hypolipidemic drugs (Jefferson, Slotte et al. 1991). The two α helices of L-FABP are thought to function as a portal that controls entry and release of ligands from the binding pocket created by the β strands (Thompson, Winter et al. 1997).

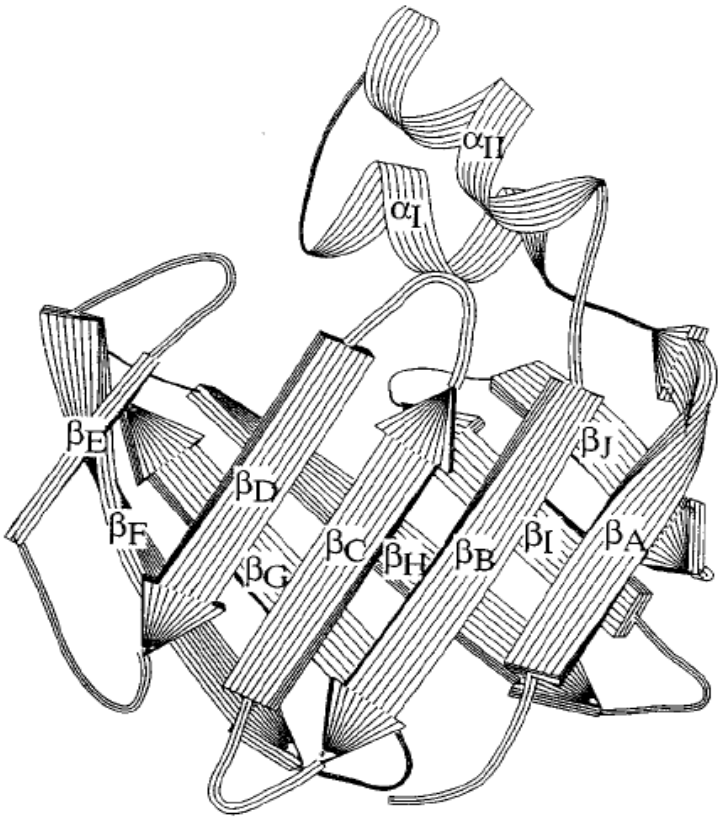

Figure 6: Crystal structure of L-FABP. It shows the typical "β-clam" structure consisting of 10 β-sheets and 2 α-helices. The representative crystal structure of rat L-FABP is shown in the protein data bank (code: 1lfo) (Thompson, Winter et al. 1997).

L-FABP can be separated into 2 to 4 isoforms by isoelectric focusing and these isoforms differ in bound endogenous fatty acids both quantitatively and qualitatively. (Frolov, Cho et al. 1997; Murphy, Edmondson et al. 1999) or chromatography (Dormann, Borchers et al. 1993; Jolly, Murphy et al. 1998; Antonenkov, Sormunen et al. 2006) (Table 2). L-FABP isoforms represent native conformations (amino acid sequence or primary structure of L-FABP protein) and delipidated (breakage of covalent or non-covalent bonds to detach lipid moieties from a protein) fractions.

Table 2: Putative L-FABP isoforms

Protein	**Species**	**Tissue**	**Number of isoform**		**Reference**
			Native	**Delipidated**	
L-FABP	Rat	Liver	3		(Ketterer, Tipping et al. 1976)
	Rat	Liver	4		(Bass 1985)
	Rat	Liver	2		(Murphy, Edmondson et al. 1999)
	Rat	Liver	2	2	(Frolov, Cho et al. 1997)
	Rat	Liver	2	2	(Jolly, Murphy et al. 1998)
	Rat	Liver	2	2	(Di Pietro and Santome 2000)
	Rat	Liver	1	1	(Antonenkov, Sormunen et al. 2006)
	Bovine	Liver	2	2	(Haunerland, Jagschies et al. 1984)
	Bovine	Liver	2	2	(Dormann, Borchers et al. 1993)

B. Oxidative Stress

Oxidative stress is a condition resulting from an imbalance between the production of free radicals and the body's antioxidant defence systems. Free radicals, which are generated as by-products of metabolism in cells, are highly unstable molecules with an unpaired electron. These molecules can react indiscriminately with organic molecules including proteins, lipids, and nucleic acids (Barzilai and Yamamoto 2004; Ohshima, Sawa et al. 2006) and are thought to play an important role in the development of many diseases.

1. Production of free radicals

1.1 Reactive oxygen species or reactive nitrogen species

An important structural feature of an atom is the number of electrons in its outer shell. By sharing electrons, atoms are bound together resulting in maximum molecular stability. When a molecule gains or loses an electron, it becomes a free radical itself. Most common free radicals are oxygen or nitrogen that contain an unpaired electron. Thus, the terms "reactive oxygen species (ROS)" or "reactive nitrogen species (RNS)" have been coined. ROS or RNS might be produced by endogenous sources such as cell aerobic metabolism and inflammation and/or by exposure to a variety of chemical and physical agents. Examples of free radicals are the hydroxyl radical ($OH^{\bullet}$), the peroxyl radical ($ROO^{\bullet}$) and the superoxide anion ($O_2^{\bullet}$), where $^{\bullet}$ denotes one or more unpaired electrons.

Large amounts of ROS are generated within cells by a wide variety of metabolic and chemical reactions, such as (1) detoxification reactions carried out by the cytochrome P-450 system (Schlezinger, Struntz et al. 2006); (2) NADPH oxidation system (Shiotani, Shimada et al. 2007); (3) electron transport systems such as those present in

photosynthesis, mitochondria, and microsomes (Okuda, Li et al. 2002; Tafur and Mills 2008); (4) those created by various enzymes and biomolecules: chloramphenicol (Paez, Becerra et al. 2008), xanthine oxidase (Ohta, Matsura et al. 2007), cyclooxygenase (Li, Hortmann et al. 2008), lipoxygenase (Chung, Toriba et al. 2008); (5) exposure to exogenous chemicals including pollution, smoke, radiation, pesticide, drug consumption, hormones, and other xenobiotic chemicals (Wells, Bhuller et al. 2005); and (6) a decrease in the antioxidant capacity of cells (van de Poll, Dejong et al. 2008).

1.2 Lipid peroxidation

1.2.1 Oxidative modification of lipids

Lipid peroxidation refers to the oxidative degradation of lipids. It most often affects polyunsaturated fatty acids because they contain multiple cabon-cabon double bonds which expose methylene groups that possess especially reactive hydrogens. Free radicals formed during normal or pathological processes can attack lipid membranes, react with unsaturated lipids, and initiate a set of chain reactions resulting in lipid peroxidation (Figure 7). The overall process of lipid peroxidation consists of three stages: initiation, propagation, and termination.

The formation of a lipid radical ($L^{\bullet}$) is the key event in the initiation stage. This can occur by an initiator free radical ($R^{\bullet}$) attacking a hydrogen atom in a polyunsaturated fatty acid side chain forming a carbon-centered lipid radical ($L^{\bullet}$) (see Figure 7a). The propagation step begins with the lipid radical ($L^{\bullet}$), which is rapidly quenched by the addition of molecular oxygen to generate a lipid peroxyl radical ($LOO^{\bullet}$) (see Figure 7b). The next step of propagation occurs when the peroxyl radical ($LOO^{\bullet}$) attacks an adjacent

fatty acid side chain to generate a lipid hydroperoxide (LOOH) (see Figure 7c). Lipid hydroperoxide (LOOH) is the first and relatively stable product of lipid peroxidation reaction and this product may further react with other lipids to produce a new lipid radical (Porter, Caldwell et al. 1995). Under conditions where lipid peroxidation is continuously initiated a termination reaction, which destroys two radicals at once to form non-radical products (NRP), limits the extent of the process.

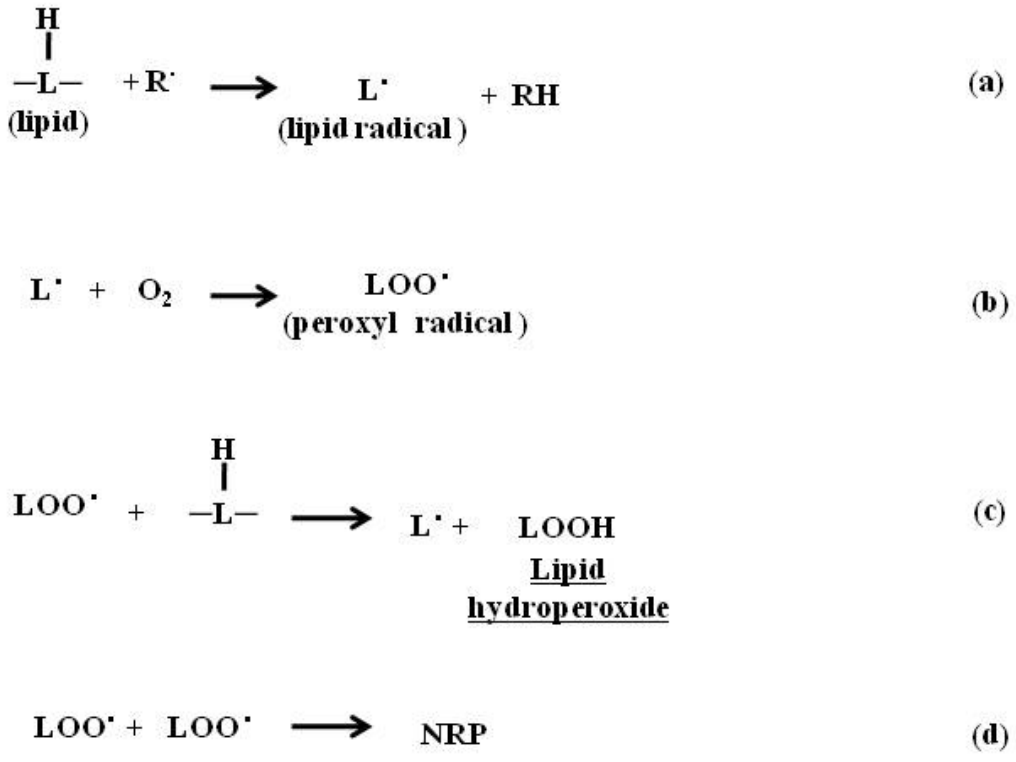

Figure 7: Schematic diagram of free radical chain reactions leading to lipid peroxidation. Abbreviations: L•: lipid radical; LOO•: lipid peroxyl radical; LOOH: lipid hydroperoxide; NRP: non-radical products.

A number of compounds are involved in the direct production of oxidizing radicals to initiate lipid peroxidation. Further peroxidation chain reactions occur by secondary processes involving enzyme activation. Among these, the best examples are the activities of lipoxygenases, phospholipase A2, glucose-6-phosphatase, cytochrome P-450, and the calcium sequestration capacity. Lipoxygenases are activated by hydrogen peroxide and lipid hydroperoxides (Kitaguchi, Ohkubo et al. 2005). Propagation of lipid peroxidation also occurs via NADPH cytochrome-P450 reductase (Sevanian, Nordenbrand et al. 1990). Activation of lipoxygenases occurs in response to disrupted membrane structures or compositions (Akhilender Naidu, Abhinender Naidu et al. 1994). Lipid membranes catalyzed by phospholipase A2 acting at the phospholipids glycerol backbone generate free lysophospholipids and free fatty acids (Hyvonen, Oorni et al. 2001). Lysophospholipids left in the membrane can disrupt membrane structure and function (Tatulian 2001).

1.2.2 Consequences of lipid peroxidation

The consequence of lipid peroxidation is degradation of the membrane's polyunsaturated fatty acids with a subsequent disorganization of membrane structure and disturbance in membrane function (Zhang, Stanley et al. 2006). Aldehydic molecules are generated from lipid peroxidation. These include ketoaldehydes, malondialdehyde (MDA), 4-hydroxy-2-nonenal (HNE), glyoxal, and 4-oxo-2-nonenal (ONE). MDA is one of the most abundant specific aldehydes resulting from lipid peroxidation (Esterbauer, Schaur et al. 1991). Aldehydes are reacted with proteins, DNA, and phospholipids and can generate a variety of intra- and inter-molecular covalent adducts. They are considered the ultimate mediators of the toxic effects elicited by oxidative stress in biological systems.

Collectively, lipid peroxidation products produce a range of biological activities. For example, the products of lipid peroxidation may reduce membrane fluidity, increase permeability, impair integrity, inactivate membrane bound enzymes and receptors. One of the important effects induced by lipid peroxidation is DNA mutagenesis by forming DNA adducts. Increased lipid peroxidation products is also thought to be involved in the pathogenesis of chronic hepatitis C (Konishi, Iwasa et al. 2006) and the progression of non-alcoholic fatty liver disease to fibrosis (Albano, Mottaran et al. 2005). Finally, lipid peroxidation is likely to be involved in the pathogenesis of various renal (Aygen, Celiker et al. 2008), neurologic (Chen, Na et al. 2008) and cardiovascular (Castelao and Gago-Dominguez 2008) diseases.

1.3 Oxidation of DNA

1.3.1 Oxidative modification of DNA

Oxidative alterations to nucleic acid polymers has been shown to cause various types of damage to DNA at either the bases producing single and double strand DNA breaks, or the sugar-phosphate backbone to induce clustered sites, tandem lesions, etc (Evans, Dizdaroglu et al. 2004). Hydroxyl radicals add to double bonds of heterocyclic DNA bases such that the bases undergo ring saturation, opening, contraction, and hydroxylation (Xu, Wu et al. 1999). Further reactions of radicals, which result from the damage of DNA bases, can result in a variety of sugar modifications and numerous end products. Some sugar products are released from DNA as free modified sugars, whereas others remain within DNA or constitute end groups of broken DNA strands (Muller and Gurster 1993).

Exocyclic adducts represent the most frequent form of damage to DNA caused by ROS. Reactive lipid peroxidation products such as MDA and 4-HNE can react with DNA bases in vitro and in vivo to form exocyclic DNA adducts (which serve as biomarkers in stages of oxidative stress) (Poli, Schaur et al. 2008; Warnakulasuriya, Parkkila et al. 2008). MDA can react with DNA bases G, A and C to form adducts of deoxyguanosine (M1G), deoxyadenosine (M1A) and deoxycytidine (M1C), respectively (Marnett 2000). The reactive lipid peroxidation products 4-HNE can be oxidized and are able to attack the nitrogen atoms in DNA bases to generate etheno-DNA-base adducts such as 1,*N*6-ethenodeoxyadenosine (εdA) 3, *N*4-ethenodeoxycytidine (εdC) and *N*2,3-ethenodeoxyguanosine (εdG) (Loureiro, Di Mascio et al. 2000).

1.3.2 Consequences of DNA oxidation

Oxidative stress can produce a multiplicity of DNA lesions with potentially serious consequences. One of the most important consequences of oxidative stress induced DNA damage is mutagenesis (Lee, O'Connor et al. 2002). Oxidative product induced DNA damage leads to disruption in transcription, translation and DNA replication, and gives rise to mutations, which can lead to cancer initiation, and cell senescence or death (Ames, Shigenaga et al. 1993). DNA damage can also disturb cell signalling pathways (Miyasaka, Nagai et al. 2007). DNA damage has been implicated in the development of various human cancers (de Gruijl, van Kranen et al. 2001; Yuki, Maniwa et al. 2008; Rao, Klein et al. 2009; Wu, Lin et al. 2009), neurodegenerative diseases and ageing processes (Kyng, May et al. 2005; Wang, Lukas et al. 2008).

1.4 Oxidation of protein

1.4.1 Oxidative modification of protein

Protein oxidation is defined as the covalent modification of a protein induced either directly by ROS or indirectly by reactions with secondary by-products of oxidative stress. Agents are responsible for oxidative damage and protein oxidation including chemical reagents (H_2O_2, $Fe^{+2,}$ Cu^{+}, etc), UV light, oxidative reductase enzymes (xanthine oxidase, myeloperoxidase, cytochrome P-450 enzymes), drugs and their metabolites. Protein modifications induced by ROS include sulfur oxidation (cysteine disulfides, S-thiolation, methionine sulfoxide), formation of protein carbonyls, tyrosine crosslinks, tryptophanyl modifications and amino acid interconversions (Stadtman and Levine 2000).

Protein carbonylation may result from an accumulation of ROS themselves or from accumulated lipid peroxidation products such as MDA, which are known to react with lysine residues to form carbonyl derivatives (Liu and Wang 2005). Oxidative attack of a polypeptide backbone is initiated by $^{\bullet}OH$-dependent oxidation of an amino acid hydrogen atom. The alkyl, alkyl peroxyl, and alkoxyl radicals formed in this pathway may undergo side reactions with other amino acid residues to generate a new carbon-centered radical. Table 3 provides examples of amino acids most susceptible to oxidation and their oxidants.

Table 3: Amino acids most susceptible to oxidation

Amino acids	**Oxidation products**
Cysteine	Cysteine sulfenic acid, cysteinesulfinate, cysteic acid
Methionine	Methionine sulfoxide, methionine sulfone
Tryptophan	4-,5-,6-, and 7-Hydroxytryptophan, nitro-trypophan
Tyrosine	p-Hydroxyphenylacetaldehyde, nitro-and dityrosine
Histidine	N-benzoyl-2-oxohistidine, asparagines, aspartic acid,
Arginine	Glutamic semialdehyde
Lysine	Aminoadipic semialdehyde

1.4.2 Consequences of protein oxidative modification

Oxidative damage to a specific protein, particularly at its active site, can induce a progressive loss of a particular biochemical function. Oxidized proteins often lose function and undergo selective degradation (Chevion, Berenshtein et al. 2000). ROS can cause biological dysfunction through oxidation of amino acid side chains/or protein backbone, which may in turn lead to the formation of protein cross-linkages and fragmentation (Kowalik-Jankowska, Rajewska et al. 2006). Protein carbonylation can affect enzyme activities or alter the susceptibility of the modified protein to proteolysis (Berlett and Stadtman 1997). Oxidation of proteins plays an essential role in the pathogenesis of different diseases including aging (Abd El Mohsen, Iravani et al. 2005), Alzheimer's disease (Korolainen and Pirttila 2009), atherosclerosis (Serdar, Aslan et al. 2006), renal disease (Drueke, Witko-Sarsat et al. 2002) and liver diseases (Ahmed, Thornalley et al. 2004; Wei, Chen et al. 2006).

C. **Hepatocellular Oxidative Stress**

1. General aspects

In the healthy liver, hepatocytes produce low amounts of ROS which are normally inactivated by various cellular antioxidant systems. If the liver becomes inflamed or infected, its ability to suppress ROS production may become impaired. In chronic liver diseases, however, there is an over production of ROS resulting in oxidative stress, such that the normal antioxidant capacity of the cell becomes overwhelmed. Chronic liver disease is characterised by the processes of inflammation and fibrosis that leads to cirrhosis and hepatocellular carcinoma. Increasing evidence demonstrates that alterations in cellular

ROS generation play a crucial role in the various steps that initiate and regulate the progression of liver dieases. Indeed, cellular oxidative stress has been detected in patients with alcohol abuse (Wu, Zhai et al. 2006), hepatitis C virus infection (Okuda, Li et al. 2002), iron overload (Ounjaijean, Thephinlap et al. 2008), drug toxicity (Masutani 2001), chronic cholestasis (D'Odorico, Melis et al. 1999), and hepatic fibrosis (Yang, Chang et al. 2008). It should be noted that, oxidative stress is not only a potentially toxic consequence of chronic liver injury but also contributes to excessive tissue remodeling and fibrosis (Parola and Robino 2001). Thus, researchers are attempting to better understand the cellular and molecular mechanisms leading to oxidative stress and the cellular results of being chronically exposed to high levels of ROS.

2. Pathogenesis

ROS suppresses hepatocyte proliferation, stimulates hepatic stellate cells (HSC) activation, promotes extracellular matrix (ECM) production, and likely plays an important role in the initiation of liver damage (Perez de Obanos, Lopez-Zabalza et al. 2007). Activation of HSC, a process responsible for the excessive production of fibrosis tissue in the development of cirrhosis, is mediated by cytokines and ROS released from damaged hepatocytes and/or activated Kupffer cells (liver macrophages) or even HSC themselves (Cubero and Nieto 2008). Endothelial and Kupffer cells are necessary for the effective defence against invading microorganisms and oxidative stress in the liver. After frequent exposure to oxidative products, especially endotoxins such as lipopolysaccharide (LPS), Kupffer cells become activated and in turn stimulate hepatocyte metabolic activity via the production of additional reactive species and proinflammatory cytokines (Catala, Anton et

al. 1999). Increased metabolic activity in hepatocytes causes further increases in ROS production and results in the development of hepatocyte hypoxia. This contributes to hepatocyte death by both necrotic and apoptotic mechanisms (Arteel, Raleigh et al. 1996). ROS also play a key role in mediating the pathologic manifestations of endothelial cells dysfunction, such as increased vascular endothelial permeability and leukocyte adhesion (Szocs 2004).

The role of ROS in the pathogenesis of the liver is depicted in Figure 8. ROS can be liberated through a variety of physiological and pharmacological events such as age, obesity, ethanol consumption, virus, lipid alteration, carbohydrate metabolism, and xenobiotic metabolism (Parola and Robino 2001). The extent of the ROS effect depends on the activated inflammatory cells such as neutrophil and Kupffer cells (Bilzer, Jaeschke et al. 1999; Jaeschke and Hasegawa 2006). Oxidative stress affects tissue and cellular events such as apoptosis, necrosis and regeneration by regulating numerous cytokines, growth factors and hormones (Thannickal and Fanburg 2000). In particular, pro-inflammatory cytokines such as interleukin 6 (IL-6), tumor necrosis factor-α (TNF-α), and fibrogenic cytokines such as transforming growth factor (TGF-β) have been identified as key mediators in chronic liver damage (Pinzani and Rombouts 2004). It is now widely accepted that TGF-β is a major cytokine in the regulation of extracellular matrix (ECM) accumulation and the development of hepatic fibrosis (Border and Noble 1994). Attenuation of ROS has been demonstrated to result in the inhibition of TGF-β induced hepatic fibrosis (Yang, Chang et al. 2008).

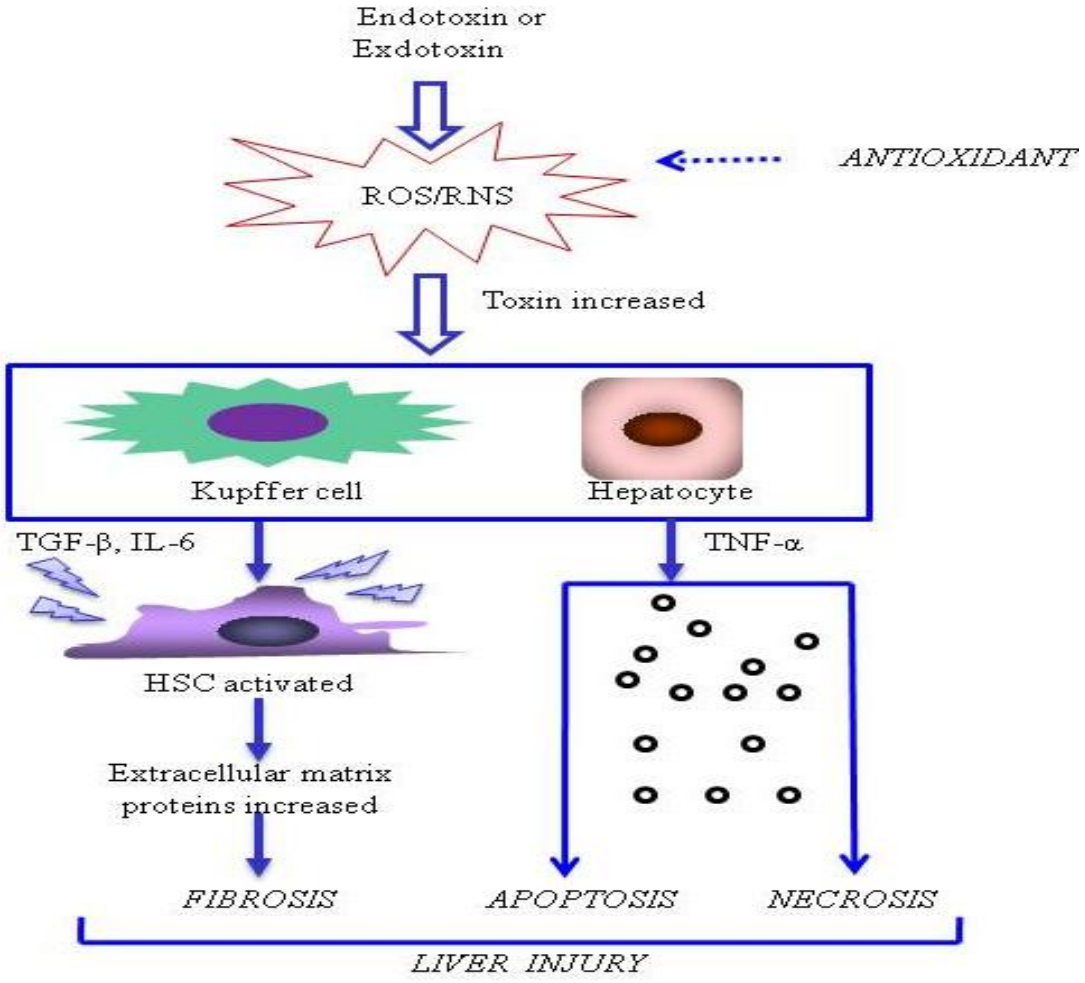

Figure 8: Effect of ROS on liver injury. Endotoxins or exdotoxins trigger a series of events in hepatocytes, Kupffer cells and hepatic stellate cells that are all believed to play important roles in the initiation and progression of liver injury such as fibrosis, apoptosis or necrosis.

3. The signalling pathway involved in ROS induced liver diseases

While ROS are predominantly implicated in causing a variety of cellular responses ranging from proliferation to cell death, they may also reflect the balance between a variety of intracellular signalling proteins that are activated in response to oxidative stress (Palmer and Paulson 1997). Exogenous ROS can trigger a variety of cytokines and growth factors that bind to different classes of receptors (see Figure 9) while endogenous ROS are largely generated by mitochondrial enzymes (particularly NADPH-cytochrome P450) and can induce hepatocyte damage. Protein tyrosine phosphatases (PTPs) have been demonstrated to be stimulated by ROS to induce tyrosine phosphorylation events, which play an important role in redox control and cell signalling (Gupta and Luan 2003). The information is transmitted *via* the activation of mitogen-activated protein kinases (MAPKs) signalling pathway (Ballif and Blenis 2001), which consists of extracellular signal-regulated kinases (ERK), c-Jun N-terminal kinases (JNK), and p38kinases (p38MAPK). The ERK pathway is linked to the regulation of cell proliferation, while the JNK and p38MAPK pathways are strongly tied to oxidative stress. The activation of JNK by ROS in hepatocytes is considered to be a pro-apoptotic event (Marderstein, Bucher et al. 2003). MAPKs interact with upstream mediators such as growth factor receptors, G proteins (Ras) and tyrosine kinases, and downstream mediators such as nuclear factor-κB (NF-κB) and the activator protein 1 (AP-1) to regulate a wide array of cellular processes, including proliferation, differentiation, and apoptosis (Lopez-Ilasaca, Crespo et al. 1997).

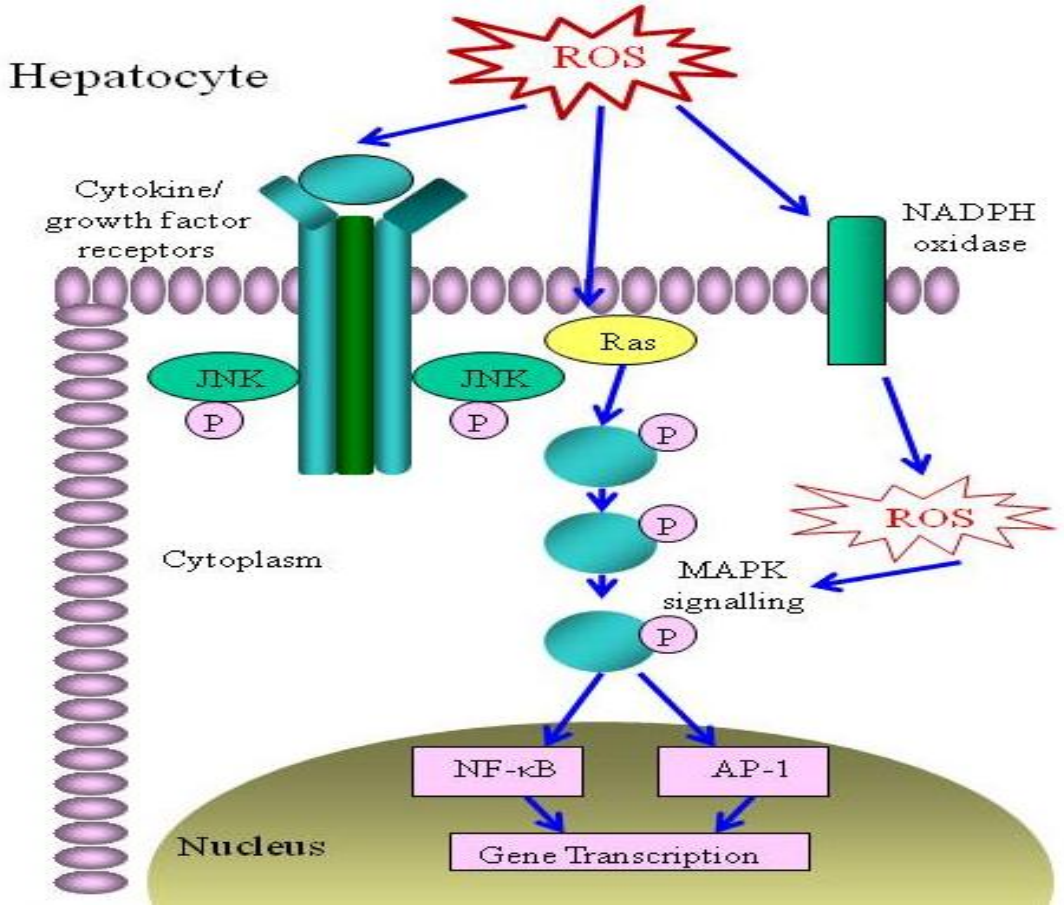

Figure 9: Factors involved in ROS induced liver diseases. ROS activate cytokines/growth factors on hepatocytes, which leads to the upregulation of several signalling cascades most importantly JNK, Ras, and MAPK signalling pathways. These signalling cascades result in the activation of several redox-regulated transcription factors (AP-1, NF-κB, etc). Abbreviations: AP-1: activator protein-1; NF-κB (nuclear factor kappa B).

Growth factor receptors activated by ROS include epidermal growth factor receptor (EGFR) (Bae, Kang et al. 1997), platelet-derived growth factor receptor (PDGFR) (Catarzi, Degl'Innocenti et al. 2002) and vascular endothelial growth factor receptor (VEGFR) (Neufeld, Cohen et al. 1999). ROS can also play an important physiological role as a secondary messenger by activating certain transcriptional factors such as NF-κB and the AP-1 family factors (Czaja, Liu et al. 2003; Storz 2005). Activation of these transcriptional factors is thought to be involved in cell transformation, proliferation, and cell survival (Baldwin 1996; Brown, Nigh et al. 1998). Transcription of NF-κB and AP1 are potentially associated with ROS-triggered tumor progression (Hsu, Young et al. 2000).

D. Antioxidant

1. Antioxidant Systems

Antioxidants are defined as any substance that when present at low concentrations relative to an oxidizable substrate, significantly delays or prevents oxidation of that substrate. Because oxidative stress plays a central role in liver disease pathogenesis and progression, use of antioxidants has been proposed as being of therapeutic benefit in an effort to prevent or attenuate liver damage. Various compounds have been classified as hydrophilic or hydrophobic antioxidants. Table 4 summarizes some of the antioxidants proposed to protect the liver from injury in animal and human trials. Lipophilic antioxidants, such as carotenoids and tocopherols, protect lipophilic environments while hydrophilic antioxidants are involved in the cellular defence against free radicals in the hydrophilic environment.

Table 4: List of hydrophilic antioxidants and lipophilic antioxidants

Hydrophilic Antioxidant	**Lipophilic Antioxidants**
Superoxide dismutase (SOD), Catalase	Tocopherols
Glutathione peroxidase (Gpx)	Flavonoids
Glutathione	Carotenes
Albumin, ascorbic acid, uric acid	Coenzyme Q_{10}
Bilirubin	Silymarin

2. Hydrophilic Antioxidants

Cells contain several antioxidant enzymes, which can catalyze the breakdown of free radical species in the cytosol and thereby act as hydrophilic antioxidants. These include superoxide dismutase (SOD), glutathione peroxidase (GPx), catalase, and glutathione. The first line of defence against oxidative stress is provided by SOD, a group of metal-containing enzymes located in the mitochondrial matrix. SOD is known to catalyze the dismutation of superoxide anion to oxygen and hydrogen peroxide (Johnson and Giulivi 2005) and is strongly modulated by the redox state of the cell. GPxs constitute a family of selenium-containing enzymes that are found in the cytoplasm of nearly all mammalian tissues. GPxs are able to detoxify cellular organic peroxides and hydrogen peroxide by oxidizing two molecules of glutathione. Catalase is mainly located in cellular peroxisomes and to some extent in the cytosol of mammalian cells. By catalyzing the conversion of hydrogen peroxide to water and oxygen, catalase plays a significant role in the development of tolerance to cellular oxidative stress especially in the case of limited glutathione availability. Figure 10 shows the antioxidant system provided by enzymes in the cytosol against oxidative stress induced by the metabolism of long-chain fatty acids. Various reports describe the activation of antioxidant enzymes in the setting of tissue injury and liver diseases such as ischemia/reperfusion injury (Zapletal, Heyne et al. 2008), non-alcoholic fatty liver disease (Bujanda, Hijona et al. 2008), alcoholic liver disease (Prakash, Gunasekaran et al. 2008), viral hepatitis (Pushpavalli, Veeramani et al. 2008).

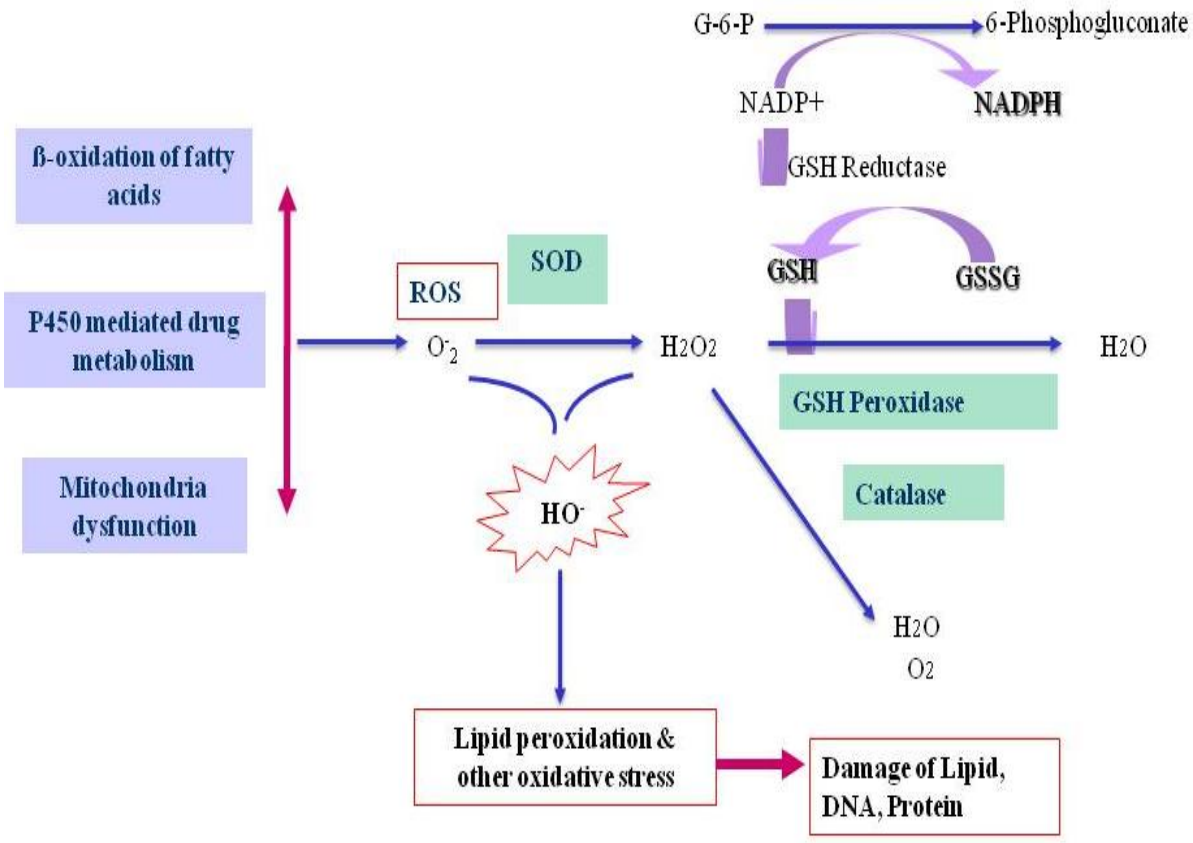

Figure 10: ROS and hydrophilic antioxidant defence systems. Superoxide anion radical is formed by the process of β-oxidation of fatty acids, P450 metabolism, mitochondria dysfunction or NAD(P)H oxidase mediated oxidation. A number of antioxidant defence systems have evolved to combat the accumulation of ROS. These include superoxide dismutase (SOD), glutathione peroxidase (GPx), catalase, and glutathione. Abbreviations: GSH, reduced glutathione; GSSG, oxidized glutathione.

Hydrophilic antioxidants also include non-enzymatic antioxidants such as albumin, ascorbic acid, uric acid, bilirubin, etc which are responsible for much of the blood's ability to trap free radicals (Krijgsman, Papadakis et al. 2002). These serum substances are sometimes included in routine clinical serum biochemistry measurements in patients (Delimaris, Georgopoulos et al. 2008). Albumin may be an important antioxidant since it contains sulphydryl (SH) groups that can react with hydrogen peroxide and peroxyl radicals. Albumin also contains thiol groups which are able to scavenge reactive oxygen and nitrogen species (Faure, Troncy et al. 2005). It has been shown that albumin can bind and remove reactive oxygen species in vitro, thereby regulating cell molecules that are active in mediating inflammatory reactions (Kouoh, Gressier et al. 1999). Albumin can also influence plasma redox status by binding heavy metals, which can otherwise transform into redox-active forms (Kragh-Hansen, Chuang et al. 2002).

Ascorbic acid is a powerful water-soluble, chain-breaking antioxidant that has several antioxidant effects including the ability to donate electrons to most water-soluble radicals and oxidants such as superoxide, hydrogen peroxide, the hydroxyl radical, hypochlorous acid, aqueous peroxyl radicals, and singlet oxygen. In the plasma and within cells, ascorbic acid acts as a primary antioxidant to scavenge ROS generated from cellular metabolism (Torres, Galleguillos et al. 2008). Ascorbic acid can also interact with plasma membranes by donating electrons to α-tocopheroxyl radicals (Iglesias, Pazos et al. 2009). Indeed, the combination of ascorbic acid and α-tocopherol treatment has been reported to normalize liver enzymes abnormalities in patients with fatty liver disease induced oxidative stress (Ersoz, Gunsar et al. 2005). Therefore, ascorbic acid has the potential to protect both cytosolic and membrane components of cells from oxidant damage.

3. Lipophilic antioxidants

Contradictory results have been obtained regarding the hepatoprotection provided by lipophilic antioxidants such as coenzyme Q, tocopherols, β-carotene, flavonoids and silymarin. Coenzyme Q is a powerful lipophilic antioxidant and oxygen free radical scavenger found in mitochondrial enzymes. It improves the function of mitochondria which produce energy in cells. It is found in relatively high concentrations in the heart, kidney, liver, and pancreas. Coenzyme Q contributes to the stability of plasma membranes by inserting itself into phospholipids and generating antioxidants such as ascorbate and α-tocopherol (Quiles, Ramirez-Tortosa et al. 1999).

Tocopherols consist of several forms: α, β, γ, and δ. All forms have antioxidant properties but α-tocopherol is thought to be the most active form (Kaiser, Di Mascio et al. 1990). As a major active lipid-soluble and chain-breaking antioxidant within cell membranes (Cochrane 1991) and lipoproteins, α- tocopherol is able to inhibit the generation of singlet oxygen free radicals and most importantly protects polyunsaturated fatty acids in membranes against lipid peroxidation (Gavazza and Catala 2006). Several studies have clearly demonstrated that α-tocopherol levels correlate inversely with the production of oxidative stress products and extent of liver damage (Masalkar and Abhang 2005). The maintenance of normal concentrations of α-tocopherol appears to be essential in the prevention of lipid peroxidation induced by alcohol consumption (Nanji, Yang et al. 1996) and cirrhosis (Brown, Poulos et al. 1997).

Carotenoids also serve as a source of lipid-soluble antioxidants to protect lipid membranes against lipid peroxidation (Dixon, Shie et al. 1998). Beta-Carotene is

considered to be one of the most abundant and potent carotenoids present in food sources. Recent evidence has shown that β-carotene is an effective scavenger of singlet oxygen and inhibits peroxyl radicals, which are generated in the process of lipid peroxidation (Bando, Hayashi et al. 2004).

Finally, flavonoids are lipid-soluble antioxidants that have been reported to prevent or delay the progression of a number of diseases resulting from oxidative damage (Frei and Higdon 2003) including liver diseases (Luceri, Giovannelli et al. 2008). The antioxidant properties of flavonoids include chelating capacity, interacting with membranes and inhibition lipid peroxidation (Santos, Uyemura et al. 1998; Erlejman, Verstraeten et al. 2004).

4. Interaction between hydrophilic and lipophilic antioxidants

Interactions between hydrophilic and lipophilic antioxidants provide a beneficial effect in tissues. For example, ascorbic acid, α-tocopherol and Coenzyme Q (CoQ) are involved in a trans-membrane electron transport recycle system in plasma membranes as outlined in Figure 11. Ascorbic acid is located at the hydrophilic cell surface. Both CoQ and α-tocopherol are in the hydrophobic phospholipids bilayer. Co-administration of ascorbic acid and α-tocopherol resulted in a substantial reduction in the levels of lipid peroxidative products (Huang and May 2003; Maliakel, Kagiya et al. 2008; Tikare, Das Gupta et al. 2008). The tocopheroxyl radical formed as a result of the initial reduction of a lipid peroxyl radical, is regenerated to α-tocopherol by acceptance of a hydrogen ion from ascorbic acid. CoQ could also interchange electrons with ascorbate (Roginsky, Bruchelt et al. 1998), leading to regeneration of $CoQH_2$. The major source of electrons comes either

from different NAD(P)H-dehydrogenases such as NADH-cytochrome b_5 reductase, NAD(P)H:quinone oxidoreductase 1 (NQO1) on the plasma membrane (Forthoffer, Gomez-Diaz et al. 2002) or from ascorbate free radical-reductase in the cytosol (De Cabo, Cabello et al. 2004). This process allows for the transport of radicals from a lipophilic to an aqueous compartment where antioxidant enzymes are operative.

Cooperative interactions have also been described within the class of lipophilic antioxidants. β-carotene and α-tocopherol have been reported to act synergistically to inhibit lipid peroxidation resulting from peroxyl radicals (Stratton and Liebler 1997). Finally, mixtures of carotenoids are superior to single compounds in preventing β-oxidation of lipids in multilamellar liposomes.

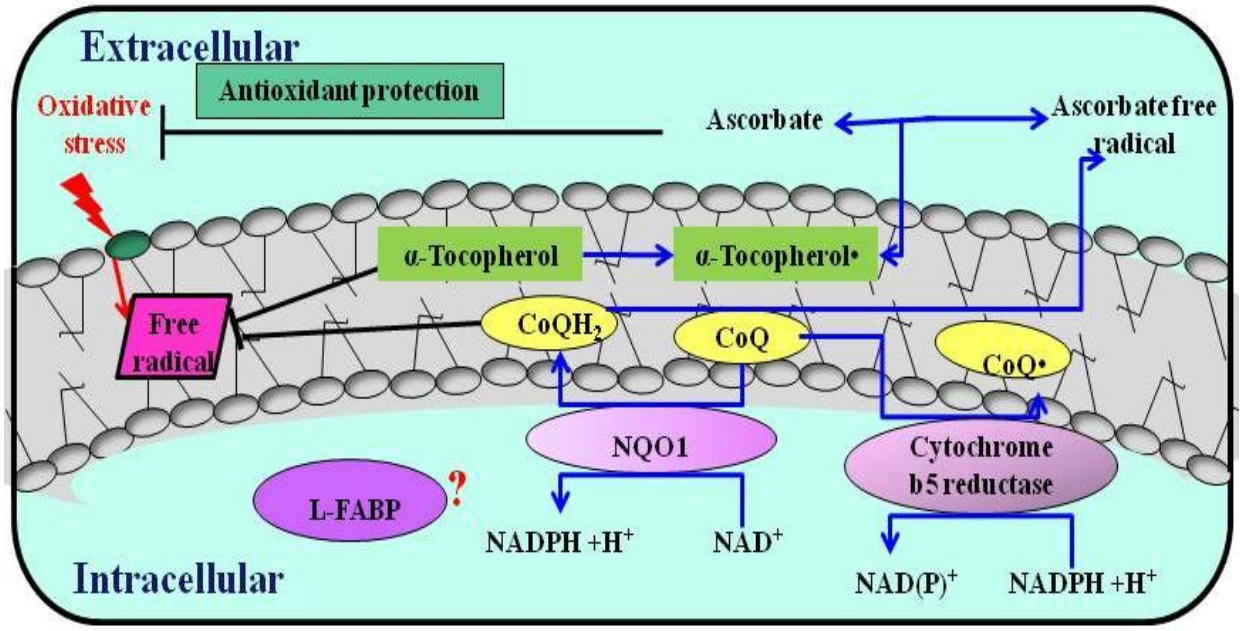

Figure 11: Plasma membrane redox system. Abbreviations: NQO1, NAD(P)H quinone oxidoreductase 1.

5. Antioxidant function

As discussed above there are many antioxidant systems available to cells to combat free radicals. However, a novel antioxidant that has escaped detection is L-FABP.

Recent work by our group showed that L-FABP plays an important role in the cell's antioxidant defence mechanism (Wang, Gong et al. 2005; Rajaraman, Wang et al. 2007; Wang, Shen et al. 2007). Using an L-FABP cDNA transfection model Wang et al have reported that hepatocytes containing L-FABP were associated with significant lower levels of ROS than cells without L-FABP (Wang, Gong et al. 2005). Moreover, in a bile-duct ligated animal model of cholestasis, clofibrate induced L-FABP was associated with reduced lipid peroxidation products and improved hepatic function (Wang, Shen et al. 2007).

The antioxidative function of L-FABP is thought to be due to its amino acid composition. L-FABP contains one cysteine and several methionine groups (She, Wang et al. 2002). Methionine (Figure 12) and cysteine (Figure 13) are amino acids with well defined functions in the redox reactions of cells. High resolution X-ray and NMR structure analyses reveal that Met^{113} is buried in the hydrophobic core of L-FABP, while Cys-69 and other methionine residues are located on the surface of the protein (Thompson, Winter et al. 1997). Methionine and cysteine residues regulate the biological activity of proteins by alterating catalytic efficiency and modulation of the surface hydrophobicity of the protein. In redox reactions, methionine is readily oxidized to methionine sulfoxide and cysteine can be oxidized to cysteine disulfide by free radicals. The oxidation of surface exposed methionines and cysteines thus serves to protect other residues from oxidative damage. Covalent S-thiolation of cysteine modification in rat and bovine liver L-FABP has been

reported (Sato, Baba et al. 1996). Most biological systems contain disulfide reductases and methionine sulfoxide reductases that can convert the oxidized forms of cysteine and methionine back to their unmodified forms. These are the only amino acids that can be converted back to their unoxidized form. Thus, the role of L-FABP can be expanded beyond intracellular transport to a novel function as an antioxidant protein.

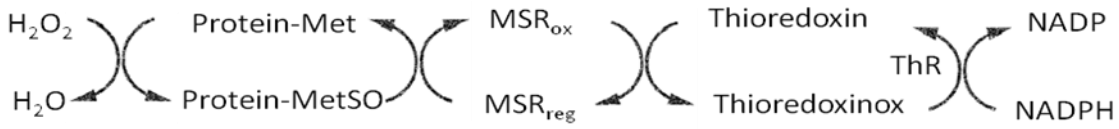

$H_2O_2 + Met \longrightarrow MetSO + H_2O$ (a)

$MetSO + MSR \longrightarrow Met + MSR_{ox} + H_2O$ (b)

$MSR_{ox} + Thioredoxin \longrightarrow MSR_{reg} + Thioredoxinox$ (c)

$Thioredoxinox + ThR \xrightarrow{NADPH} Thioredoxin + NADP^{+}$ (d)

Figure 12: The oxidation and reduction of catalytic reaction for methionine residues Methionine (Met) is readily oxidized to methionine sulfoxide (MetSO) by many different forms of ROS (a). In the reaction hydrogen peroxide (H_2O_2) is used to represent ROS. The MetSO is reduced by methionine sulfoxide reductase (MSR) which itself becomes oxidized (b). The reduced form of MSR is regenerated by thioredoxin (c) whose oxidized form is then regenerated by thioredoxin reductase (ThR) which uses NADPH as an electron donor (d). Abbreviations: reg: regenerated; ox: oxidized.

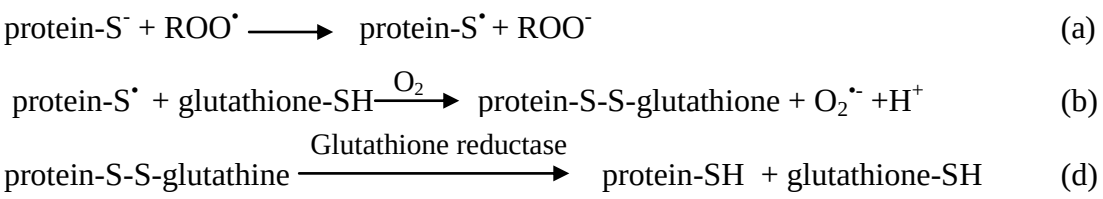

Figure 13: Cysteine residues may participate in S-thiolation/dethiolation reactions. In the first reaction (a) a protein containing cysteine residue is oxidized to form protein sulfhydryls producing sulfenic acids and thiyl radicals. Subsequently, the oxidized protein is then reversed by forming S-glutathiolated protein (b). The S-glutathiolated protein is continuously reduced by glutathione reductase.

II. Hypothesis & Objectives

Hypothesis

Recent findings in our laboratory indicated that modulating L-FABP expression influences the cellular antioxidant defence system *in vivo* (Wang, Gong et al. 2005; Rajaraman, Wang et al. 2007; Wang, Shen et al. 2007). However, the mechanism for regulating L-FABP when it serves as an antioxidant remains to be determined. In the experiments, we test the hypothesis that PPAR activation in hepatocytes results in increased L-FABP antioxidant activity and the abundance of methionine residues within the L-FABP molecule interact with ROS to achieve an antioxidant state.

Objective

The principal objectives of this work were to: 1) determine the mechanism of PPAR in the regulation of L-FABP expression and antioxidant activity; and 2) determine the antioxidant mechanism of L-FABP using recombinant rat L-FABP.

III. MATERIALS AND METHODS

A. Materials

Chemicals used in this thesis were purchased from the companies listed in Table 5.

Table 5: Materials used in experiments

Product	Company
100bp DNA ladder (250µg)	Invitrogen
100mM dNTP set, PCR Grade	Invitrogen
Actinomycin-D	Sigma
Acrylamide	Sigma
Anti-rabbit IgG	Amersham
α-tocopherol	Sigma
2,2′-azobis(2,4-dimethylvaleronitrile)	Woho
2,2′-azobis(2-amidinopropane) dihydrochloride	Woho
BamHI enzyme	Roche
BCA protein assay reagent	PIERCE
Bis-acrylamide	Sigma
Cell culture flask	Fisher
Centrifuge tubes	Fisher
Clofibrate	Sigma
[α-^{32}P]-CTP	GE health care
[α-^{32}P]-dCTP	GE health care
DH5α Competent Cells	Invitrogen
DNase	Roche
Dulbecco's Modified Eagle Medium	GIBCO/BRL
Fetal bovine serum	VWR
Glutathione 4B	Amersham
Glutamine	Sigma
GFX PCR DNA and Gel Band Purification Kit	GE health care

[^{3}H] palmitic acid	PerkinElmer Life
GW-9662	Sigma
isopropyl-β-D-thio-galactoside (IPTG)	Alfa Aesar
LB broth	Fisher
Lipofectamine2000	Invitrogen
Methanol	VWR
MK-886	Sigma
Oligo(dT) 12-18 primer	Promega
PCR thermowell tubes	Fisher
Penicillin, Ampicillin	GIBCO/BRL
pGEX-6P-2	Amersham
Phenol/chloroform/isomyl alcohol (25:24:1)	Sigma-Aldrich
Pipet tips	Invitrogen
Prescission protease	Amersham
Protein Assay Kit	Bio-Rad
Proteinase inhibitor	Invitrogen
Proteinase K	Invitrogen
RNase, DNase-free	Roche
1,1,3,3-tetra-methoxypropane	Sigma
2-thiobarbituric acid	Sigma
trichloroacetic acid	VWR
T4 DNA ligase	Promega
Taq DNA Polymerase	Qiagen
Trypsin	GIBCO/BRL
Tris-base	Sigma-Aldrich
Tween-20	Sigma
vitamin C	Sigma
Western blot membrane	Fisher
nitrocellulose blotting membrane	GE healthcare
XhoI enzyme	Roche

B. Methods

1. Cell line and culture conditions

L-FABP expressing CRL-1548 hepatoma cells used in this thesis were maintained on 100×20mm culture dishes overlaid with DMEM (Dulbecco's Modified Eagle's Medium) or DF-10 (DMEM/Nutrient Mixture F-10 Ham's) medium containing 10% fetal bovine serum, 100 IU/ ml penicillin, and streptomycin (50units/ml) and kept in a 37^{o}C incubator with a humidified atmosphere of 5% CO_2 and 95% air. Clofibrate, PPARα antagonist MK886, and PPARγ antagonist GW9662 were dissolved in dimethyl sulfoxide (DMSO) and added to DF-10 media (DMSO < 0.1% v/v in final solution). Concentrations of the pharmacological agents were based on their effective dose. Control cells were incubated with DMSO using the same volume as in the drug study. Cells were exposed to DF-10 media containing clofibrate and/or PPARα antagonist MK886, and/or PPARγ antagonist GW9662.

2. RNA isolation

TRIZOL LS reagent was employed to extract total RNA from CRL-1548 cells and liver tissues as described in the manufacturer's manual (Invitrogen, CA, USA). Approximately 50~100 mg of rat liver tissue was homogenized in 0.75 ml of TRIZOL LS reagent using a power homogenizer (Polytron, Elkhart, Indiana). To lyse the CRL-1548 cells, 0.3~0.4 ml of TRIZOL LS reagent was directly added to the 3.5 cm diameter dish. And the cell lysate passed several times through a pipette. The homogenized samples were incubated for 5 minutes at 15 to 30°C to permit the complete dissociation of nucleoprotein

complexes and then 0.2 ml of chloroform was added. Sample tubes were shaken vigorously by hand for 15 seconds, incubated at 15 to 30°C for 2 to 15 minutes and centrifuged at 12,000 × *g* for 15 minutes at 4°C. Following centrifugation, the aqueous phase containing RNA was transferred to a clean tube, and incubated with 0.5 ml of isopropyl alcohol to precipitate the RNA at 15 to 30°C for 10 minutes. The RNA precipitate was formed by centrifugation at 12,000 × *g* for 10 minutes at 4°C. At least 1 ml of 75% ethanol was used to wash the RNA and centrifuged at 7,500 × *g* for 5 minutes at 4°C. The RNA pellet was air-dried and eluted in RNase-free water at 1 µg/µl which was determined using a spectrophotometer (Bio-Rad Smart Spec 3000 Spectrophotometer, Life Science Research Division, Mississauga, Canada). Good quality RNA had an $A_{260/280}$ ratio of 1.8 to 2.0. RNA was stored at -70°C until required.

3. Reverse transcriptase polymerase chain reaction (RT-PCR)

The first-strand cDNA was synthesized by the Advantage RT-for-PCR kit. Total RNA (1 µg) was dissolved in diethylpyrocarbonate (DEPC)-treated doubled-distilled water (ddH2O) to achieve a final volume of 12.5 µl. Subsequently, 1 µl oligo(dT) primer, 4 µl of 5 × reaction buffer, 1 µl of 10 mM dNTP mix, 0.5 µl recombinant RNase inhibitor, and 1 µl Moloney murine leukemia virus reverse transcriptase were added and incubated for 1 h at 42°C. At the end of the reverse transcription procedure the reaction mixture was heated to 94°C for 5 min and brought up to a final volume of 100 µl with DEPC-H_2O.

PCR was performed by using the Taq DNA Polymerase kit (Qiagen, Mississauga, Canada). Taq DNA Polymerase is a thermostable DNA polymerase used for amplifying short segments of DNA. QIAGEN PCR Buffer contains both KCl and $(NH_4)_2SO_4$

providing a wide annealing temperature window and tolerance to variable Mg^{2+} concentration. Q-solution facilitates amplification of difficult templates by modifying the melting behaviour of DNA.

A typical 50 µl RT-PCR reaction is shown in Table 6. Gene-specific PCR primers for rat L-FABP were designed by the Oligo 5.1 program from a cDNA sequence obtained from GenBank (GenBank BC086947) and synthesized by Invitrogen (Invitrogen, Burlington, Canada). The sense primer was 5'- GCC ACC ATG AAC TTC TCC G-3' and the antisense primer was 5'- AGT CAC GGA CTT TAT GCC TTT-3'. PCR product length was 318 bp. Specific rat GAPDH was purchased from Clontech (5507-3) with an expected PCR size of 986 bp. PCR reactions were performed in an Eppendoff Master Cycler (Westbury, NY, USA). PCR amplification was carried out in 30 cycles of denatu.ration at 94˚C for 45 seconds, annealing at 54˚C (L-FABP) and 60˚C (GAPDH) for 30 seconds, elongation at 72˚C for 120 seconds with additional 7 minutes final extension at 72˚C using an Eppendorf Master Cycler. The PCR product was analyzed using a 1.2% agarose gel. Identity of PCR products was confirmed by sequencing PCR products at the DNA-sequencing facility of the Manitoba Institute of Cell Biology (Winnipeg, Canada).

Table 6: RT-PCR reaction components

Components	**Volumes (µl)**
cDNA template	5
10X PCR Buffer	5
5X PCR Buffer	10
25mM $MgCl_2$	4
dNTP mix (10mM each)	1
Forward Primer	1
Reverse Primer	1
Tag DNA Polymerase	0.4
RNase-free Water	22.5
Total volume	50

4. Protein sample preparation from cell culture

After washing twice with ice cold phosphate-buffered saline (PBS), cellular protein was extracted by dissolving cells in 500 µl cold RIPA lysis buffer (1x = 50 mM Tris-HCl pH 7.4, 150 mM NaCl, 1 mM EDTA, 5 µg/ml aprotinin, 1 mM PMSF (phenylmethanesulfonylfluoride), 5 µg/ml leupeptin, 1% Triton X-100, 1% sodium deoxycholate, 0.1% sodium dodecyl sulfate) and collected into a microcentrifuge tube. Protease inhibitors were added to prevent the digestion of the sample by its own enzymes. Cell pellets (~10^8 cells) were incubated with lysis buffer on ice (to avoid protein denaturing) for 20 minutes and vortexed 2 to 3 times for approximately 1 sec each. The lysate was centrifuged at 12,000 *g* for 10 minutes at 4°C and the supernatant was transferred into a clean tube. Protein concentration was measured by the BCA (PIERCE, Rockford, USA) assay. Protein samples were stored at -80°C until required. Appropriate amount of proteins were subjected to Western blot analysis.

5. Western blot analyses

The Western blot is an analytical technique used to detect specific proteins in a given sample of tissue homogenate or extract. Twenty micrograms of total cell protein was employed to detect L-FABP expression by Western blot analysis. Protein samples were mixed with 4x gel-loading buffer (4x = 250 mM Tris-HCl, pH 6.8, 8% sodium dodecyl sulfate (SDS), 20% glycerol, 0.2% bromophenol blue, and 5% β-mercaptoethanol), and boiled for 10 minutes to denature and unfold the proteins. The strong reducing agent β-mercaptoethanol maintained polypeptides in a denatured state and removed the secondary and tertiary structure of the protein. Proteins were then separated on a 15% (based on the molecular weight), sodium dodecyl sulfate-polyacrylamide gel (SDS-PAGE) under

reducing conditions. Proteins were covered by the negatively charged SDS and move to the positively charged electrode through the acrylamide mesh of the gel. Once separated, proteins were transferred onto Nitroplus-2000 membranes (Micron Separations, Westborough, USA). Nonspecific antibody binding was blocked by preincubation of membranes in 1x TBS-T solution (Tris-buffered saline-tween, 0.61% Tris base, 0.8% NaCl, and 500 µl Tween 20 per litter, pH 7.0) containing 5% skim milk for 1 h at room temperature. After blocking, membranes were then incubated overnight at 4°C with primary antibodies for rabbit anti-L-FABP at 1:500 and for mouse anti-β-actin at 1:1000 in 1x TBS-T solution containing 5% or 2% of skim milk, respectively. After being washed with TBS-T to remove unbound primary antibody, membranes were incubated with donkey anti-rabbit IgG for L-FABP at 1:1000 dilutions and anti-mouse antibody for β-actin at 1:1000 for 1 h at room temperature. The protein-antibody complexes were visualized by employing the enhanced chemiluminescence kit (Amersham, Sydney, Australia). Optical densities of each target protein band were determined using the computer program ImageJ (National Institutes of Health).

6. Northern blot analysis

6.1 RNA sample preparation

For *in vivo* L-FABP mRNA stability studies, cells were cultured in 100 mm diameter dishes and treated with 500 µM of clofibrate for 4 days. At the end of the treatment period, actinomycin D (4 µM) was added and further incubated for 0 to 24 h. Previous work indicated that 4 µM actinomycin D concentration was able to inhibit 93% of RNA

synthesis (Robertson, Farnell et al. 2002). Total RNA was isolated using the TRIzol LS reagent and subjected to Northern blot analyses as described below.

6.2 Random primer DNA labelling

To target RNA sequences in northern blot hybridization, a "random primed" DNA sequence was used to produce radiolabelled L-FABP cDNA strands by a random primer kit (Prime-It II, Stratagene, USA) to a specific activity of approximately 1.0 X 10^9 cpm/µg. The method was originally introduced by Feinberg and Vogelstein (Feinberg and Vogelstein 1983), which is based on the hybridization of oligonucleotides of all possible sequences to the denatured DNA template to be labelled. The reaction mixture contains 35 µl of random oligonucleotides (1 ml TE buffer stock, O.D A_{260}=50), 70 µl of labelling mixture (7 mM each of dATP, dGTP, dTTP, 18 M Tris/HC1 pH 8.0, 2 M $MgCl_2$, 18µl β-mercaptoethanol). The L-FABP DNA template (125 ng) was diluted to 12 µl with sterile double distilled water) and then added into a microcentrifuge tube, denatured by heating to 100°C for 10 minutes, and immediately placed on ice for 5 minutes. The denatured DNA was mixed with 4.5 µl of reaction mixture, 3 µl of 3,000 Ci/mmole [α-^{32}P]-dCTP, 0.5 µl of Klenow Polymerase I and incubated at room temperature for 1~3 hours. Using the random oligonucleotides as primers, the complementary DNA strand was synthesized by DNA polymerase I. To separate the labelled probe from free isotope, the labelling mixture was added on top of a Nick column (after washing with TE buffer) 480 µl of TE buffer added, and buffer subsequently collected into a microcentrifuge tube. Once the TE buffer was eluted, the nick column on top of the microcentrifuge tube was changed. The TE buffer (500 µl) was added again and recollected in a new microcentrifuge tube which contained

the labelled probe. The DNA probe was counted on a Geiger counter (Measurements, Inc. Texas, USA). The labelled probe was heated to 100°C for 5 minutes and then allowed to cool on ice-water. After a brief centrifugation (7500 rpm, 2 seconds), the labelled probe was added directly to the bottom of a hybridization tube.

6.3 Northern blot

Total RNA (20 µg/sample) was mixed with 17 µl RNA loading buffer (16.88% formaldehyde, 50.63% formamide, 10.13% 10 x MOPS, 21.94% DNA loading buffer, 0.04% 10mg/ml EtBr (ethidum bromide)) in eppendorf centrifuge tubes and incubated at 55°C to 65°C for 20 minutes in a water bath. Total RNA was loaded on a 1% agarose gel containing formaldehyde (0.05%) and separated by gel electrophoresis using 1 x MOPS as the running buffer. After electrophoresis, the gel was transferred to GT-zeta nylon membranes (Bio-Rad, Burlington, Canada) using 10 x SSC solution (1 x SSC = 150 mM NaCl, 15 mM sodium citrate, pH 7.0). The RNA was crosslinked to the membrane using an ultraviolet oven (Bio-Rad, Burlington, Canada) set at 80°C for 2 minutes.

Membranes were then prehybridized at 42°C for 3 hours with hybridization buffer (50% formamide, 0.12 M Na_2HPO_4, pH 7.2, 0.25 M NaCl, 7% w/v SDS, 4% ddH_2O). The labelled DNA probe (as described above) was then placed into a hybridization tube with the membrane followed by hybridization with ^{32}P labelled rat L-FABP cDNA at 42°C overnight. Following hybridization, membranes were washed twice in 2 x SSC containing 0.1% SDS at room temperature for 15 minutes each and once in 0.1 x SSC containing 0.1% SDS at 65 °C for 15 minutes. Membranes were then exposed to X-ray film. Signal intensities were measured by densitometry using the program ImageJ (National Institutes

of Health). Relative expression of L-FABP mRNA was calculated by dividing the densities of L-FABP mRNA by the loading control (28S RNA).

7. Nuclear run-off assay

7.1 Nuclear isolation

Cellular nuclei were isolated as described by Fivaz et al. (Fivaz, Chiarra Bassi et al. 2000). Following 4-days of clofibrate, PPARα, or PPARγ treatment, CRL-1548 cells were harvested, homogenized, and nuclei collected after a brief spin at 500 *g* for 5 min at 4^{o}C. The isolated nuclei were resuspended in 3 ml of lysis buffer (10 mM KCl, 10 mM Tris-HCl (pH7.5), 2 mM $MgCl_2$, 15 µl of 1M DTT) followed by the addition of 30 µl 10% NP-40 to a final concentration of 0.1% (v/v). The nuclei were then centrifuged and resuspended in 200 µl of 50 mM Tris (pH 8.0), 5 mM $MgCl_2$, 0.1 mM EDTA and 0.25 M sucrose per 5 $\times 10^7$ nuclei, and stored in liquid nitrogen until required.

7.2 Preparation of ^{32}P-labeled nuclear RNA

Transcription reactions were initiated by adding an equal volume of 25 mM Tris (pH 8.0), 12.5 mM $MgCl_2$, 0.3 M KCl, 1.25 mM ATP, 1.25 mM GTP, 1.25 mM UTP, and 2.5 mM DTT, 200 U/ml RNase inhibitor to 220 µl nuclei suspension with 12 µl [α-^{32}P]dCTP (3000 Ci/mmol). Reactions were stopped by adding 10 µl RQ1-DNase 1 (Promega, Ottawa, Canada) and incubated at 30°C for 10 min. DNase I treatment was able to eliminate unwanted DNA sequences and was stopped by adding 18 µl 10% (w/v) SDS in 0.5 M Tris, pH 7.4, 1.5 µl 0.5M EDTA, and 1.5 µl of 10 mg/ml proteinase K. After 5 min incubation at 37^{o}C, 3 µl yeast tRNA (10mg/ml) and 400 µl of denaturing solution (4 M

guanidinium thiocyanate, 25 mM sodium citrate, 0.005% (w/v) N-lauryl sarcosine and 0.007% β-mercaptoethanol) were added to the reaction mixture. The elongated ^{32}P-labeled nascent nuclear RNAs were extracted and stored at -70°C for 2 h to precipitate. The RNA pellet was dissolved in 1 ml of 10 mM Ntris (hydroxymethyl) methyl-2-aminoethanesulfonic acid (Mates, Perez-Gomez et al.), pH 7.4, 0.2% SDS and 10 mM EDTA at a concentration of 1×10^7 cpm/ml.

7.3 Immobilization of cDNA on nitrocellulose membranes

cDNAs designed for L-FABP and GAPDH were immobilized onto a nitrocellulose blotting membrane (GE healthcare, Baie d'Urfe, Quebec) using a UV Crosslinker (UVP, Upland, USA). The targeted L-FABP cDNA and loading controls (cDNAs of GAPDH) were obtained by RT-PCR with TRIzol, for rat L-FABP, using a forward primer 5'- GCC ACC ATG AAC TTC TCC G-3', and reverse primer 5'- AGT CAC GGA CTT TAT GCC TTT-3', which yielded a 318-bp product; for rat GAPDH, using a forward primer 5'-AGA CAA GAT GGT GAA GGT CGG-3' and reverse primer 5'-GGG TGC AGC GAA CTT TAT TG-3', providing a 918-bp product. cDNA fragments were denatured by incubation at 37°C for 15 min in 0.2 M NaOH and then neutralized by 6×SSC (0.9 M NaCl, 0.09 Na_3citrate·$2H_2O$, pH 7.0). Immobilization of the DNA sample was achieved by blotting 10 μg denatured DNA/slot on nitrocellulose membrane at 55 mbar vacuum pressure using a slot-blot apparatus (Minifold II, Schleicher & Schuell, Germany). After blotting was completed the DNA was UV-linked (Bio-Rad laboratories, Hercules, USA) to the membrane for 2 min.

7.4 Hybridization of labelled transcript with immobilized cDNA and detection

The blot containing immobilized DNA was prehybridized for 2 h in formamide prehybridization buffer (5×SSC, 5 × Denhardt's solutions, 50% (v/v) formamide, 100 µg/ml denatured salmon sperm DNA and 0.5% (w/v) SDS) at 65°C. After prehybridization the blot was hybridized with 1 ml RNA TES solution and 1 ml TES/NaCl solution in hybridization buffer at 65 °C for 36 h. After hybridization, the blot was washed, wrapped in a plastic sheet, and exposed to X-ray film at −70 °C for 4 days.

8. siRNA Transfection

Small interfering RNA (siRNA) is a class of double-stranded RNA molecules consisting of approximately 20-25 nucleotides (usually 21nt) that interfere with the expression of a specific gene. The process begins with dsRNA (double stranded RNA) being broken down with Dicer (an enzyme that converts either long dsRNAs or small hairpin RNAs into siRNAs) into small fragments approximately 21nt in length. Each siRNA fragment has 2 nucleotide overhangs on their 3' ends to help incorporate siRNA into RISC (RNA-induced silencing complex). This RISC then binds to and cleaves mRNA, knocking out the corresponding gene.

L-FABP siRNA was used to examine the effects of knocking down L-FABP gene expression. Shortly before transfection 8 x 10^4 CRL-1548 cells were seeded per well of a 24-well plate in 500 µl of a DF-10 culture medium containing serum and antibiotics. RNA sense sequence of rat L-FABP siRNA was 5′-r (GAU GGA GGG UGA CAA UAA A) dTdT-3′. RNA antisense sequence of rat L-FABP siRNA was 5′-r (UUU AUU GUC ACC CUC CAU C) dTdT-3′. Negative or non-silencing control siRNA had no significant

sequence homology to any known rat gene. These siRNAs were resuspended and annealed according to the manufacturer's instructions to a stock concentration of 20 μM. Subsequently, 100 μl of 5 nM siRNA and 3 μl of HiPerFect reagent were mixed and incubated at room temperature for 5 min. The transfection mixture containing either L-FABP siRNA or negative control siRNA was then added drop wise to cells cultured on 24-well plates on days 1 and 3. Cells were incubated at 37°C for 96 h and treated daily with 500 μM clofibrate. Cell extracts were then prepared for L-FABP Western blot analysis.

9. Measurement of antioxidant activity in vivo

Fluorescein probes have been widely employed to monitor oxidative activity in cells (Tsuchiya, Suematsu et al. 1994). 2'-7'-Dichlorofluorescein (DCFH) was employed as a marker for measuring free radical levels in cells. The oxidation of DCFH is thought to occur as a result of the reaction of H_2O_2 with peroxidase, cytochrome *c*, etc (LeBel, Ischiropoulos et al. 1992). When the diacetate form of DCFH is added to cells, it diffuses across the cell membrane and is hydrolyzed by intracellular esterase to liberate DCFH which, upon reaction with oxidizing species, is converted to the highly fluorescent compound 2'-7'-dichlorofluorescein (DCF). The fluorescence intensity can be easily measured and is the basis of the popular cellular assay for oxidative stress.

Cells were grown in black plastic 96-well plates with DF-10 culture medium for determination of oxidant production as previously described (Rajaraman, Wang et al. 2007). Briefly, cells were washed twice with Ca^{++}/Mg^{++}-PBS and incubated with 100 μM 2, 7-dichlorofluorescein diacetate ($DCFH_2$-DA) at room temperature in the dark for 30 min. After washing the cells with PBS, oxidative stress was induced by treating the

$DCFH_2$-DA loaded cells with 200 μM hydrogen peroxide (H_2O_2) for 20 min followed by washing cells with Ca^{++}/Mg^{++}-containing PBS. Fluorescence intensity of DCF was determined using a BMG (Durham, NC, USA) Fluostar Galaxy fluorescence plate reader at a wavelength of 485 nm for excitation and 520 nm for emission excitation and emission probes were directed to the bottom of the plate. Mean fluorescence intensity was calculated from triplicate wells of control and drug-treated cells from six separate experiments.

10. Measurement of antioxidant enzyme

Total cytosolic activity of intracellular antioxidant enzymes (superoxide dismutase, glutathione peroxidase, catalase) was measured in cell lysate protein using their respective biochemical spectrophotometric assays as described in the manufacturer's manual (Sigma, Oakville, Canada).

10.1 Superoxide dismutase (SOD)

Activity of SOD in the cytosol was measured by "SOD Assay Kit-WST". This kit allows for very convenient SOD assaying by utilizing Dojindo's highly water-soluble tetrazolium salt, WST-1 (2-(4-Iodophenyl)-3-(4-nitrophenyl)-5-(2, 4-disulfophenyl) - 2H-tetrazolium, monosodium salt) that produces a water-soluble formazan dye upon reduction with a superoxide anion. The rate of O_2 reduction is linearly related to the xanthine oxidase (XO) activity which is inhibited by SOD. Therefore, the IC50 (50% inhibition activity of SOD or SOD-like materials) can be determined by a colorimetric method. The absorption spectrum of WST-1 formazan at 440 nm is proportional to the amount of superoxide anion, the SOD activity as an inhibition activity can be quantified by measuring the decrease in color development at 440nm.

Table 7 shows the amount of solution used in each well of the 96-well plate. SOD standard solution was prepared by diluting SOD with dilution buffer. Sample solution (20 µl) was added to each sample and blank 2, 20 µl of ddH_2O (double distilled water) was added to each blank 1 and blank 3. WST Working Solution (200 µl; provided by the kit) was added to each well and mixed. Dilution Buffer (provided by the kit) was added to each blank 2 and blank 3, and finally the Enzyme Working Solution (20 µl) was added to each sample and blank 1 well, and thoroughly mixed. The plate was incubated at 37 °C for 20 minutes and absorbance read at 450 nm using a microplate reader. The SOD activity was calculated using the following equation:

SOD activity (inhibition rate %) = $\{[(A_{blank\ 1} - A_{blank\ 3}) - A_{sample} - A_{blank\ 2})]/ (A_{blank\ 1} - A_{blank\ 3})\} \times 100$

Table 7: Volumes of each solution for sample, blank 1, 2 and 3

	Sample	**Blank 1**	**Blank 2**	**Blank 3**
Sample solution	20 µl		20 µl	
ddH_2O		20 µl		20 µl
WST working solution	200 µl	200 µl	200 µl	200 µl
Enzyme working solution	20 µl	20 µl		
Dilution buffer			20 µl	20 µl

10.2 Glutathione peroxidase (GPx)

The GPx kit used is based on the oxidation of glutathione (GSH) to oxidized glutathione (GSSG) catalyzed by GPx, which is then coupled to the recycling of GSSG back to GSH utilizing glutathione reductase (GR) and NADPH (β-Nicotinamide Adenine Dinucleotide Phosphate, Reduced). The decrease in NADPH absorbance measured at 340 nm during the oxidation of NADPH to $NADP^+$ is indicative of GPx activity.

The volume of "Glutathione Peroxidase Assay Buffer" is indicated in Table 8. The assay was conducted in a 1 ml quartz cuvette and measured in the spectrophotometer at 25 °C by using a thermostated cell holder. NADPH Assay Reagent (50 µl) and 10~50 µl of sample or 20~50 µl of enzyme were added into the cuvette and mixed by inversion. The total volume in the cuvette was 1 ml. Glutathione peroxidase dilutions were used as standards. The reaction was started by the addition of 10 µl of the 30 mM *tert*-Butyl Hydroperoxide Solution and mixed by inversion followed by measuring the absorbance at 340 nm using a kinetic program (initial delay: 15 seconds; interval: 10 seconds; number of readings: 6).

Table 8: Volume of glutathione peroxidase reaction scheme

	GPx assay buffer (µl)	**NADPH assay reagent (µl)**	**Enzyme (0.25 units/ml) (µl)**	**Sample (µl)**	**30mM t-Bu-OOH (µl)**
Blank	940	50		−	10
Positive control	890-920	50	20-50	−	10
Sample	890-930	50	—	10-50	10

The activity of Glutathione Peroxidase in the sample can be calculated using the formula:

Activity per extract (mmol/min/ml = Units/ml)

$$\frac{A_{340} \text{ x } DF}{6.22 \text{ x } V}$$

$A_{340} = A_{340}/\text{min}_{(Blank)} - A_{340}/\text{min}_{(sample)}$; $6.22 = \varepsilon^{mM}$ for NADPH; DF = dilution factor of sample before adding to reaction; V = sample volume in ml

Unit definition: 1 unit of glutathione peroxidase will cause the formation of 1 mM of $NADP^+$ from NADPH per minute at pH 8.0 at 25 °C in a coupled reaction in the presence of reduced glutathione, glutathione reductase, and *tert*-butyl hydroperoxide.

10.3 Catalase

Analysis of catalase activity was based on the effect that catalase catalyzes the decomposition of hydrogen peroxide (H_2O_2) to water and oxygen. A series of standard solutions of H_2O_2 were prepared fresh each day. Dilutions for preparation of the H_2O_2 standard curve are shown in Table 9. An aliquot of each solution (10 µl) was transfered to a second tube and 1 ml of the Color Reagent was added and absorbance read at 520 nm after 15 minutes incubation.

Catalase activity in samples was determined as follows: samples were added to microcentrifuge tubes at the appropriate volume (x µl; see Table 10). Then (75–x) µl of 1X Assay Buffer (50 mM potassium phosphate buffer, pH 7.0) was added to the microcentrifuge tubes. The reaction was started by adding 25 µl of the "Colorimetric Assay Substrate Solution (200 mM H_2O_2), mixed by inversion, and incubated for 1~5 minutes. The tube was inverted after adding 900 µl of the "Stop Solution (15 mM sodium azide in water)". An aliquot of the catalase enzymatic reaction (10 µl) was removed to another microcentrifuge tube. Color Reagent (1 ml; 150 mM potassium phosphate buffer, pH 7.0, containing 0.25 mM 4-aminoantipyrine and 2 mM 3, 5-dichloro-2-hydroxybenzenesulfonic acid) was added and mixed by inversion. The mixture was incubated for 15 minutes at room temperature for color development and absorbance measured at 520 nm.

Table 9: Dilitions for Preparation of the Hydrogen Peroxide Standard Curve

Volume of 10 mM H_2O_2	1 x Assay Buffer	H_2O_2 in Standard solution (µM)	H_2O_2 in Reaction Mixture (µM)
0 µl	1000 µl	0	0
125 µl	875 µl	1.25	0.0125
250 µl	750 µl	2.5	0.025
500 µl	500 µl	5.0	0.05
750 µl	250 µl	7.5	0.075

Table 10: Catalase Colorimetric Enzymatic Reaction Scheme

	Sample Volume	1 x Assay Buffer	200 mM H2O2 Solution
Blank	20 µl	75 µl	25 µl
Sample	x µl	75-x µl	25 µl

The activity of catalase in the sample can be determined using the formula:

Activity = Δµmoles (H_2O_2) x d x 100 (µmoles/min/ml) V x t

A520 (Blank) = µmoles of H_2O_2 in Blank;

A520 (Sample) = µmoles of H_2O_2 in Sample, (OD520 of 1.4 is equivalent to 0.082 µmole of H2O2);

Δµmoles (H_2O_2) = µmoles of H_2O_2 (Blank) – µmoles of H_2O_2 (Sample)

d = dilution of original sample for Catalase Reaction

t = Catalase Reaction duration (minutes)

V = sample volume in Catalase Reaction (x μl = 0.00x ml)

100 = dilution of aliquot from Catalase Reaction in

Unit definition: One unit of catalase will decompose 1.0 micromole of hydrogen peroxide to oxygen and water per minute at pH 7.0 at 25 °C at a substrate concentration of 50 mM hydrogen peroxide.

11. Recombinant L-FABP protein construction

11.1 Rat L-FABP cloning

Total RNA was isolated from rat liver and the first strand cDNA of rat L-FABP was generated by reverse transcriptase using Advantage RT (reverse transcription)-for-PCR (polymerase chain reaction) kit (CLONTECH, Palo Aito, USA). The gene-specific PCR primer for rat L-FABP was designed with an Oligo 5.1 program (National Biosciences Inc., Plymouth, USA) from the DNA sequence obtained from GenBank (BC086947). Full length L-FABP cDNA fragment was then amplified from the first strand cDNA template by PCR reactions with Tag DNA polymerase (Qiagen, Mississauga, Canada) using the L-FABP-specificity primers 5'-CTATTG CCA TGA GTT-3' (sense) and 5'-AAT AAT ATG AAA TGC AGA CTT G-3' (antisense). The forward primer contains a BamH1 site and the reverse primer contains an Xho1 site.

PCR amplification reactions involved initial denaturation at 94°C for 3 minutes, followed by 35 cycles of denaturation at 95°C for 45 seconds, annealing at 58°C for 45 seconds, extension at 72°C for 90 seconds, and then followed by 10 minutes of final extension at 72°C. PCR products (418 bp) were analyzed by electrophoresis on 1.2%

agarose gel. Identity of PCR products was confirmed by sequencing PCR products at the DNA-sequencing facility of the Manitoba Institute of Cell Biology (Winnipeg, Canada). The PCR product (418 bp) containing the full length L-FABP cDNA was subcloned into pGEX-6P-2 expression vector (Invitrogen) as described below.

11.2 Transformation of expression plasmid pGEX-6P-2 with competent E.coli

Recombinant L-FABP encoding full length of rat L-FABP sequence was constructed using the pGEX-6P-2 vector of glutathione S-transferase (GST) fusion mammalian expression system (Amersham, Oakville, Canada). Structure of pGEX-6P-2 plasmid is shown in Figure 14. The vector pGEX-6P-2 contains multiple cloning sites with PreScission Protease sequence for separation of fusion protein and restriction enzymes sites such as BamH1 and Xho1 that allows for recombinant cloning. The vector also possesses a glutathione S-transferase fusion tag for easy purification and a Lac Iq sequence for induction of fusion protein expression by the lactose analog isopropyl b-D thiogalactoside (IPTG). In addition, there is an antibiotic resistant gene (ampicillin) for the selection of bacteria between pGEX-6P-2 transformed and non-transformed. The plasmid vector pGEX-6P-2 was transformed with competent *E.coli*. After amplification, the plasmid was digested with BamHI and XhoI restriction endonucleases and purified by the GFX PCR DNA and Gel Band Purification Kit (GE Health Care, Chicago, USA). Detailed methods are described below.

Transformation was carried out by mixing 100 ng of plasmid DNA to 100 µl of DH5α competent cells (Invitrogen, Burlington, Canada) solution and incubated on ice for 30 minutes. This mixture was subjected to heat shock by immersion in a 42°C water bath

(Fisher Scientific, Ottawa, Canada) for 45 seconds without shaking and then put on ice for another 2 minutes. Pre-warmed 250 µl of LB (Luria-Bertani) medium (1% tryptome, 0.5% yeast extract, 1% NaCl, pH 7.0) was added to the mixture and incubated in a 37°C shaking incubator (New Brunswick Scientific, Edison, USA) for 1 hour. This transformation was spread on a pre-warmed LB-agar (15 g agar/l LB) plate containing 100 µg/ml of ampicillin and the plate incubated in a 37°C incubator (Precision Scientific Inc., Chicago, USA) overnight for selection the positive clones.

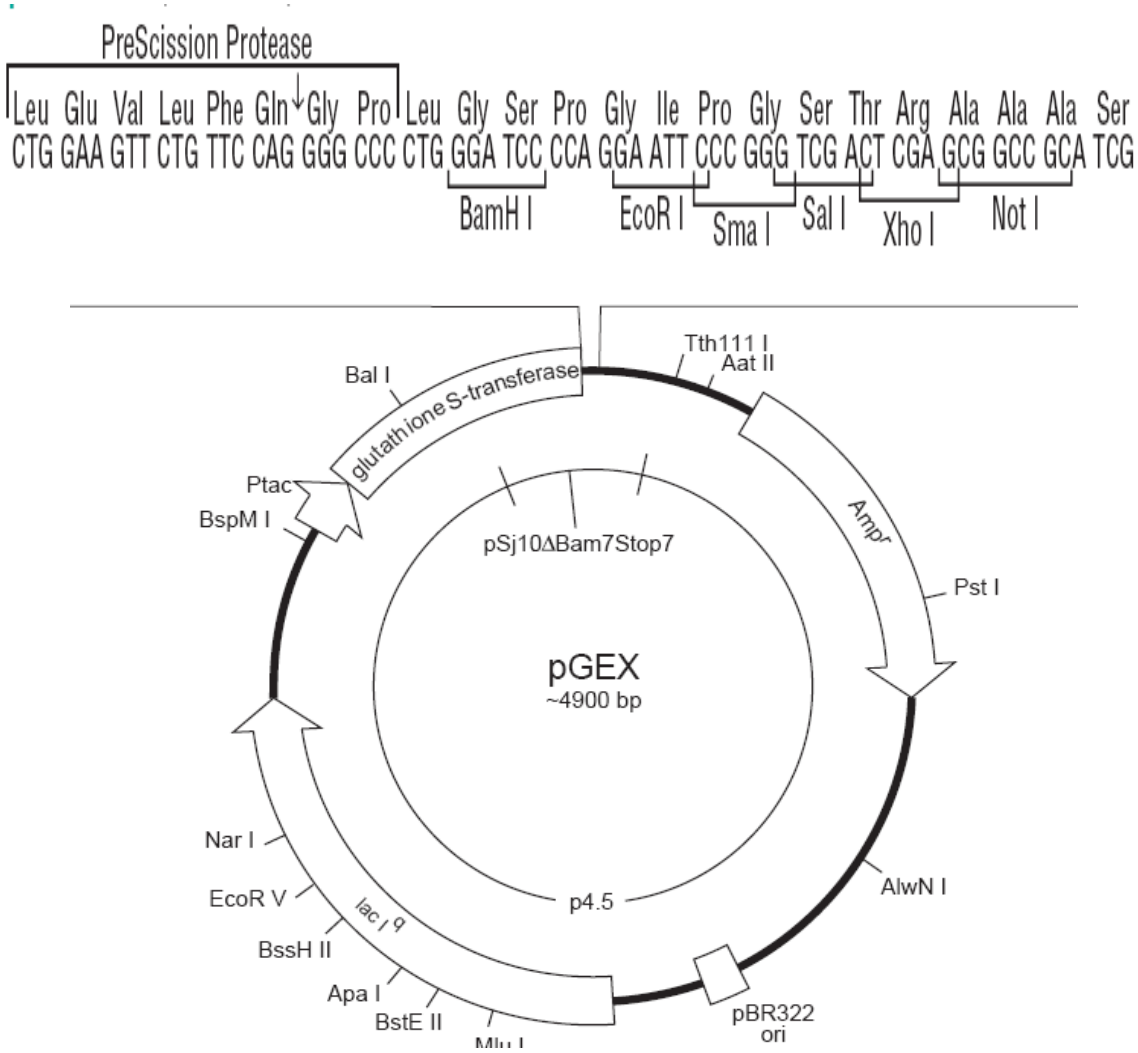

Figure 14: Map of expression vector pGEX-6P-2.

http://www4.gelifesciences.com/Aptrix/upp01077.nsf/Content/ProductsOpenDocument&parentid=976038&moduleid=38859&zone=Proteomics

11.3 Plasmid DNA isolation

Plasmid DNA isolation was performed using the alkaline (NaOH) lysis method to separate the plasmid DNA from the chromosomal DNA, polysaccharides, lipid and proteins by high salt solution (NH_4OAC) and detergent (SDS). The selected transformed colonies were put into a 12 ml culture tube containing 5 ml of LB with 100 µg/ml of ampicillin and incubated at 37°C incubator with vigorous shaking at 300 rpm overnight. Bacteria were pelleted at 1350 *g* at 4°C for 20 min. Bacterial pellets were resuspended in 100 µl suspension solution (50 mM glucose, 25 mM Tris-HCl, pH 8.0, and 10 mM EDTA pH 8.0) by pipetting up and down. An alkaline solution (200 µl of 0.2 N NaOH and 1% SDS) was freshly prepared and added into the bacterial suspension. The solution was mixed by gently inverting the tube five times and followed by incubation on ice for 5 minutes. Sodium acetate (NaOAc; 3.0 M; pH 5.0; 150 µl) was then added and the reaction tube was gently inverted 5 times to mix the solution, followed by incubation on ice for 5 min to precipitate the protein and chromosome DNA. Plasmid DNA was separated by centrifuged at 10,000 *g* at 4 °C for 5 min. The supernatant (400 µl) containing plasmid was transferred to a new eppendorf tube and an equal amount of phenol/chloroform/isoamylalcohol (25:24:1) was added to extract the DNA. The solution was mixed by inverting the tubes for 2 minutes and centrifuged at 10,000 g for 5 minutes. The supernatant was transferred to another eppendorf tube and the DNA precipitation was pelleted with two volume of 100% ethanol and incubated at -70°C for 2 hours. After centrifugation at 10,000 g at 4°C for 10 minutes, the DNA pellet was washed with 1ml 70% ethanol twice and air dried 15 minutes. The pellet was resuspended in 20 µl TE buffer (10 mM Tris, 1 mM EDTA, pH 8.0) containing 0.2 µl of 100 µg/ml DNase-free RNase

(Roche, Mississauga, ON). Concentration of plasmid DNA was determined using a spectrophotometer (Bio-Rad Smart Spec 3000 Spectrophotometer, Life Science Research Division, Mississauga, Canada). Good quality DNA had an A260/280 ratio of 1.65 to 1.85.

11.4 Restriction Enzyme Digestion

Restriction enzymes, also referred to as restriction endonucleases, are enzymes which recognize short, specific (often palindromic) DNA sequences. They cleave double-stranded DNA (dsDNA) at specific sites within or adjacent to their recognition sequences. Each restriction enzyme has specific requirements to achieve optimal activity. Purified plasmid DNA was digested with BamH1 and Xho1 restriction endonucleases (Roche, Mississauga, Canada). A proportional restriction enzyme digestion was performed in a final volume of 20 µl. Table 11 shows the volumes used in the digestion reaction.

Table 11: Volumes used in the restriction enzyme digestion reaction

Components	**Volumes (µl)**
DNA (1µg/µl)	1
Acetylated BSA (10µg/µl)	0.2
Restriction Enzyme 10 x Buffer	2
Sterile, deionized water	16.3
Restriction Enzyme (10u/µl)	0.5
Total volume	20

The solution consisted of 0.2-1.5μg of substrate DNA, restriction enzyme 10 x buffer and sterile distilled water, mixed by pipetting, then added restriction endonuclease (two to tenfold excess of enzyme over DNA). Addition of acetylated BSA to a final concentration of 0.1 mg/ml can sometimes improve the quality and efficiency of enzyme assays containing impure DNA. The digest was mixed gently by pipetting, centrifuged for a few seconds in a microcentrifuge, and then incubated at 37°C for 1~4 hours. Digestion products were analyzed by running an agarose gel. It should be noted that overnight digests are usually unnecessary and may result in degradation of the DNA.

11.5 Agarose gel electrophoresis

Agarose gel electrophoresis is the easiest and most common way of separating and analyzing DNA. The DNA fragments including plasmid DNA and subcloned DNA that were digested with restriction enzymes were analyzed by agarose electrophoresis. Agarose powder was mixed with electrophoresis 1X TAE buffer (2.0 M Tris-base, 1 M glacial acetic acid, 50 mM EDTA-Na_2, adjust to pH 7.2 with acetic acid) in a 250 ml conical flask to a desired concentration of 0.7-2%. A 0.7% gel will show good separation (resolution) of large DNA fragments (5–10 kb) and a 2% gel will show good resolution for small fragments (0.2–1 kb). The mixed solution was dissolved with the use of a microwave oven for approximately 1 minute and then 3 μl of ethidium bromide (EtBr) (10 mg/ml) was added and swirled to mix. The gel solution was slowly poured into a tank (Midi-horizontal electrophoresis unit, Bio-Rad, Hercules, USA) containing a sample comb. Bubbles were pushed to the side using a disposable Eppendorf tip. After the gel formed a solid at room temperature, the comb was removed, and gel submerged to 2–5 mm depth with 1X TAE

buffer. A DNA marker was mixed with the loading buffer (0.25% bromophenol blue, 0.25% xylene cyanol and 25% ficoll) and loaded in the first well, DNA samples with loading buffer were subsequently loaded into the sample wells. DNA fragments were separated at an appropriate voltage value (usually 100 V) for 15~30 minutes and the gel checked on an ultraviolet transilluminator (312 nm Transilluminator, Fisher Scientific, Pittsburgh, USA) for band separation. Optical densities of each target protein band were determined using the computer program ImageJ (National Institutes of Health).

11.6 DNA extraction from agarose gels

DNA subfragments were purified from agarose gels before subcloning. DNA on the agarose gel was cut out carefully using a scalpel blade on a UV light transilluminator. Gel slices containing the DNA fragment were purified using the illustra™ GFX™ PCR DNA and Gel Band Purification Kit which was designed for the rapid purification and concentration of PCR products or DNA fragments ranging in size from 50 bp to 10 kb. Gel band slice extractions were performed by incubating with 300 µl capture buffer at 65 °C for 10 minutes until melted completely. The solution was applied on a GXF spin-column for 2 minutes at room temperature and the column washed with 500 µl ethanol wash buffer. Flow-through was discarded after centrifugation at 15,000 rpm for 30 seconds. DNA was eluted from the column with the proper amount of 10mM Tris-Cl (pH 8.0) by centrifuging at 15,000 rpm for 1 minute. From 60 to 95% of DNA fragments were recovered from the agarose gel and as high as 99.5% of contaminants were removed. DNA concentration was assayed by Bio-Rad Spectrophotometer.

11.7 Construction of recombination plasmid L-FABP/ pGEX-6P-2

After restriction enzyme digestion and gel band purification, the full length L-FABP cDNA (insert) was subcloned into plasmid pGEX-6P-2 (vector) by ligation using T4 DNA ligase (Promega). About 1:1, 1:3 or 3:1 molar ratios of vector to insert DNA are normally used when cloning a fragment into a plasmid vector. The desired vector: insert ratio in this thesis was 1:3. The amount of purified DNA fragments used for ligation was calculated by the equation:

$$\text{ng of insert} = \frac{\text{ng of vector} \times \text{kb size of insert}}{\text{kb size of vector}} \times \text{molar ratio of } \frac{\text{insert}}{\text{vector}}$$

Typical ligation reactions contained 100~200 ng of digested vector to be subcloned, proper amount of purified insert DNA fragment, 10 x T4 ligase buffer, 0.1-1 units of T4 DNA ligase, and sterile distilled water in a total volume of 20 µl. Components for vector pGEX-6P-2 and insert L-FABP cDNA ligation reaction are list in Table 12. The reaction was allowed to proceed overnight at room temperature, where T4 DNA Ligase catalyzes the joining of two strands of DNA between the 5´-phosphate and the 3´-hydroxyl groups of adjacent nucleotides in the cohesive-ended configuration. The reaction solution (5~10 µl) was then used to transform 100 µl of *E.coli* DH5α competent cells as described above. The ligation DNA was cultured in 5 ml LB broth containing 100 µg/ml ampicillin and isolated following the plasmid DNA isolation method as described above. Successful ligation was confirmed by restriction enzyme digestion with BamH1 and XhoI and analyzed by agarose gel electrophoresis.

Table 12: Components for L-FABP DNA ligation reaction

Components	**Volumes**
pGEX-6P-2	200 ng
L-FABP DNA	60 ng
Ligase 10 x reaction buffer	1 µl
T4DNA ligase (u)	1 u
DNAnase/RNase Free Water	5~15 µl
Total volume	20 µl

The subcloned L-FABP cDNA sequence was confirmed by DNA sequencing (University Core DNA & Protein Services, University of Calgary, Canada) with pGEX-5' and pGEX-3' sequence. The sequence of pGEX-5' is GGG CTG GCA AGC CAC GTT TGG TG-3' and the pGEX-3' sequence 5'-CCG GGA GCT GCA TGT GTC AGA GG-3' (GE healthcare). The produced plasmid was referred as pGEX-6P-2/L-FABP.

11.8 Recombinant L-FABP protein expression

The transformation of the plasmid pGEX-6P-2/L-FABP was carried out with the *E. coli* DH5α strain to scale up the preparation of recombinant L-FABP protein expression. A single colony of bacteria from a fresh plate was selected and cultured in 5 ml LB broth containing 20 mM glucose and 100 μg/ml ampicillin. Following an overnight growth at 37°C with shaking (300 rpm), then was used to inoculate 500 ml flasks containing LB broth (with antibiotic, 1:100 dilution) and grown at 37°C with mild shaking (300 rpm) until an OD_{600}=1.0 was achieved (approximately 8-9 hr). Conditions at OD_{600}=0.6 or 0.8 were also checked but OD_{600}=1.0 was optimal for protein expression.

Expression of the L-FABP protein was induced by adding isopropyl-β-D-thio-galactoside (IPTG) (Alfa Aesar, Ward Hill, USA) to a final concentration of 0.1 mM. The plasmid pGEX-6P-2 containing recombinant L-FABP gene which is controlled by the tac promoter was amplified following induction with IPTG. The effect of IPTG was a strong induction and amplification of the recombinant pGEX-6P-2 gene. The inducing concentration of IPTG tested included 0.1-1.0 mM with 0.1mM IPTG found to be optimal for inducing the recombinant L-FABP expression. Following 6 hours of incubation at 37°C with shaking (300 rpm), cells were harvested by centrifugation (3500 g for 20 min), the pellet washed with PBS, and resuspended in lysis buffer (PBS + 1% Triton X-100, 2 μg/ml aprotinin, 1 μg/ml leupeptin, and 25 μg/ml phenylmethylsulfonyl fluoride [PMSF]). The resuspended cell suspension (40 ml) was sonicated to disrupt the cellular architecture using an UltrasonicsTM A180 sonicator (180 W maximum power output; Melbourne, Australia) with a 10 mm ultrasonic probe three times for 10 seconds per time on ice. The soluble protein fraction was recovered from the supernatant following centrifugation at 3,500 *g* for 15 min at 4~8°C. Protein fragments were analyzed by SDS-PAGE and Western blot.

11.9 Recombinant L-FABP protein purification

Protein extract was brought to 50% slurry with a glutathione-Sepharose 4B (Amersham, Oakville, Canada) solution. The final concentration of glutathione-Sepharose 4B in the solution was approximately 10-20%. The solution was incubated at room temperature for 30 min, rotating the tube end over end to ensure thorough mixing. The glutathione-Sepharose 4B bead-treated extract was centrifuged at 500 g for 5 min at 4~8°C. The pellet was washed with 1 ml ice-cold PBS (supplemented with protease inhibitors) three times followed by a final centrifugation (500 g for 5 min at 4°C) to pellet the beads. The pellet was collected and eluted by adding 50% (4°C) 20 mM reduced glutathione in 50 mM Tris-HCl (pH 8.0) for 10 min at room temperature then centrifuged at 500 *g* for 5 min at 4°C to isolate the supernatant which contained the recombinant L-FABP with GST tag. The elution step was repeated three times and the supernatant fractions collected in microcentrifuge tubes. Samples were analyzed by SDS-PAGE.

To separate the L-FABP protein from the GST/L-FABP complex, the supernatant (from above) was treated with 50% glutathione-Sepharose 4B beads and incubated for 30 minutes at room temperature, rotating the tube end over end to ensure thorough mixing. The GST/L-FABP fusion protein bound glutathione-Sepharose beads were washed with 1 ml Prescission Protease cleavage buffer (50 mM Tris–SO_4, pH 7.5, 1 mM EDTA, 1 mM DTT, and 0.01% Triton X-100) for 30 min at room temperature. To the 200 µl GST/L-FABP fusion protein bound glutathione-Sepharose beads, a mixture of 5 µl (10 units) of PreScission Protease and 495 µl of cleavage buffer was added and incubated at 4°C for 4 hours then centrifuged at 500 *g* for 5 min at 4°C to collect the supernatant. This

supernatant which contained the L-FABP protein was subsequently analyzed by SDS-PAGE and Western blot.

12. Measurement of antioxidant activity of recombinant L-FABP in vitro

We used 2', 7'-dichlorofluorescein-diacetate (DCFHDA) to assess the intracellular free radical levels released by H_2O_2. Fluorescence probes have been used *in vitro* and in cellular assays to provide a convenient and sensitive method to detect ROS. Thus, DCFH-DA was used to uncover the antioxidant capacity of our recombinant L-FABP in *in vitro* studies. The DCFH-DA was initially de-esterified to generate the oxidation substrate 2'7'-dichlorofluorescein (DCFH). The de-esterification reaction was performed by mixing 125 μl of a 1.5 mM DCFH-DA solution in EtOH with 0.5 ml of 0.01 N NaOH for 30 min at room temperature in the dark. The mixture was neutralized with 2.5 ml of 20 mM sodium phosphate buffer (pH 7.0) to give a final concentration of 60 μM of the activated DCFH dye stock solution. The de-esterified DCFH-DA could then be oxidized by free radicals to a highly fluorescent dichlorofluorescein (DCF) whose absorbance could be quantitated at 504 nm spectrophotometrically. Oxidation reactions were carried out in 96 well CoStar plates using 10–30 μM dye stock solution with 200 μM hydrogen peroxide (H_2O_2) (Pittsburgh, PA) and different concentrations of L-FABP.

13. Isolation of lipoproteins

Plasma fractions (density less than 1.21 g/ml) were separated from fresh human plasma by ultra-centrifugation (40000 rpm) in the presence of 1 mM EDTA. After dialysis, plasma lipoproteins were applied on a lysine-Sepharose 4B affinity chromatography

column. Unbound lipoproteins were used to prepare LDL (density 1.019–1.063) using ultracentrifugation. Lipoproteins were stored in sealed tubes filled with nitrogen and kept in the dark at 4°C to prevent oxidization during storage. Protein concentrations of LDL were measured by a BCA protein kit (Fisher Scientific Inc, Rockford, USA).

14. The induction of lipid peroxidation

Lipoprotein peroxidation was induced by two oxygen derived free radical generators: a hydrophilic radical generator 2, 2'-azobis (2-amidinopropane) dihydrochloride (AAPH), and a lipophilic radical generator 2, 2'-azobis (2, 4-dimethylvaleronitrile) (AMVN). AAPH was dissolved in deionized water whereas AMVN was dissolved in 95% ethanol. Both free radical generators were prepared fresh and incubated with LDL (1 mg cholesterol/ml) with or without different concentrations of antioxidants for 90 minutes at 37°C. The lipid peroxidation product (MDA) was determined by the thiobarbituric acid-reactive substance (TBARS) method (Buege and Aust 1978).

15. Triobarbituric acid reactive substances (TBARS) assay

Thiobarbituric acid reacting substances (TBARS) assay is the most commonly used colorimetric method for the detection of lipid peroxidation in biological systems. The TBARS test is easy to perform, inexpensive, and reliable (Valenzuela 1991). The TBARS assay is used to demonstrate reactive aldehydes from lipid peroxidation, which has been widely accepted as a general marker of free radical production. The most commonly measured TBARS is MDA. Figure 15 shows a schematic of the TBARS reaction. After incubation of the free radical generator with LDL (1 mg cholesterol/ml), with or without

different concentration of antioxidants for 90 minutes at 37°C, the reaction was terminated by addition of 1 ml thiobarbituric acid (TBA) reagent (0.67% TBA, 15% trichloroacetic acid, 0.25 N HCl). In the reaction mixture, the lipid peroxidation product MDA reacted with thiobarbituric acid under high temperature (100°C) and acidic conditions for 15 minutes resulting in the development of a pink chromogen. Samples were then centrifuged and cooled on ice. With the generation of free radicals, up to 98% of MDA that reacts with TBA is formed from the decomposition of lipid peroxides during the incubation stage of the assay and the products were measured at 535 nm absorbance in a spectrophotometer. Freshly diluted malondialdehyde bis (dimethyl acetal 1, 1, 3, 3-tetramethoxypropane) was used as a reference standard and the thiobarbituric acid reactive substances were expressed as MDA equivalents.

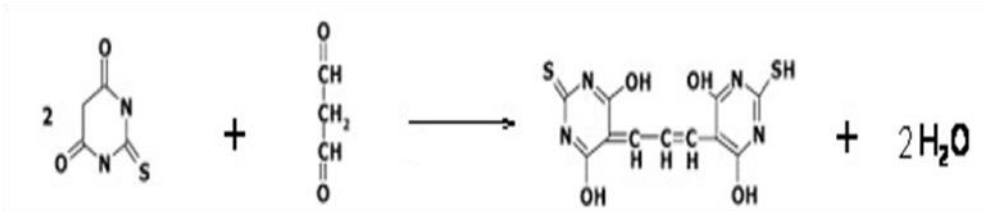

Thiobarbituric acid Malondialdehyde MDA-TBA adduct

Figure 15: Thiobarbituric acid reaction.

16. MALDI-QqTOF mass spectrometry

Matrix-assisted laser desorption/ ionization time-of-flight mass spectrometry (MALDI-TOF MS) has emerged as a powerful tool for identification and characterization of proteins (Egelhofer, Bussow et al. 2000). Protein mass analysis and peptide mapping was performed to detect the sequence of recombinant L-FABP and the oxidative modifications of recombinant L-FABP incubated with different free radical generators.

Samples were initially dialyzed to remove any salts present in samples. Tubes for dialysis were treated in an adequate amount of water for 10 minutes to remove glycerol. For heavy metal and sulfide removal, the tubing was incubated with $NaHCO_3$ for 1 min at 80°C, washed in water for 2 min at 60°C and 10 mM EDTA-NA for 1 min at room temperature, and finally washed in water for 5 min at room temperature. L-FABP solutions were placed into dialysis tubing; the tubing sealed at both ends using special clips, and dialyzed against distilled water. Dialyzed proteins were run on 15% SDS-PAGE gel to verify size and purification procedure after overnight dialysis.

She et al. (She, Wang et al. 2002) previously reported that two enzymatic digestions, one with typsin and the other with an endoprotease Glu-C, were sufficient to obtain the complete sequence information of FABP by mass spectrometry. L-FABP proteins (~5 µg) were, therefore, digested with 50 ng sequencing grade trypsin or endoprotease Glu-C (Roche Diagnostic Corp., Cambridge, Canada) in 25 mM ammonium bicarbonate, and the solution incubated at 37^{o}C for 6 hrs. Analyses of the proteolytic peptides were performed on Applied Biosystems / MDS Sciex QStar XL quadrupole time-of-flight (QqTOF) mass spectrometer by matrix assisted laser desorption ionization (MALDI) at positive ionization mode. The instrument was equipped with a MALDI II

source and a UV nitrogen laser operating at 337 nm. Samples were prepared at the ratio of 1:1 (v/v) of the peptide digest to matrix (*i.e.* 2, 5-dihydroxybenzoic acid, DHB) in 50% acetonitrile/water, and subsequently dried on a stainless steel MALDI plate at room temperature. After MALDI MS mapping, the individual peptide sequences were identified by MS/MS measurements using argon as the collision gas. The intact mass of L-FABP was determined by MALDI and also confirmed by nanospray ESI TOF mass spectrometry using the same instrument. In the case of ESI, the protein sample was dissolved in 50% methanol/0.1% formic acid solution.

Peptide fingerprinting masses were searched by MS-Fit program against the NCBI database using Protein Prospector at the UCSF web site (http://prospector.ucsf.edu), whereas the MS/MS ions search on each tandem mass spectrum was performed through the Mascot search engine (Matrix Science, http://www.matrixscience.com). These searches consider up to three missed enzyme cleavage sites and the modifications of methionine oxidation, asparagine and glutamine deamidation to aspartic acid and glutamic acid, N-terminal pyroglutamation. Mass tolerance between calculated and observed masses used for database search was considered at the range of ± 100 ppm for MS peaks and ± 0.2 Da for MS/MS fragment ions. If no result was retrieved by the automated database search then a manual data interpretation was conducted on the spectrum based on the L-FABP predicted sequence.

17. Purification of [^{3}H]-palmitate

Manufacturer supplied [^{3}H]-palmitate (PerkinElmer Life, Montreal, Canada) (56.5 Ci/mmol) with a radiochemical purity of 97.8% was further purified prior to use by

the ethanol extraction procedure as described previously by our lab (Elmadhoun, Wang et al. 1998). [^{3}H]-Palmitate (1.0 ml) supplied in ethanol was added to 0.98 ml of distilled water (18-MΩ/cm) containing 0.1 ml of NaOH (1N) and approximately 1 mg thymol blue. The solution was mixed with 1.2 ml of heptane and vortexed for 60 sec and allowed to separate into two phases. After separation, the heptane phase was discarded, fresh heptane added, and the procedure repeated twice. All of the heptane phase fractions were collected and the aqueous phase was acidified using two drops of HCl (6N) and the mixture vortexed for 60 sec. The purified [^{3}H]-palmitate in the heptane phase was harvested, fresh heptane added to the acidified aqueous phase, and the procedure was repeated. The heptane phases were combined from two times harvests. The heptane phase containing the purified palmitate was evaporated until approximately 10~20 µl heptane remained. At this time 1 ml of 100% ethanol was added. The purified [^{3}H]-palmitate was stored in ethanol at -20°C until used.

18. Determination of L-FABP binding affinity

The unbound [^{3}H]-palmitate concentration was determined using the heptane: buffer partition ratio previously assessed for this type of analysis (Burczynski, Pond et al. 1993; Elmadhoun, Wang et al. 1998). Purified [^{3}H]-palmitate was added to solutions of PBS containing 50 µM L-FABP that was freshly prepared prior to each experiment in a 20 ml scintillation vial. Heptane was layered overtop and the mixture capped using the scintillation vial which has been previously fitted with a hematocrit tube (0.2 mm thickness and 10 mm long; Fisher Scientific, ON) secured to the cap by contact cement. Tubes were shaken slowly (80 rpm) in a Gyrotory Water Bath Shaker (New Brunswick Scientific,

Canada) at 37°C to ensure proper equilibration between the two phases. Samples were taken at the end of 24 or 48 hrs from both phases and analyzed for radioactivity using a Beckman LS6500TA liquid scintillation counter. Sampling from buffer phase was done through the hematocrit tube using a 200 μl Hamilton syringe whereas sampling from the heptane phase was done through a 200 μl eppendorf pipette.

The partition ratio PR was calculated as,

$$PR = TR_h / TR_b$$

where, TR_h is the total radioactivity in the heptane phase and TR_b is the total radioactivity measured in the buffer phase. The heptane-to-buffer partition ratio was calculated as the total radioactivity in the heptane phase divided by the total radioactivity in the buffer phase. The predicted [^{3}H]-palmitic acid heptane-to-buffer partition ratio in the absence of a protein (PR^-) was expressed as

$$PR^- = Pc / (1+Kd / [H^+])$$

where P_c is the fatty acid partition coefficient ($10^{5.64}$) (Smith and Tanford 1973), K_d is the dissociation constant ($10^{-4.9}$ M) (Moran, Burczynski et al. 1987) for palmitic acid, and [H^+] is the H^+ concentration of the aqueous phase ($10^{-7.4}$ M). The predicted heptane-to-buffer partition ratio was calculated to be 1,376.

The unbound [^{3}H]-palmitate fraction (α) was calculated using

$$\alpha = PR^+ / PR^-$$

where PR^+ is the heptane: buffer partition ratio of [^{3}H]-palmitate in the presence of L-FABP and PR^- is the heptane: buffer partition ratio in the absence of L-FABP.

Data were obtained from six separate experiments.

19. Statistical analyses:

Statistical analyses of the treatment groups were carried out by student *t* test (unpaired) where 2 groups were compared while a one-way ANOVA was used for multiple comparisons. In Northern blot analyses, L-FABP RNA half-lives (time to reach 50% of original concentration) were estimated from plots of relative L-FABP RNA levels vs. time. Statistical differences with P values<0.05 were calculated significant.

III. RESULTS AND DISCUSSION

1. Regulation of L-FABP gene expression and antioxidant activity by PPARs

1.1 Introduction

Increased levels of L-FABP are seen in the livers and intestines of animals fed high-fat diets (Bass, Manning et al. 1985; Bass 1988) and growth hormone is known to induce L-FABP mRNA in hypophysectomised rats (Berry, Yoon et al. 1993). The most marked increase in L-FABP expression occurs after administration of peroxisome proliferators. Peroxisome proliferators are a group of structurally diverse chemicals that cause a dramatic increase in the size and number of peroxisomes (Corton, Lapinskas et al. 2000). Clofibrate is one of the peroxisome proliferator activated receptor (PPAR) agonists and is known to be a significant inducer of L-FABP expression (Luxon, Milliano et al. 2000; Antonenkov, Sormunen et al. 2006; Rajaraman, Wang et al. 2007). However, the mechanism of this group of drugs in modulating L-FABP expression and its subsequent influence on antioxidant activity remains to be determined. L-FABP expression could take place at one or multiple steps that may involve transcriptional, post-transcriptional, and/or post-translational control. Previous work has shown the increase in L-FABP expression after clofibrate treatment occurred 4 days following treatment (Rajaraman and Burczynski 2004; Rajaraman, Wang et al. 2007), suggesting that translational events are rate-limiting. The altered level of L-FABP by clofibrate, however, may result from a change in the rate of

gene transcription, turnover of transcript, or turnover of protein. In the current study, we explored the regulation of L-FABP expression and antioxidant activity by the peroxisome proliferator agonist and antagonist using CRL-1548 hepatoma cells and RNA interference.

1.2 Results

1.2.1 Regulation of L-FABP expression

To understand the mechanism of clofibrate regulation of L-FABP, expression of L-FABP in CRL-1548 hepatoma cells after clofibrate treatment was examined. As shown in Figure 16, clofibrate (500 μM) significantly increased the amount of L-FABP in a time and dose dependent manner. L-FABP levels were significantly increased compared to control (no clofibrate) following two days of clofibrate treatment ($p<0.05$) and continued to increase during the 4 days treatment regime (Figure 16A). Figure 16B shows the clofibrate concentration effect on L-FABP following 4 days treatment. There was no statistical difference between 500 μM or 1000 μM clofibrate treatment but statistically significant increases in L-FABP levels were seen following 4 days treatment with 250, 500, and 1000 μM clofibrate ($p<0.05$, $p<0.01$).

To further understand the regulation of L-FABP by clofibrate, CRL-1548 cells were treated with clofibrate (500 μM), PPARα antagonist (MK-886), PPARγ antagonist (GW-9662), clofibrate (500 μM) plus MK-886, and clofibrate plus GW-9662. Figure 17 shows a dose dependent inhibition in the clofibrate increased L-FABP expression by 1, 10, and 20 μM MK-886 or GW-9662 compared to 500 μM clofibrate treatment alone. Co-treatment of cells with clofibrate and 20 μM of MK-886 (or GW-9662) significantly reduced the L-FABP level ($p<0.001$) compared to either 1 μM or 10 μM cotreatment

groups (Figure 17). Therefore, we chose MK-886 (20 μM) and GW-9662 (20 μM), to further elucidate the role of clofibrate on L-FABP levels. Treatment of CRL-1548 cells with clofibrate significantly increased L-FABP (Figure 18; $p<0.01$), while treatment with the PPARγ antagonist GW-9662 did not affect L-FABP levels (Figure 18; $p>0.001$) from that of control cells. Treatment with the PPARα antagonist MK-886 reduced the intracellular L-FABP level compared to control cells but no significant difference. Co-treatment of cells with clofibrate and GW-9662 significantly reduced the L-FABP level ($p<0.01$) compared to the clofibrate group. L-FABP levels, however, were still greater than those of the control (no drug treatment) group ($P<0.05$) (Figure 18). Co-treatment of cells with clofibrate plus MK-886, however, blocked the clofibrate induced increase of L-FABP to values that were lower than control but not statistically different to that of MK-866 treatment alone.

L-FABP mRNA levels (Figure 19) were significantly increased following clofibrate treatment ($P<0.001$). Co-treatment with clofibrate plus GW-9662 was not associated with any significant reduction in L-FABP mRNA levels compared to the clofibrate group. Co-treatment with clofibrate plus MK-886, however, reduced L-FABP mRNA level ($p<0.001$), but it was still significantly higher than control level ($p<0.05$; Figure 19).

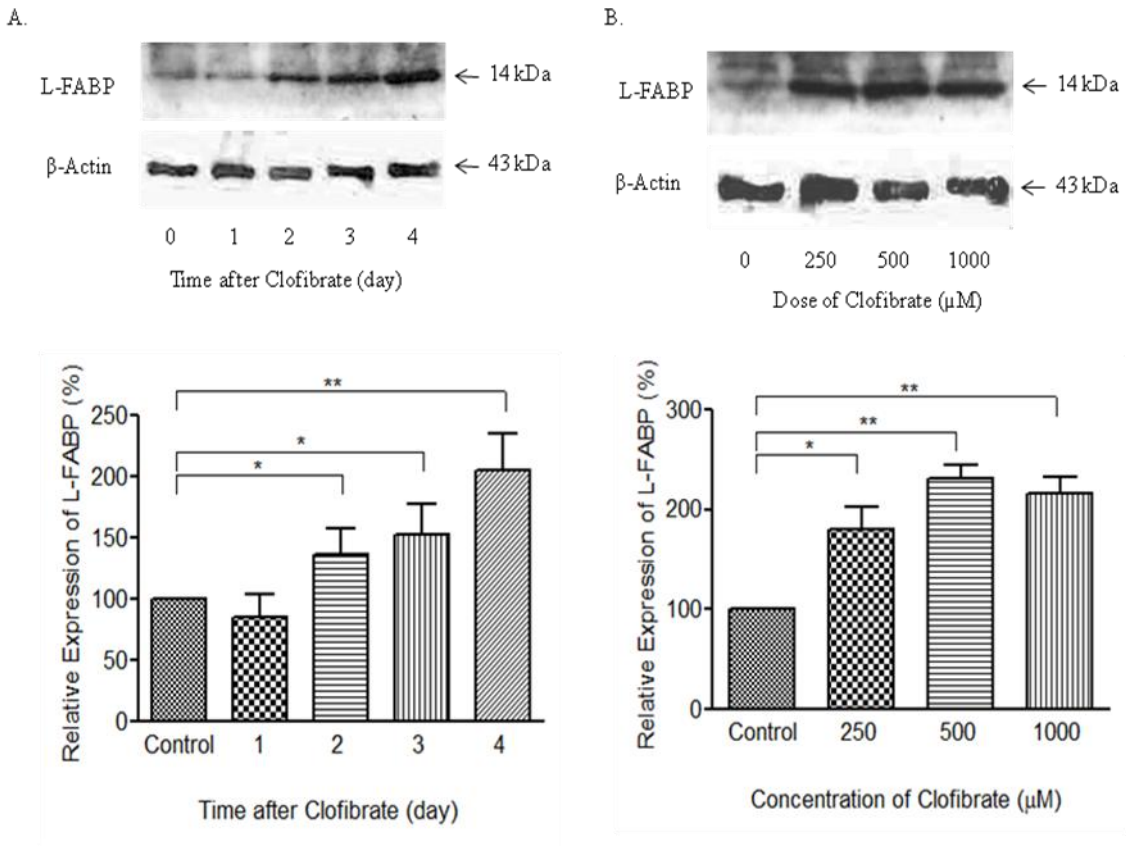

Figure 16: Western blot analyses of L-FABP levels from control and clofibrate (500μM) treated CRL-1548 hepatoma cells. (A) Top - Western blot of L-FABP level from representative cells that were treated with 500μM clofibrate for 1 to 4 days. (B) Top – Representative western blot of L-FABP from cell treated with 250 μM, 500 μM, and 1000 μM clofibrate after 4 days. Bottom - Histogram representing integrated density values for L-FABP from four different experiments. Band densities were quantified and expressed as mean ± SD. *P < 0.05, **P < 0.01.

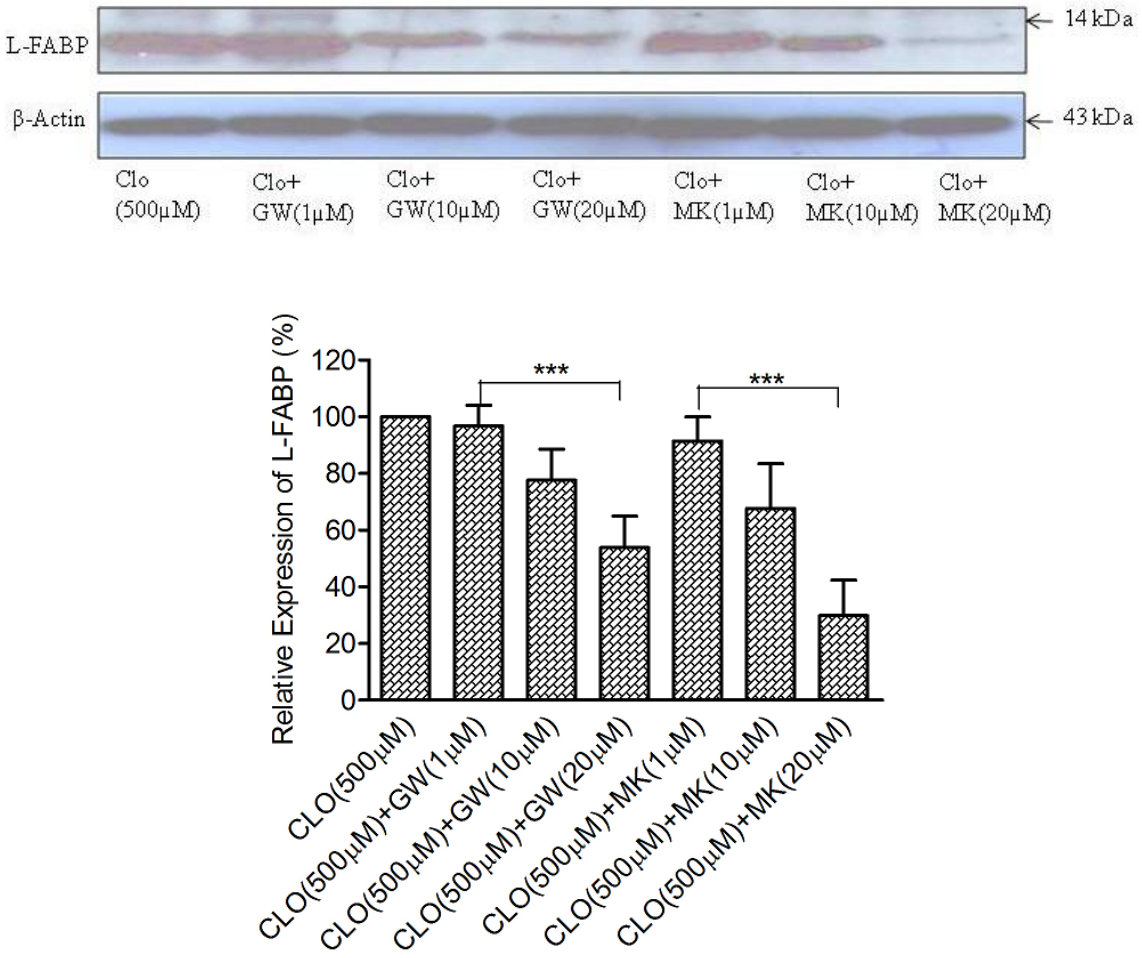

Figure 17: Western blot analyses of L-FABP levels from clofibrate (500 μM), co-treatment with clofibrate (500 μM) and PPARα antagonist MK-886 (1, 10 and 20 μM), or co-treatment with clofibrate (500 μM) and PPARγ antagonist GW-9662 (1, 10 and 20 μM) treated cells. Top: L-FABP level from treated CRL-1548 cells. Bottom: Histogram representing integrated density values for L-FABP from four experiments. Band densities were quantified and expressed as mean ± SD. ***P < 0.001.

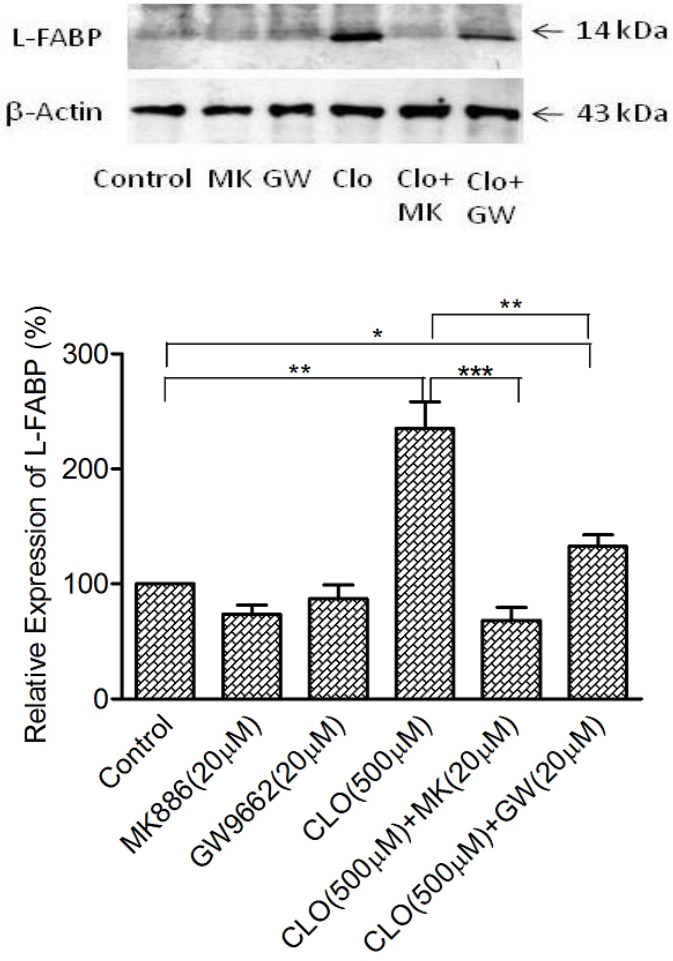

Figure 18: Western blot analyses of L-FABP levels from control (no drug treatment), clofibrate (500 μM), and PPARα antagonist MK-886 (20 μM), PPARγ antagonist GW-9662 (20 μM), co-treatment with clofibrate (500 μM) and MK-886 (20 μM, CLO+MK), and clofibrate (500 μM) and GW-9662 (20 μM, CLO+GW) treated cells. Top: L-FABP level from treated CRL-1548 cells. Bottom: Histogram representing integrated density value for L-FABP from four experiments. Band densities were quantified and expressed as mean ± SD. *P < 0.05, **P < 0.01, ***P < 0.001.

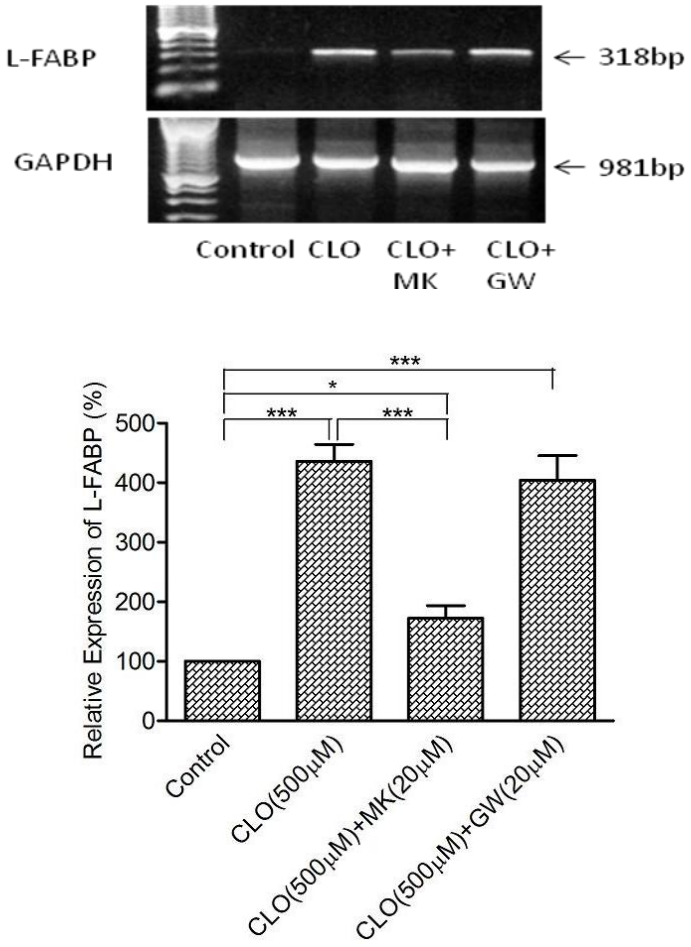

Figure 19: RT-PCR analysis of L-FABP mRNA expression in control (no drug treatment), clofibrate (500 µM), and cells co-treated with the PPARα antagonist MK-886 (20 µM) and clofibrate (500 µM) (CLO+MK); and cotreatment with PPARγ antagonist GW-9662 (20 µM) and clofibrate (500 µM) (CLO+GW) on day 4. Top: RT-PCR products of 318 bp L-FABP mRNA and 981 bp product of GAPDH mRNA. Bottom: Histogram representing integrated density value of L-FABP amplification product/integrated density value of GAPDH mRNA amplification product from four independent experiments. Band densities were quantified and expressed as mean ± SD. *P < 0.05, ***P < 0.001.

1.2.2 L-FABP mRNA stability

Inhibition of mRNA synthesis in cells by actinomycin D allowed for measurements of cellular L-FABP mRNA stability. CRL-1548 hepatoma cells were treated with 500 µM clofibrate for 4 days. Following the treatment period (time=0 h), 4 µM actinomycin D was added to the cell culture medium. Total RNA was extracted from cells harvested at 6 hr intervals and analyzed for L-FABP mRNA using Northern blot to investigate the relative degradation rate. Figure 20 shows that the degradation of L-FABP mRNA over time after transcriptional blockade occurred much faster in control cells compared with that of the clofibrate-treated cells. Clofibrate treatment increased the half-life (time to reduction to 50% of original level) of the L-FABP mRNA from 14 hrs in control cells to 23 hrs in clofibrate-treated cells.

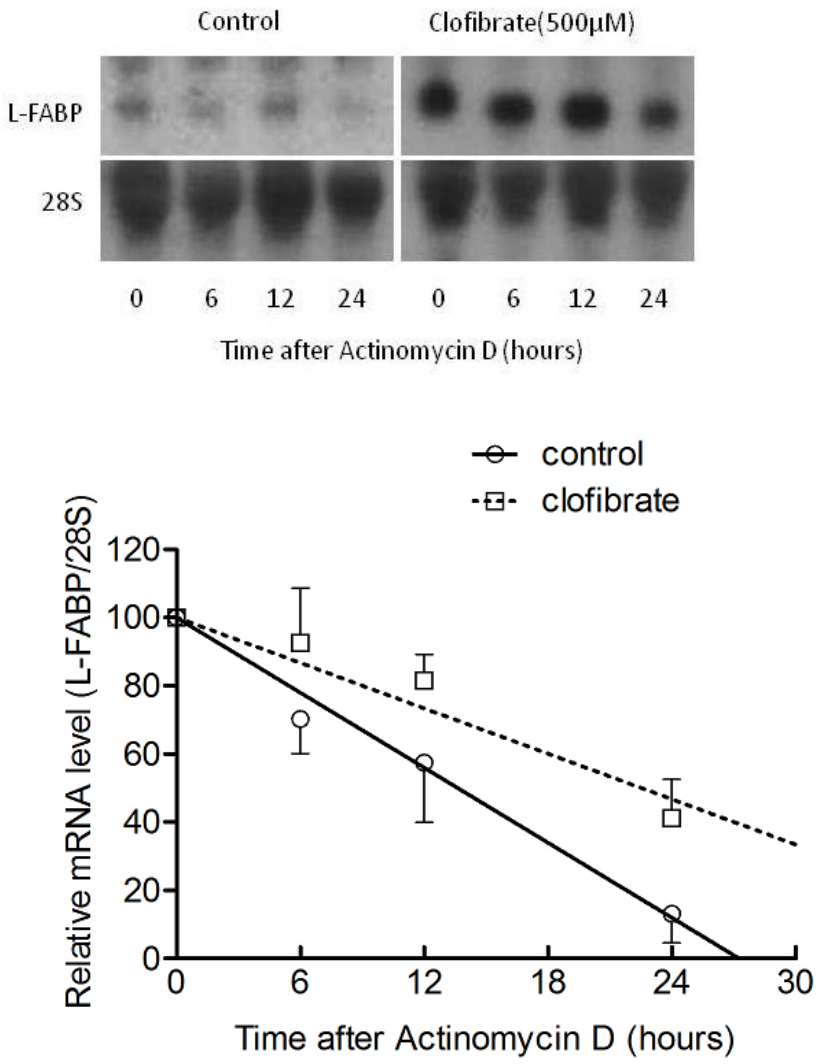

Figure 20: Northern Blot analysis of L-FABP mRNA stability in 1548 cells. Total RNA was extracted from control and clofibrate (500 µM) treated cells harvested at 0, 6, 12, 24 hr intervals and analyzed for L-FABP mRNA expression by Northern blot. Top: Representative Northern blot from control and clofibrate treated cells. Bottom: Regression analysis of L-FABP mRNA expression vs. time after actinomycin D treatment.

1.2.3 L-FABP mRNA transcription

The nuclear run-off assay allowed for the detection of changes in the transcriptional rate of L-FABP nascent mRNA. Nascent mRNA transcripts that had already been initiated and elongated in isolated nuclei were labelled with [^{32}P]-dCTP and hybridized to L-FABP or GAPDH-specific probes. Results showed that treatment of clofibrate significantly increased nascent L-FABP RNA synthesis, where GAPDH nascent mRNA was used as a loading control (Figure 21). These results suggest that clofibrate acts as a transcriptional factor and enhances the transcriptional rate of L-FABP.

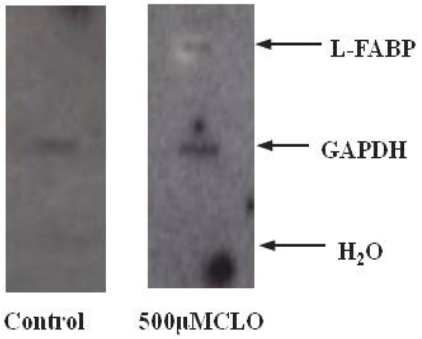

Figure 21: Nuclear run-off analysis of nascent L-FABP mRNA transcription rate in control and treated CRL-1548 cells. Cells were treated with clofibrate (500 μM) for 4 days. Nuclei were isolated from control and treated cells. The nascent mRNA transcripts were elongated with labelled [α-^{32}P] dCTP. The figure represents autoradiogram of L-FABP from treated cells. GAPDH was used as the loading control. H_2O was used as the negative control.

1.2.4 L-FABP antioxidant activity

We then assessed whether clofibrate induced L-FABP possessed the antioxidant activity. As shown in the Figure 22, 500 μM clofibrate treatment significantly reduced ($p<0.001$) intracellular ROS levels as determined by a reduction in DCF fluorescence. Treatment with the PPARα antagonist MK 866 (20 μM) or PPARγ antagonist GW-9662 (20 μM) alone showed no significant effect on ROS levels than control values. Co-treatment with clofibrate plus the PPARγ antagonist GW 9662, however, showed a significant reversal of the clofibrate effect on DCF levels ($P<0.001$). There were still significant amounts of ROS in this co-treatment group compared to the control group ($p<0.001$). Co-treatment with the PPARα antagonist MK 886 and clofibrate showed a complete reversal of the clofibrate reduced intracellular ROS levels ($P<0.001$). Clofibrate and/or the PPAR antagonists did not affect the activities of SOD, GPx, or catalase activity (see Table 13), suggesting that the reduction in free radical levels following clofibrate treatment was likely due to functional increases in L-FABP levels.

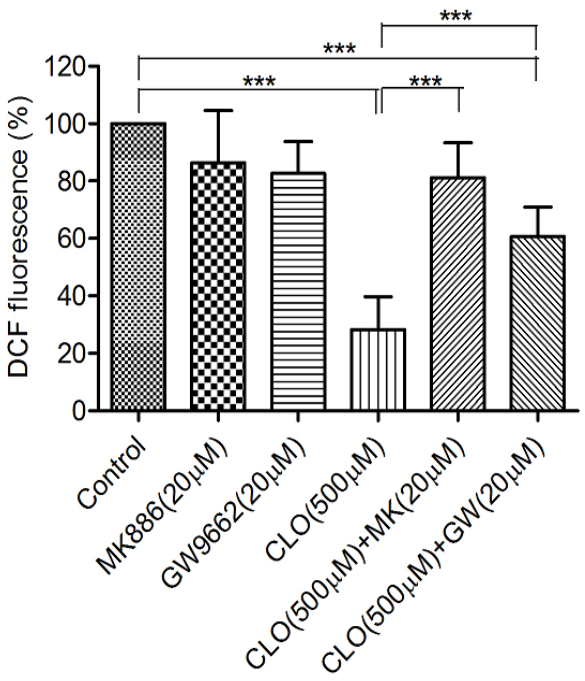

Figure 22: Intracellular ROS levels induced by H_2O_2 treatment in CRL-1548 hepatoma cells. DCF fluorescence levels were quantified and expressed as mean ± SD, n = 6. ***P < 0.001.

To further support the notion that L-FABP upregulation is implicated in the clofibrate-promoted ROS suppression we used RNA interference (siRNA) to silence the expression of L-FABP. Cells were treated with 500 μM clofibrate everyday for 4 days. During this treatment period cells were transfected with L-FABP siRNA on days 1 and 3. The reduction in L-FABP protein level was assessed by Western blot (Figure 23) and the antioxidant activity assessed by DCF fluorescence (Figure 24). Cells transfected with siRNA targeted against L-FABP showed a substantial decrease of L-FABP at 24 h post transfection (data not shown), with maximum reduction at 96 h post transfection (Figure 23). As shown in Figure 23, L-FABP expression was significantly higher than in the control group (no drug treatment) after 500 μM clofibrate treatment ($p<0.001$). In CRL-1548 cells transfected with siRNA targeted against L-FABP, the level of L-FABP in 500 μM clofibrate treatment showed a substantial decrease at 24 h post transfection (data not shown), with maximum reduction (66.01±2.56%, $p<0.001$) at 96 h post transfection compared to either non-transfected or negative siRNA transfected in clofibrate treated cells (Figure 23). Figure 24 revealed that 500 μM clofibrate treatment significantly reduced ($p<0.001$) intracellular ROS levels compared to the control group (no clofibrate), non-transfected cells. After L-FABP siRNA transfection, ROS levels in the control group (no clofibrate, L-FABP siRNA transfected) were significantly higher than in control group ($p<0.05$; Figure 24). This result indicated that the background L-FABP level in the control group was slightly decreased after L-FABP siRNA transfection. ROS levels in the clofibrate treated group were significantly reversed after transfected with L-FABP siRNA compared to the non-transfected clofibrate group ($p<0.001$). Thus, these data support the notion that the reduction in ROS levels was due to clofibrate's upregulation of L-FABP.

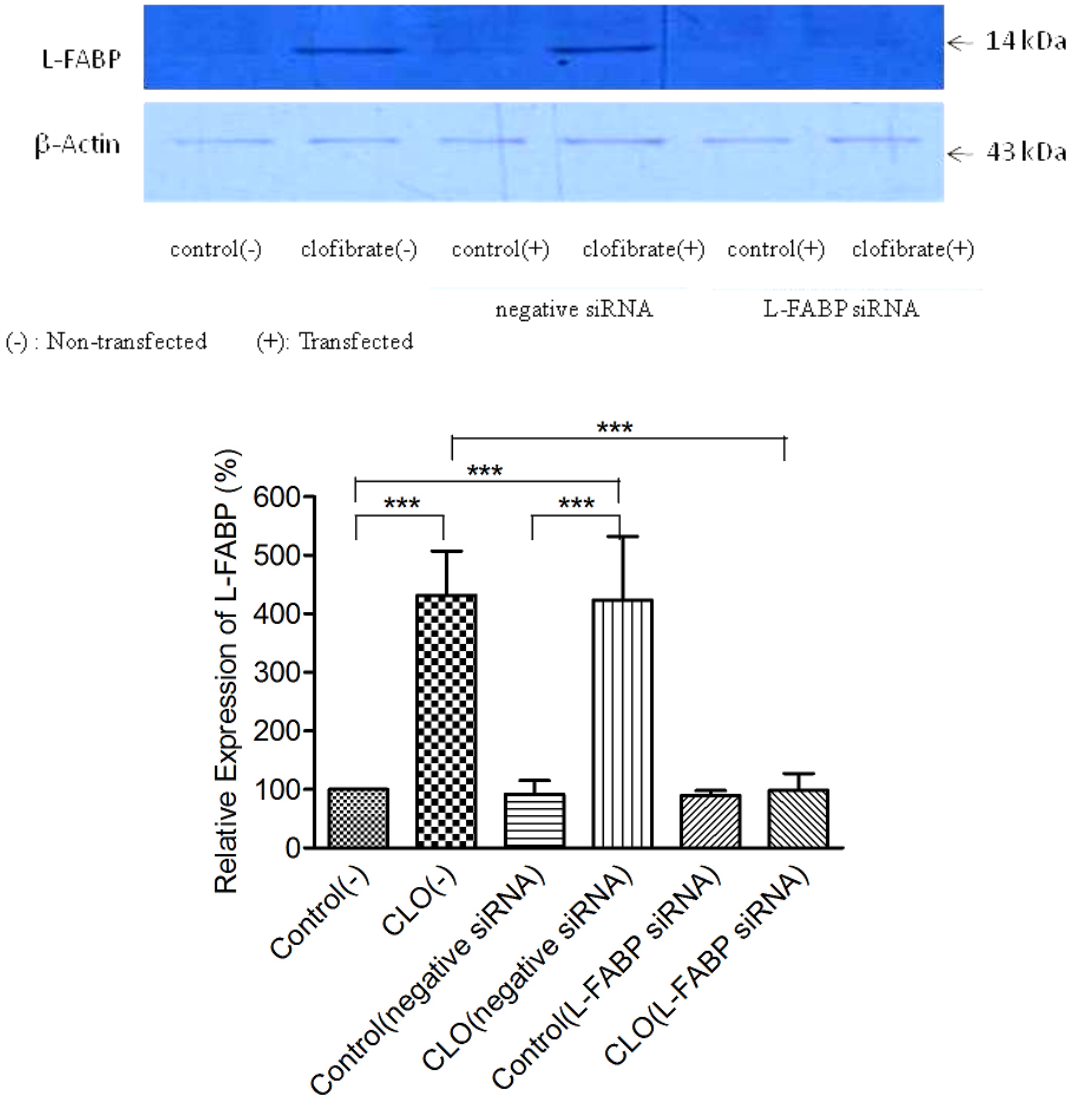

Figure 23: Western blot analysis of L-FABP levels from control (no drug treatment); clofibrate (500 µM) treated cells with/without negative siRNA or L-FABP siRNA transfection. Control (-): control cells with no drug treatment; CLO (-): clofibrate (500 µM) treated cells without siRNA transfection; Control (negative siRNA): control cells with negative siRNA transfection; CLO (negative siRNA): clofibrate treated cells with negative siRNA transfection; Control (L-FABP siRNA): control cells with L-FABP siRNA

transfection; CLO (L-FABP siRNA): clofibrate treated cells with L-FABP siRNA transfection. Top: L-FABP level from treated CRL-1548 cells. Bottom: Histogram representing integrated density values for L-FABP from four experiments. Band densities were quantified and expressed as mean ± SD. n=4, ***P < 0.001.

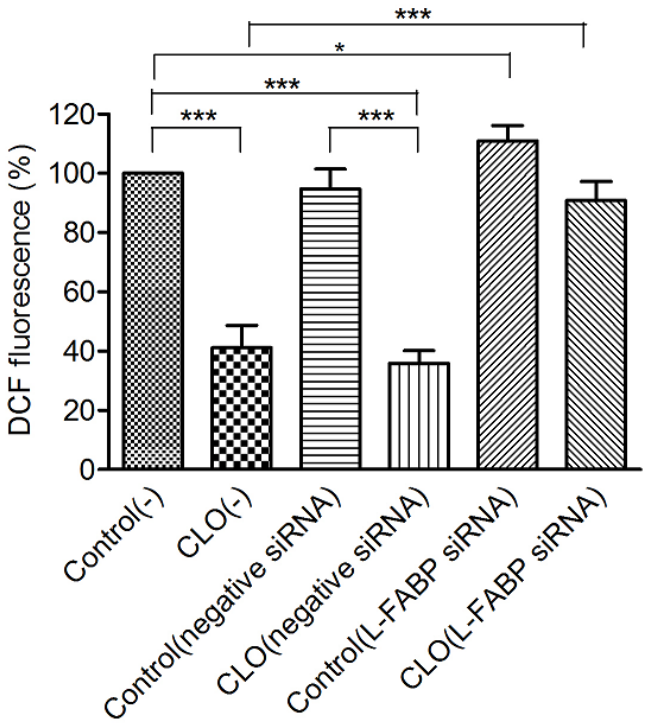

Figure 24: Intracellular ROS levels induced by H_2O_2 treatment in CRL-1548 hepatoma cells after using RNA interference (siRNA) to silence the expression of L-FABP. Control (-): control cells with no drug treatment; CLO (-): clofibrate (500 µM) treated cells without siRNA transfection; Control (negative siRNA): control cells with negative siRNA transfection; CLO (negative siRNA): clofibrate treated cells with negative siRNA transfection; Control (L-FABP siRNA): control cells with L-FABP siRNA transfection; CLO (L-FABP siRNA): clofibrate treated cells with L-FABP siRNA transfection. Data indicate mean ± SD, n = 6. *P < 0.05, ***P < 0.001.

Table 13: Clofibrate did not alter SOD, GPx and catalase activities in CRL-1548 hepatoma cells.

	SOD	**GPx**	**Catalase**
Control	81.37 ± 15.9	8.04± 1.8	37 ± 4.6
Clofibrate (500µM)	78.96 ±8.08	9.65±2.1	32 ± 4.8
Clofibrate (500µM) + MK886 (20µM)	79.66 ± 10.8	11.25± 1.9	29 ± 4.9
Clofibrate (500µM) + GW9662 (20µM)	81.62 ± 10.5	9.57± 1.8	22±4.2

SOD activity was measured in units where one unit of activity was defined as the amount of enzyme that decreased initial rate of xanthine oxidase to half its maximal value. GPx enzyme activity was measured in µM NADPH oxidized/min. The activity of catalase was measured in units of catalase decomposing µM H_2O_2 consumed/min. Data are represented as mean ± SD from 6 independent experiments.

1.3 Discussion

L-FABP has been reported to be associated with significant antioxidant activity (Wang, Gong et al. 2005). Complications from diseases involving oxidative stress would, therefore, be expected to be attenuated as L-FABP levels are increased. Although L-FABP levels may be manipulated by various methods, the most effective method is through pharmacological intervention. The present results show that L-FABP levels and antioxidant activity were strongly modified by the PPAR agonist clofibrate. Fibrates are known to increase L-FABP levels (Baumgardner, Shankar et al. 2008) by binding to the PPARα subunits (Bishop-Bailey 2000; van Raalte, Li et al. 2004). Thus, L-FABP helps to induce its own levels indirectly by transporting these ligands to the PPAR subunits. The transfer of ligands between L-FABP and PPARα as well as PPARγ occurs by a direct protein-protein interaction whereby the bound ligand is directly off-loaded to the PPAR subunit (Wolfrum, Borrmann et al. 2001). The PPARα (MK886) and PPARγ (GW9662) antagonists prevent the peroxisome proliferator induced activation of gene expression. MK886 associates with the ligand binding site of PPARα which prevents the conformational change in the gene ligand binding domain (Kehrer, Biswal et al. 2001). Therefore, it has an impact on the interaction with other activators to further inhibit the transcription of the L-FABP gene. As a potent antagonist of PPARγ, GW9662 covalently modifies a cysteine residue in the ligand-binding site of PPARγ (Leesnitzer, Parks et al. 2002).

The mechanism of clofibrate treatment on increasing L-FABP levels was also investigated. An elevated level of L-FABP mRNA by clofibrate treatment could result from an increase in L-FABP RNA synthesis, a decrease in L-FABP mRNA degradation, or

both. In this study nuclei were *harvested* and transcription rates were estimated by a nuclear *run-off* assay which allowed for the specific detection of changes in the L-FABP transcription rate of *nascent RNA (nRNA)* induced by clofibrate. When nuclei were harvested from control and clofibrate-treated groups, changes in L-FABP nRNA were found between these two groups, indicating that clofibrate treatment increased the transcription rate of genes that encode for L-FABP. Stability of L-FABP mRNA was evaluated by using actinomycin D to inactivate mRNA synthesis. Results showed that clofibrate also significantly increased the stability of L-FABP mRNA from 14 hours (0 μM of clofibrate) to 23 hours (500 μM clofibrate), suggesting reduced degradation of mRNA. These findings were consistent with the observation that L-FABP levels were elevated following 2 days of clofibrate treatment.

A novel property of L-FABP is its ability to suppress free radicals levels in the cytosol (Wang, Gong et al. 2005; Rajaraman, Wang et al. 2007) and its hepatoprotective effect in liver disease (Wang, Shen et al. 2007). In this study we also assessed L-FABP's potential to suppress free radical levels when L-FABP levels were first increased by clofibrate treatment followed by ROS release by hydrogen peroxide; and second whether PPARα or PPARγ antagonist treatment affected intracellular free radical levels. As predicted clofibrate treatment was associated with increased L-FABP levels and significantly reduced ROS levels (Figures 18 and 22). Cells treated with the PPARα antagonist alone also lowered L-FABP levels in control cells but did not affect intracellular ROS levels; while treatment with the PPARγ antagonist alone did not affect L-FABP or ROS levels. Use of the PPAR antagonists (Figure 18) following clofibrate treatment, however, reversed the clofibrate induced increases in L-FABP levels with the PPARα

antagonist being more effective than the PPARγ antagonist. Figure 22 also showed that GW-9662 significantly reversed the antioxidant activity induced by clofibrate but the DCF fluorescence values were still lower than control values ($p<0.001$). It is conceivable that GW-9662 may have some intrinsic activity as a partial antagonist at the PPARα receptor (Seimandi, Lemaire et al. 2005). That MK-866 suppressed clofibrate induced increases in L-FABP values to levels that were similar to that of control (Figure 18) is not surprising given that MK-866 is a PPARα antagonist. Finally, by using RNA interference (siRNA) we were able to further demonstrate that L-FABP's antioxidant property stem from increased L-FABP expression induced by clofibrate (Figure 23), the reduction in DCF fluorescence by clofibrate (Figure 24) was eliminated, suggesting that the cellular antioxidant activity was due to L-FABP. Of significance in this study was the finding that neither clofibrate nor the PPAR antagonist treatment affected the levels of the nascent antioxidant enzymes (Table 13).

While the above findings clearly indicate clofibrate induction of L-FABP as the key determinant in developing an antioxidant state, alternative explanations must also be considered. Specifically, clofibrate treatment has been reported to up-regulate acyl-CoA binding protein (ACBP) in rat hepatocytes which is known to bind long chain fatty acyl-CoA esters (Vanden Heuvel, Sterchele et al. 1993). Thus, it is possible that the lower ROS levels observed following clofibrate treatment may also have resulted from an up-regulation of L-FABP, ACBP, or both. ACBP is an 86 amino acid protein that lacks cysteine residues but contains 3 methionine residues (Mikkelsen, Hojrup et al. 1987). ACBP expression is directly regulated by PPARγ and possibly also by PPARα through the PPAR-response element (PPRE)(Helledie, Grontved et al. 2002). Over-expression of

ACBP is associated with reduced PPAR mRNA levels in livers of triglyceride fed animals (Oikari, Ahtialansaari et al. 2008). Thus, ACBP may act as a negative regulator of PPAR activation and function physiologically as a PPAR antagonist. If so, treatment with GW-9662 (PPARγ antagonist) should result in reduced ACBP levels. However, the intracellular ROS levels were not affected by GW-9662 treatment (Figure 22). Furthermore, if the reduction in ROS levels from clofibrate were due partially due to ACBP activity then the reversal in ROS levels seen with MK-886 should still be significantly different from control levels. Finally, the contribution to the overall antioxidant effect by ACBP is likely to be minimal since the concentration of ACBP is approximately eight-fold lower than that of L-FABP in liver cytosol (Hashimoto and Hayashi 2002).

2. Recombinant Rat L-FABP protein construction using Glutathione-S-transferase (GST) fusion system

2.1 Introduction

To elucidate the mechanism of L-FABP's antioxidant activity, large quantities of L-FABP need to be isolated. One way to isolate the protein is to sacrifice a large number of animals, isolate L-FABP from liver tissue, and conduct *in vitro* studies. A more efficient method is to produce recombinant L-FABP.

Whilst a number of systems have been described for the production of recombinant rat L-FABP in *Escherichia coli* (Cistola, Sacchettini et al. 1989; Hubbell, Behnke et al. 1994; Rolf, Oudenampsen-Kruger et al. 1995; Velkov, Chuang et al. 2005), several of the established purification procedures report the presence of additional contaminants. Purification of recombinant L-FABP is also a complicated and time-consuming procedure. In most cases, purification strategies consist of ammonium sulfate precipitation (Davies, Thumser et al. 1999) followed by dialysis or gel filtration and ion-exchange chromatography (Hubbell, Behnke et al. 1994; Maatman, van Moerkerk et al. 1994; Rolf, Oudenampsen-Kruger et al. 1995). In contrast to previously published procedures, the advent of affinity tags makes purification faster, more efficient, and significantly reduces contaminants, complexity and the time involved, with much higher yields and homogeneous preparations of the protein. Affinity tags enhance the solubility, and even promote the proper folding of their fusion partners. In this thesis we constructed L-FABP in a GST fusion system. The recombinant L-FABP in the study was expressed

successfully and purified to near homogeneity using glutathione-sepharose transferase 4B beads. The results indicated that the GST fusion system is favourable for the production and purification of recombinant L-FABP from *E. coli*, and allows for further protein functional studies.

2.2 Results

2.2.1 Expression of recombinant GST/L-FABP from E. coli

The cDNA fragment encoding the complete rat L-FABP sequence was cloned into the pGEX-6P-2 plasmid (Figure 25) downstream of the hybrid GST *tag* promoter to allow for the inducible and efficient intracellular expression of rat GST/L-FABP in *E. coli* (see Figure 26). Following sonication and removal of the bacterial cell pellet, the highly soluble GST/L-FABP complex was isolated from bacterial cytosolic proteins. Optimal expression time was evaluated by determining the extent of protein accumulation and degradation using SDS–PAGE analysis of cellular lysates over 1-8 hr. Following 6 hr of induction the GST/L-FABP tag reached a peak intracellular concentration of approximately 80% of total *E. coli* intracellular protein and 0.1mM IPTG was sufficient to induce a maximum level of GST/L-FABP expression. Figure 27 provided the results from SDS-PAGE analyse which revealed a strong 40 kDa protein band in cell lysates induced by IPTG (Figure 27A, lane 2). This band was much weaker in cells not exposed to IPTG (Figure 27A, lane 1).

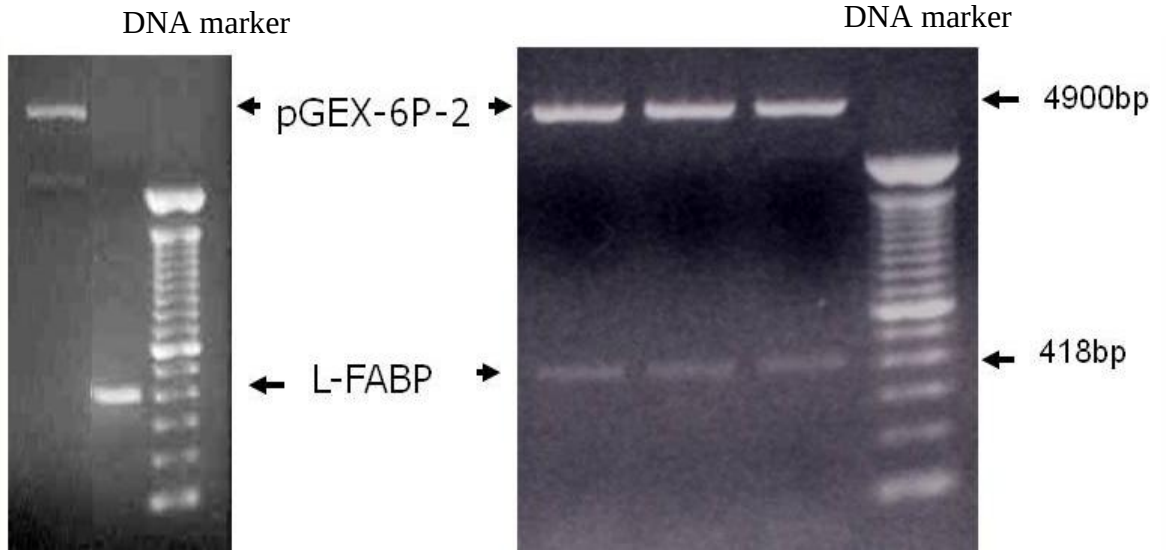

Figure 25: Analysis of recombinant pGEX-6P-2/L-FABP using restriction enzyme digestion. The left panel indicates the size of pGEX-6P-2 & L-FABP before ligation. The right panel displays restriction map of recombinant pGEX-6P-2/L-FABP. Plasmid DNAs from three bacteria colonies were prepared by mini-prep and digested by BamH1 and Xho1. Reconstructed pGEX-6P-2/L-FABP showed two bands after digestion of BamH1 and Xho1, one is pGEX-6P-2 at 4900bp and the other is L-FABP at 418bp. The right lane in each graph represents the DNA marker.

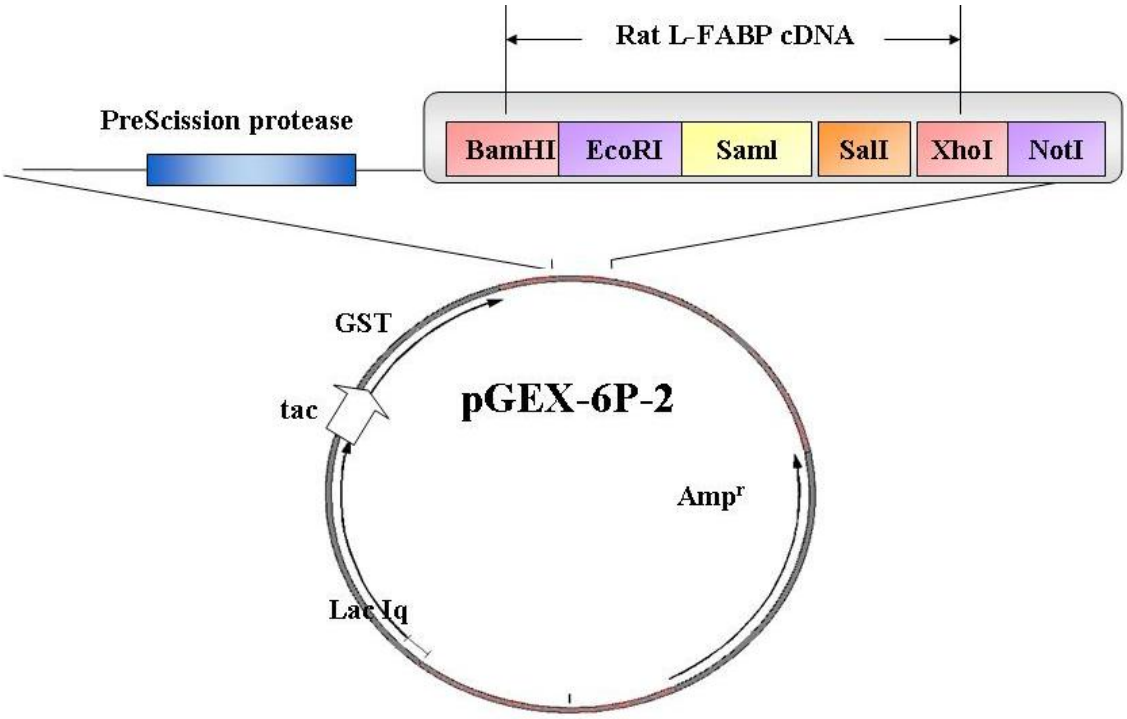

Figure 26: Schematic representation of the pGEX-6P-2-L-FABP expression vector employed for biosynthesis of rat L-FABP in *E. coli*. Vector pGEX-6P-2 is a glutathione S-transferase fusion vector, which contains a multiple cloning site with PreScission Protease sequence for separation of the fusion protein and RE such as BamH1 and Xho1; a glutathione S-transferase fusion tag for easy purification; a $LacI^q$ sequence for induction of fusion protein expression by the lactose analog isopropyl b-D thiogalactoside (IPTG); and an antibiotic resistant gene (ampicillin) for the selection of bacteria between pGEX-6P-2 transformed and non-transformed cells.

2.2.2 Rapid Purification of recombinant GST/L-FABP from E. coli

GST/L-FABP was purified to homogeneity by three successive elution steps using GST 4B beads which precipitated 85% of the GST/L-FABP (Figure 27A, lane 3). This elution method had the highest resolution and optimal elution characteristics for GST/L-FABP separation. Following elution, no contaminants were detected and approximately 50-60 mg of GST/L-FABP was obtained from a 500 ml culture. SDS-PAGE gel lanes were loaded with 20 μg protein per well in order to allow for the detection of impurities. These contaminants were not present as observed by SDS–PAGE on 15% polyacrylamide gels (Figure 27A, lane 3) indicating that the contaminants could be effectively separated from the GST/L-FABP by GST 4B beads. As expected, the GST/L-FABP fusion protein band was detected at approximately 40 kDa in the SDS-PAGE gel which was in strong agreement with our predicted size, since the GST and L-FABP molecular weights are 26 and 14 kDa, respectively.

2.2.3 Expression of the recombinant L-FABP

Purified recombinant L-FABP was successfully isolated after incubating the GST/L-FABP complex with PreScission Protease and cleavage buffer (Figure 27A, lane 4). The SDS-PAGE results (Figure 27B) showed that our recombinant L-FABP (Figure 27B, lane 3) had the same molecular weight (approximately 14 kD) as L-FABP isolated from 1548 hepatoma cells (Figure 27B, lane 1) and L-FABP isolated from 1548 hepatoma cells treated with clofibrate (Figure 27B, lane 2). Western blot results from 1548 hepatoma cell lysates showed strong immunoreactivity with our polyclonal antibody raised against rat L-FABP (Figure 27C) as did our recombinant purified rat L-FABP. Bar graphs on the right

hand side of Figures 27D and 27E depict the relative expression of L-FABP on SDS-PAGE and Western blot, respectively.

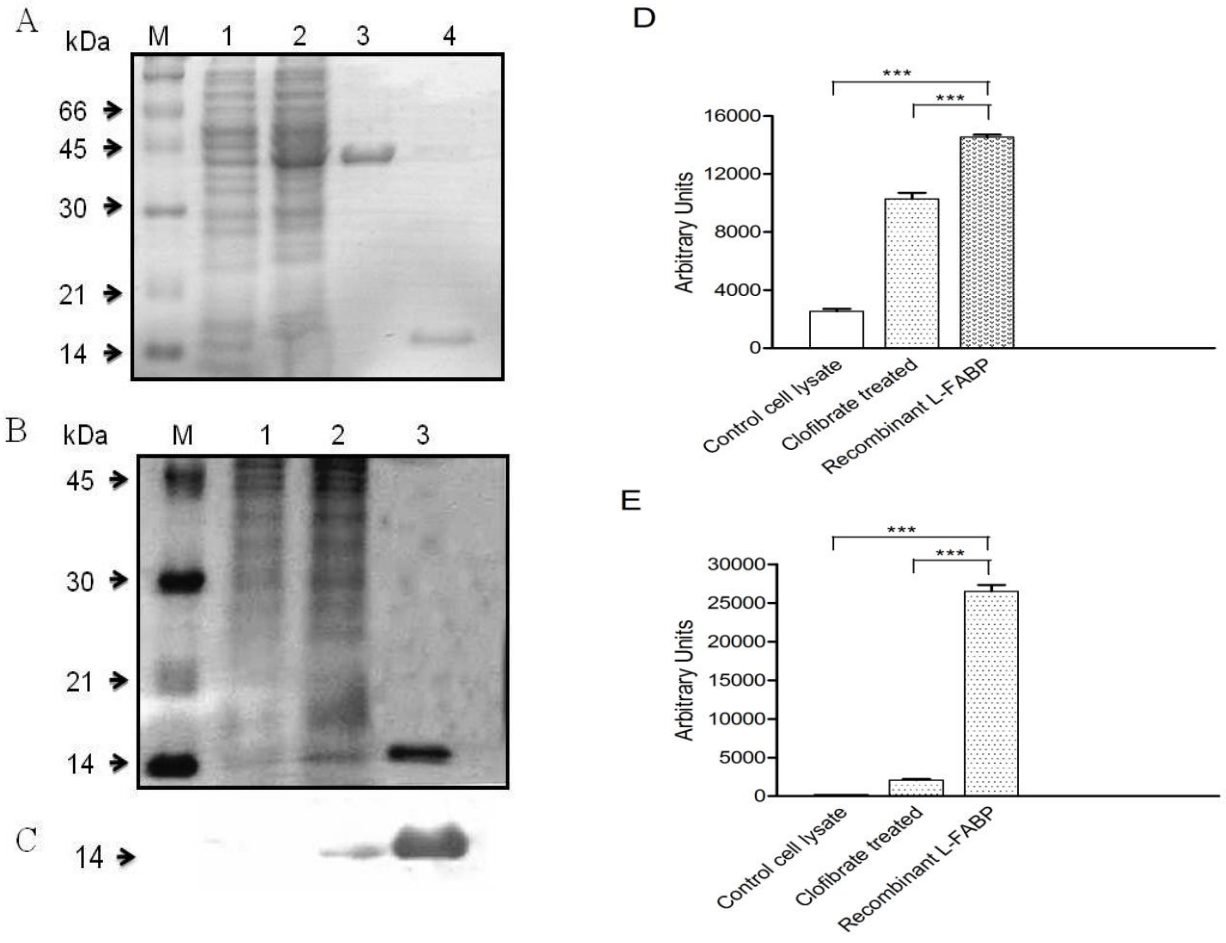

Figure 27: Expression and purification of GST/L-FABP fusion protein and L-FABP using *E. coli* DH5α cells and the GST fusion system (Figure 27A). Protein samples were analyzed by SDS-PAGE and stained with Coomassie brilliant blue. Lane M, molecular weight markers; Lane 1, bacteria not treated with IPTG (6 hrs); Lane 2, bacteria treated with IPTG (0.1 mM) to induce GST/L-FABP production (6 hrs post induction with 0.1 mM IPTG); Lane 3, purified GST/L-FABP complex. Lane 4, expression of L-FABP from the fusion protein complex GST/L-FABP. Figure 27B identifies recombinant L-FABP and L-FABP purified from rat 1548 hepatoma cytosol by SDS-PAGE. Purified recombinant L-FABP has a molecular weight of approximately 14 kDa which is similar to the L-FABP expressed in control hepatoma cells induced by clofibrate. Lane M, molecular weight markers; Lane 1, control cytosolic proteins from 1548 hepatoma cells; Lane 2, 1548 hepatoma cytosolic proteins induced by 500 µM clofibrate for 4 days; Lane 3, purified recombinant L-FABP from *E.coli*. Figure 27C identifies purified rat L-FABP and cytosolic proteins from rat 1548 hepatoma cells by Western blot with antibody raised against rat L-FABP. The purified rat recombinant L-FABP has strong immunoreactivity with the antibody against L-FABP. The Western blot corresponds to the lanes in SDS-PAGE (Figure 27B). Figure 27D summarizes the data from SDS-PAGE analysis (n=4). Recombinant L-FABP expression was significantly higher in bacterial cells than control and clofibrate treated hepatoma cells ($P<0.001$). Figure 27E summarizes data from the integrated density values of L-FABP from three Western blot experiments also showing much greater amounts of L-FABP present in the recombinant sample. Band densities were quantified and expressed as mean ± SD. ***$P < 0.001$ compared to recombinant L-FABP.

2.2.4 MALDI QqTOF mass spectrometry of recombinant L-FABP

Recombinant L-FABP was analyzed following separation using chromatography by MALDI QqTOF MS. The amino acid sequence of our recombinant rat L-FABP (Table 14) was identical with that of L-FABP isolated from rat liver (She et al, 2002). MALDI-TOF analysis showed the presence of a major mass peak at *m*/*z* of 15,275.9 (Figure 28). Peptide mass fingerprinting of the L-FABP was carried out by in-solution digestion with endoproteinase Glu-C, trypsin and analyzed by MALDI-TOF MS (Figure 29) and MS/MS. Total measured mass (15274.9 Da) of L-FABP was greater than that predicted based on the amino acid sequence (14272.450 Da). The increased mass was attributed to additional amino acids on the N-terminal end (Figure 30, Figure 31) and S-glutathionylation of the cysteine group (Figure 32) (see discussion).

Table 14: L-FABP protein sequence identification by MALDI QqTOF mass spectrometry

001 **M**NFSGKYQVQ SQENFEPF**M**K A**M**GLPEDLIQ KGKDIKGVSE IVHEGKKVKL

051 TITYGSKVIH NEFTLGEE**C**E LET**M**TGEKVK AVVK**M**EGDNK **M**VTTFKGIKS

101 VTEFNGDTIT NT**M**TLGDIVY KRVSKRI

A total of 7 methionines located at the L-FABP sequence positions Met^{1}, Met^{19}, Met^{22}, Met^{74}, Met^{85}, Met^{91}, and Met^{113}. The single cysteine is located at sequence position Cys^{69}.

Enzyme	Observed Peptide	Peptide sequence	Meas. value m/z	Calc. mass MH+
Trypsin	Tag-1-6	**PGLSGLAT**MNFSGK	1379.695	1379.699
	7-20	YQVQSQENFEPFMK	1774.804	1774.811
	21-31	AMGLPEDLIQK	1214.648	1214.645
	21-33	AMGLPEDLIQKGK	1399.767	1399.761
	21-36	AMGLPEDLIQKGKDIK	1755.972	1755.967
	37-46	GVSEIVHEGK	1054.549	1054.553
	37-47	GVSEIVHEGKK	1182.652	1182.648
	50-57	LTITYGSK	882.492	882.493
	58-80	VIHNEFTLGEE**C***ELETMTGEKVK	2941.316	2941.326
	81-96	AVVKMEGDNKMVTTFK	1797.919	1797.924
	97-122	GIKSVTEFNGDTITNTMTLGDIVYKR	2873.467	2873.471
	100-121	SVTEFNGDTITNTMTLGDIVYK	2419.176	2419.179
	100-122	SVTEFNGDTITNTMTLGDIVYKR	2575.268	2575.271
	100-125	SVTEFNGDTITNTMTLGDIVYKRVSK	2889.469	2889.466
Glu-C	Tag-1-13	**PGLSGLAT**MNFSGKYQVQSQE	2242.085	2242.081
	14-26	NFEPFMKAMGLPE	1510.703	1510.707
	27-40	DLIQKGKDIKGVSE	1529.851	1529.853
	14-40	NFEPFMKAMGLPEDLIQKGKDIKGVSE	3021.525	3021.542
	14-44	NFEPFMKAMGLPEDLIQKGKDIKGVSEIVHE	3499.683	3499.796
	45-62	GKKVKLTITYGSKVIHNE	2015.158	2015.165
	78-86	KVKAVVKME	1031.623	1031.628
	87-103	GDNKMVTTFKGIKSVTE	1854.958	1854.963
	104-121	FNGDTITNTMTLGDIVYK	2002.977	2002.979
	104-127	FNGDTITNTMTLGDIVYKRVSKRI	2742.473	2742.461

* Cys69 is glutathionylated

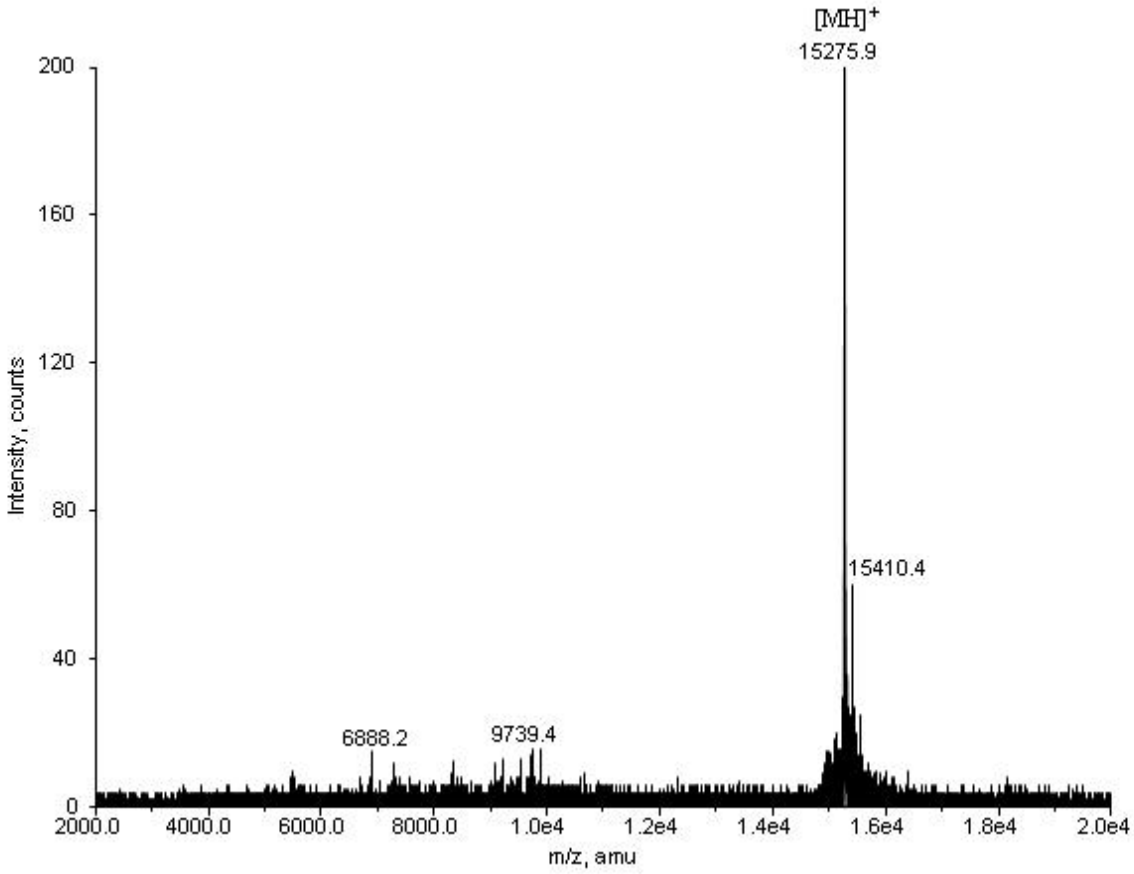

Figure 28: MALDI-TOF MS spectrum of recombinant L-FABP. Recombinant L-FABP was separated from any impurities by column chromatography, desalted, and subjected to MALDI-TOF MS analysis. The high intensity peak at *m*/*z* 15,275.9 corresponds to the molecular mass of the purified recombinant L-FABP, whereas the higher peak at m/z 15,410.4 is considered as the protein adduct with DHB matrix.

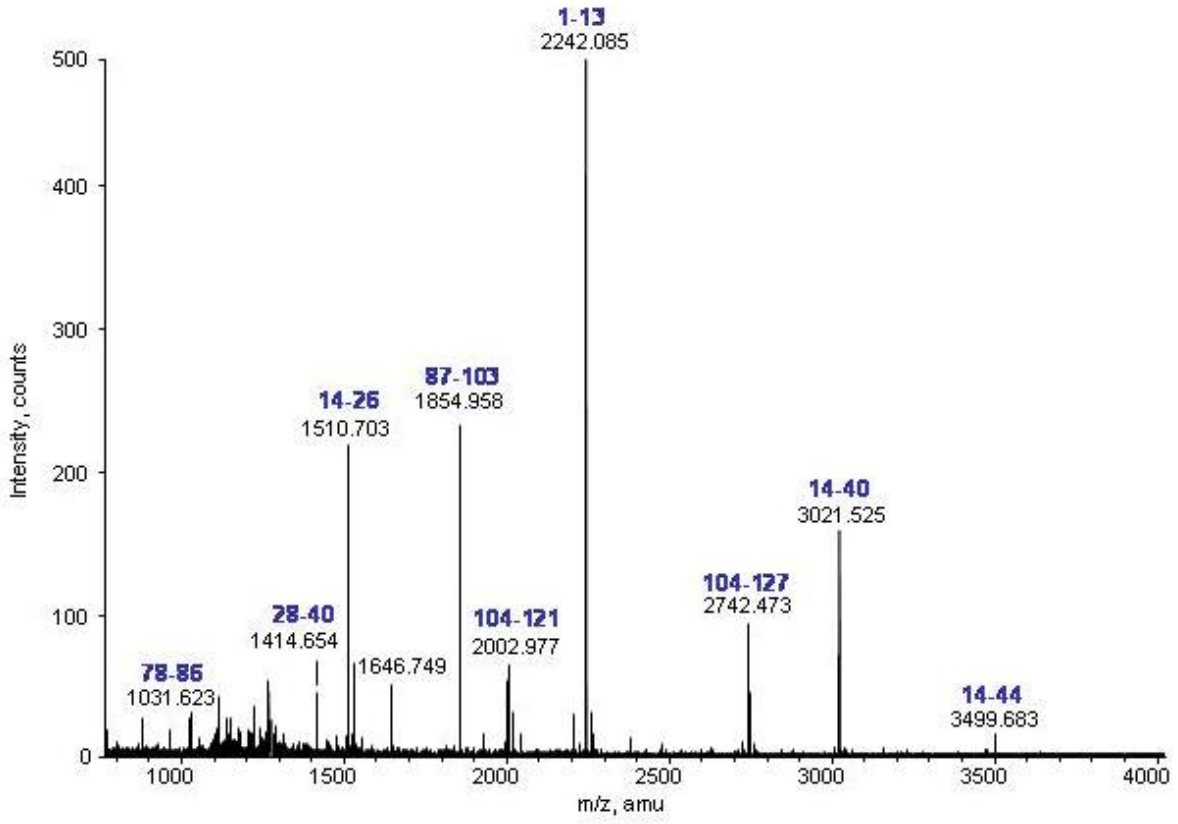

Figure 29: MALDI-TOF MS spectrum of the endoproteinase Glu-C digests of recombinant L-FABP.

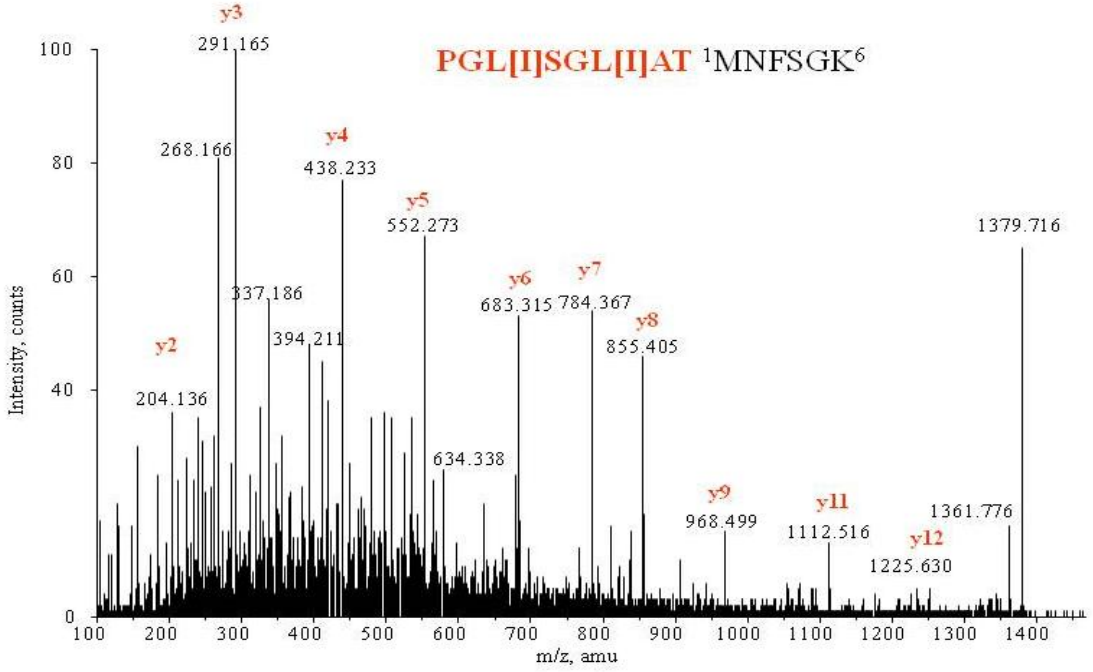

Figure 30: MS/MS spectrum of a Glu-C digested peptide at m/z 1526.70.

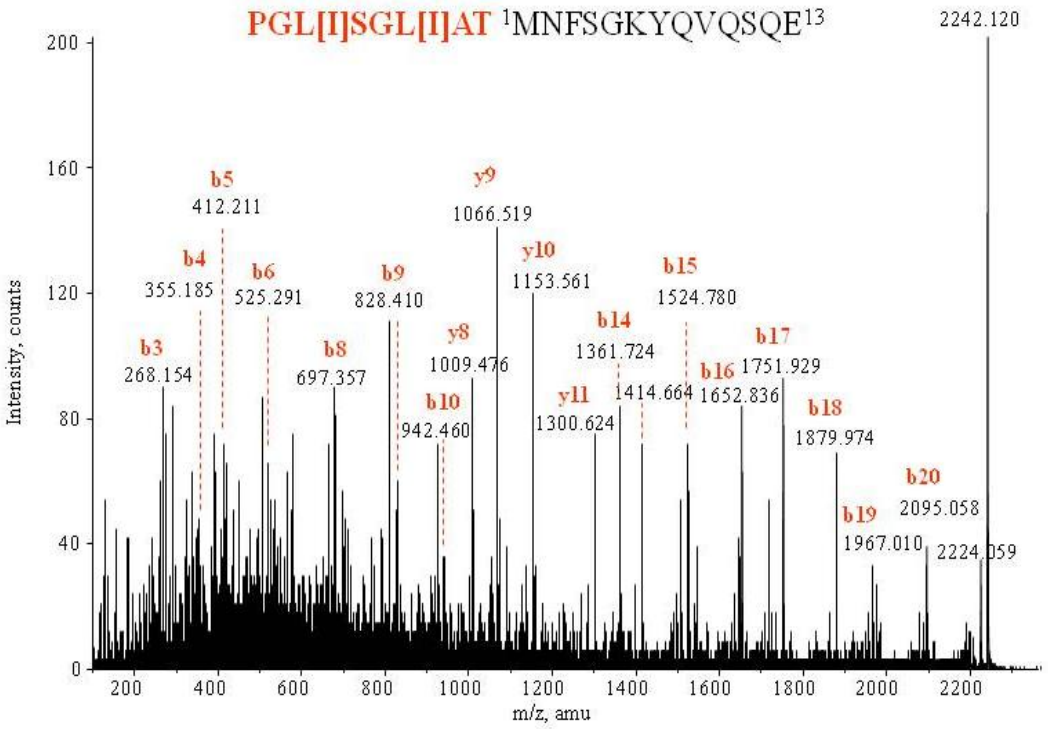

Figure 31: MS/MS spectrum of a trypsin digested peptide at m/z 1379.71. The amino acid sequence PGLSGLAT was present in the front of the protein synthesis start codon methionine. Presence of the PGLSGLAT artificial sequence observed at the N-terminal was derived from the GST infusion linker excised by PreScission protease.

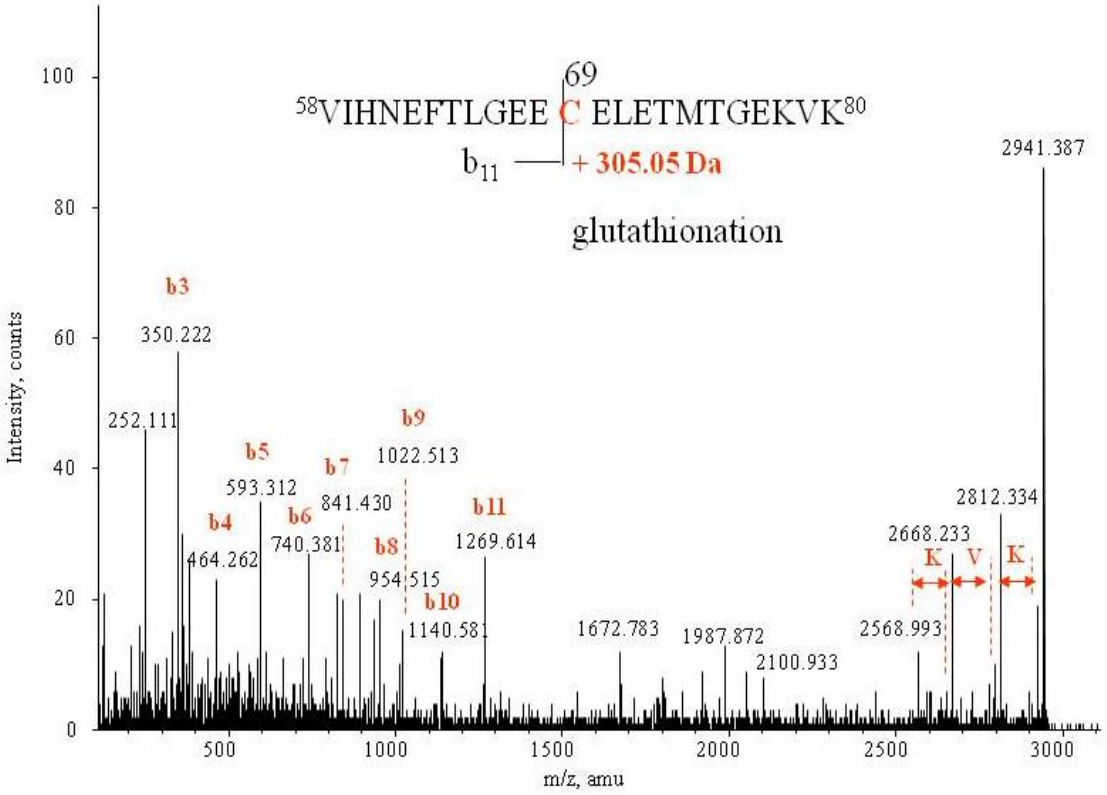

Figure 32: MS/MS spectrum of a trypsin digested peptide at m/z 2941.31. The sequence of the peptide (58-80) at m/z 2941.316 was confirmed as VIHNEFTLGEE **C**ELETMTGEKVK after trypsin digestion in MS/MS spectrum. This segment includes the incorporation of a glutathione onto Cys-69 yielding an additional mass of 305 Da.

2.2.5 Antioxidant activity of recombinant L-FABP

The DCF fluorescence assay was used as a convenient screening method for assessing the extent of the antioxidative potential of recombinant L-FABP. As shown in Figure 33, recombinant L-FABP inhibited H_2O_2 induced free radical release as observed by a decrease in DCF fluorescence intensity. Moreover, inhibition of the released free radicals was slightly increased with a corresponding increase in L-FABP concentration. Suppression of free radical release was greatest at 200 μM L-FABP which was be 65.8%±1.5% of control values ($P<0.001$).

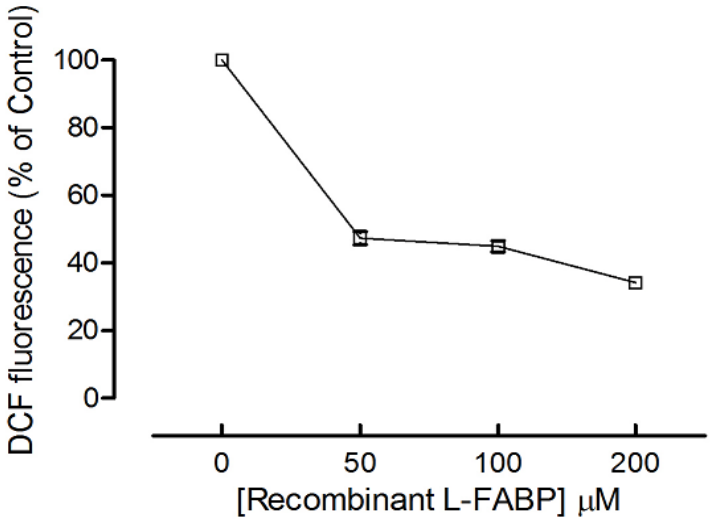

Figure 33: Reactive oxygen species (ROS) levels versus recombinant L-FABP concentration. ROS levels were assessed by quantitating the DCF fluorescence intensity at the various concentrations of recombinant L-FABP. The DCFH-DA was de-esterified in vitro and gave a final concentration of 60 μM of the stock solution. Reactions were carried out using 10–30 μM activated DCFH stock solution in 96 well plates with 200 μM H_2O_2 and varying concentrations of L-FABP as shown on the X-axis. Data represent mean ± SD (n = 4). (Note: Due to the small variation in the data obtained, error bars were not visible.)

2.3 Discussion

Expression of recombinant protein GST/L-FABP from E. coli

Several hosts such as E. coli (Liu, Flamoe et al. 2004), lactococcus (El Khattabi, van Roosmalen et al. 2008), yeast (Colbert, Anilionis et al. 1984), insect (Mathur, Das et al. 1996), and mammalian cell (Roopashree, Chai et al. 1995) cultures are being used for the specific purpose of expressing, growing, and isolating recombinant proteins. Due to the well-characterized genome, easy and inexpensive method for cultivation, high-throughput protein production and the various techniques available for genetic manipulation, *E. coli* remains the most common host system for protein expression in industrial applications. Various biochemical and genetic engineering strategies have been developed towards high-level gene expression in *E.coli* (Jana and Deb 2005). The most effective means to enhance recombinant protein production is to boost gene expression at a transcriptional level using a strong promoter system. Among them, the *tac* (de Boer, Comstock et al. 1983) and its derivatives such as *lacUV5* (Amann, Brosius et al. 1983), *lac* promoter (Polisky, Bishop et al. 1976), and *trc* (Brosius, Grosse et al. 1983) inducible by lactose or its analogue isopropyl-D-thiogalactopyranoside (IPTG) have been adopted extensively (Hallett, Grimshaw et al. 1990). Our studies established the presence of additional features in the constructed expression vector pGEX-6P-2 which contain a strong *tac* promoter, a multiple cloning site behind a unique *NcoI* site providing a translational start codon, and a *lacIq* allele of the lac repressor (Figure 26). The *tac* promoter is regulated by a *lac* repressor. A *lacIq* gene is a mutant of the *lac*I gene that synthesizes approximately 10-fold more repressor than the wild type (Muller-Hill, Crapo et al. 1968). The *lac*Iq gene product is a

repressor protein that binds to the operator region of the *tac* promoter preventing expression until induced by IPTG as shown in Figure 27A, lane 2. This maintains tight control over expression of the insert. In addition to offering chemically inducible and high-level expression, the vector allows mild chemical elution conditions for release of fusion proteins from the affinity medium. Thus, potentially detrimental effects on antigenicity and functional activity of the isolated protein are minimized.

Rapid Purification of recombinant GST/L-FABP from E. coli

This thesis describes the successful expression of plasmid encoded L-FABP in *E. coli using* a simple purification system. An affinity tag allowed for a more efficient and rapid purification of the recombinant protein. The most popular affinity tag is glutathione S-transferase (GST) (Smith and Johnson 1988). A large protein tag, such as GST, usually recognizes small ligands, is less expensive to use, and allows for more robust chromatography matrices in protein isolation. GST tagged proteins have been shown to be very water soluble with no observed aggregation (Martinez-Torrecuadrada, Romero et al. 2005). Proper protein folding is critical for pharmacological activity. Baneyx and Mujacic reported that recombinant GST tagged proteins retain proper folding characteristics when expressed in *E. coli* (Baneyx and Mujacic 2004) and prevent oxidative aggregation (Kaplan, Husler et al. 1997). The GST/L-FABP complex in these studies was hydrophilic with no observed aggregation (Figure 27A, lane 3), suggesting a proper folding pattern for the recombinant protein.

As will be discovered, after removal of the GST tag from the soluble GST/L-FABP complex, L-FABP demonstrated high antioxidant activity. This result highlights the most

important advantage of this system being that purified L-FABP retained its pharmacological activity while proteins expressed with the GST tag are devoid of activity until the GST tag is cleaved (Krautwald and Baccarini 1993). Therefore, this expression and purification system for L-FABP is critical for *in vitro* studies examining the chemical and biological properties of a protein.

Expression of the recombinant L-FABP

For functional and structural studies, enzymatic methods are most commonly used to remove affinity tags. Many enzymes such as factor Xa, enteropeptidase, and thrombin often cleave fusion proteins at locations other than the desired site (Choi, Song et al. 2001; Jenny, Mann et al. 2003). By contrast, the PreScission enzyme cleaves the GST tag with greater sequence specificity generating the target protein (Figure 27A, lane 4). After cleavage, the PreScission enzyme remains on the target protein after removal of the GST tag located at the N-terminal, preventing protein degradation and maintaining the immunogenicity of the protein (Carr, Miller et al. 1999). PreScission enzyme cleavage purification was carried out under simple conditions where contact between the cleavage buffer and recombinant L-FABP was easy to manipulate. PreScission protease is also active over a wide range of pH, ionic strength, and high efficiency (Furutani, Hata et al. 2005). Compared to enzymatic cleavage (PreScission protease), use of chemical cleavage (dithiothreitol; DTT) takes much longer for complete cleavage and recovery of the recombinant protein. Use of DTT cleavage was reported to occur by 16 hrs and took almost 40 hrs for complete cleavage (Chong, Mersha et al. 1997). Use of chymotrypsin-like “main proteinase” was unable to cleave more than 15% of its substrate during the

incubation period (van Aken, Benckhuijsen et al. 2006). Compared to the concentration used with "main proteinase", use of PreScission protease required a 20-fold lower enzyme concentration and was completed in 4 hr (Figure 27A, lane 4).

MALDI MS/MS identification of the FABP sequence

MS/MS measurements of the N-terminal peptide at m/z 2242.085 in Figure 31 showed that the amino acid sequence PGLSGLAT was present in the front of the protein synthesis start codon methionine. Presence of the PGLSGLAT artificial sequence (with an increased mass of 696.382 Da) observed at the N-terminal was derived from the GST infusion linker excised by PreScission protease. This peptide fragment has been reported to prevent protein degradation (Carr, Miller et al. 1999). The sequence of the peptide (58-80) at m/z 2941.316 was confirmed as VIHNEFTLGEE**C**ELETMTGEKVK after trypsin digestion in MS/MS spectrum (Figure 32). This segment includes the incorporation of a glutathione onto Cys-69 yielding an additional mass of 305 Da. This finding is consistent with the recombinant GST/L-FABP eluted by reduced glutathione. Thus, the additional mass of 696.382 Da together with the mass of the S-glutathionylation product (305.068 Da) yielded our total L-FABP mass of 15273.900 Da. The S-glutationylation modification may potentially serve to protect sulfhydryl groups in proteins from irreversible oxidation (Kenchappa and Ravindranath 2003). A more complete MALDI MS analysis of the observed peptide sequences of two enzymatic digests by trypsin and endoprotease Glu-C was shown in Table 14.

Antioxidant activity of recombinant L-FABP

The antioxidant activity of our recombinant L-FABP was measured using the DCF fluorescence assay to evaluate its protective function. Since L-FABP makes up approximately 2% of total cellular protein in hepatocytes or about 200-400 µM (Burnett, Lysenko et al. 1979), the antioxidant potential of L-FABP can be expected to be significant. As shown in Figure 33, by using H_2O_2 as a nonspecific free radical generator, 200 µM of recombinant L-FABP inactivated 65.8%±1.5% of the free radicals released by H_2O_2. Thus, L-FABP can inactivate a significant portion of the free radicals released through metabolic processes. Following clofibrate treatment the concentration of L-FABP could rise 2-3-fold (Bass, Manning et al. 1985), which would result in an even greater impact on intracellular free radical levels and further contribute to free radical scavenging activity. It is, therefore, not surprising that L-FABP protects the liver during periods of oxidative stress as was associated with cholestatic liver disease (Wang, Shen et al. 2007), hepatic steatosis (Harano, Yasui et al. 2006), or alcohol-induced liver injury (Gyamfi, Damjanov et al. 2008).

MALDI-TOF analysis (Table 14) showed that the recombinant L-FABP contained one cysteine and seven methionines in its amino acid sequence which was identical to the sequence reported by others (Murphy, Edmondson et al. 1999; She, Wang et al. 2002). Methionine residues in proteins are known to be oxidized to methionine sulfoxides [Met(O)] by reactive oxygen species and can be reduced back to the original form by methionine sulfoxide reductase (Levine, Mosoni et al. 1996). Similarly, the single cysteine group (Cys^{69}) of L-FABP in the presence of free radicals can form a sulfonic acid

intermediate (Cys-SOH) that is subsequently reduced by forming an intradisulfide bond through the action of thioredoxin (Wood, Schroder et al. 2003).

One of the cell's principal antioxidant defence mechanism includes glutathione (GSH). The reduced state of the cysteine in glutathione, for example, is used in the cell as a source of reducing equivalents protecting it from oxidative stress. Thus, it was proposed that the cysteine and seven methionine groups in L-FABP were responsible for the antioxidant activity of L-FABP. Utilization of cysteine and/or methionine mutant L-FABP in future experiments will facilitate dissection of the binding reaction in the absence of catalysis and the structural organization of the binding cavity with free radicals or ligands present.

In conclusion, our data indicate that the GST fusion system provides a simple and convenient way to produce large quantities of recombinant L-FABP. These data also serve to demonstrate that our recombinant L-FABP can decrease free radical levels in an *in vitro* system. Although the mechanism for L-FABP's free radical scavenging effects remained to be elucidated, it is highly likely that the cysteine and methinione amino acids are involved.

3. L-FABP antioxidant defence mechanism

3.1 Introduction

A unique property of L-FABP that has recently been uncovered is its antioxidant effect. L-FABP is known to bind polyunsaturated fatty acids (Ek, Cistola et al. 1997) and long-chain fatty acid peroxidation products (Raza, Pongubala et al. 1989). By binding polyunsaturated fatty acids, L-FABP modulates the availability of these fatty acids to intracellular oxidative pathways and in this manner, controls the amount of reactive oxygen species released within the cell. In addition to these well established functions, recent studies have shown that L-FABP plays a further role in the cellular antioxidant defence mechanism (Wang, Gong et al. 2005; Rajaraman, Wang et al. 2007; Wang, Shen et al. 2007). Using an L-FABP cDNA transfection model Wang et al (Wang, Gong et al. 2005) reported that hepatocytes containing L-FABP were associated with significantly lower levels of reactive oxygen species (ROS) compared to hepatocytes devoid of L-FABP. Using a bile-duct ligated model of cholestasis, the group further showed that clofibrate increased L-FABP levels were associated with improved hepatic function and reduced lipid peroxidation products (Wang, Shen et al. 2007). As discussed previously, the antioxidative function of L-FABP is thought to be due to its amino acid composition. L-FABP contains one cysteine and several methionine groups which are known to take part in cellular redox cycling. Thus, although the actual mechanism for the L-FABP antioxidant property is not known it is likely to involve these amino acids. Also unknown is whether L-FABP preferentially inactivates ROS released in the hydrophilic cytosolic environment

or in lipophilic environments such as membranes. In this part of the study, the mechanism and efficiency of the L-FABP antioxidant property in both aqueous and lipid environments were investigated. Free radicals were generated by either hydrophilic or lipophilic radical generators, where 2,2'-azobis(2-amidinopropane) dihydrochloride (AAPH) and 2,2'-azobis(2,4-dimethylvaleronitrile) (AMVN) were used as the source of water- and lipid-soluble peroxyl radicals, respectively (Niki 1990).

3.2 Results

3.2.1 Lipid peroxidation in the presence of AAPH and AMVN in vitro

In order to compare the effectiveness of antioxidants in both hydrophilic and lipophilic free radical generating systems, it was necessary to examine the effects of AAPH and AMVN free radical generators in a LDL solution. Levels of the lipid peroxidation product MDA were first examined as a function of varying concentrations of AMVN or AAPH (Figure. 34). The lipid soluble peroxyl radical generating system (AMVN) induced greater MDA production in LDL than the water soluble system (AAPH). Thus, for subsequent comparative work it was necessary to use AAPH and AMVN concentrations which induced similar amounts of MDA production (10 mM AMVN and 40 mM AAPH). Therefore, these concentrations were used in all *in vitro* studies.

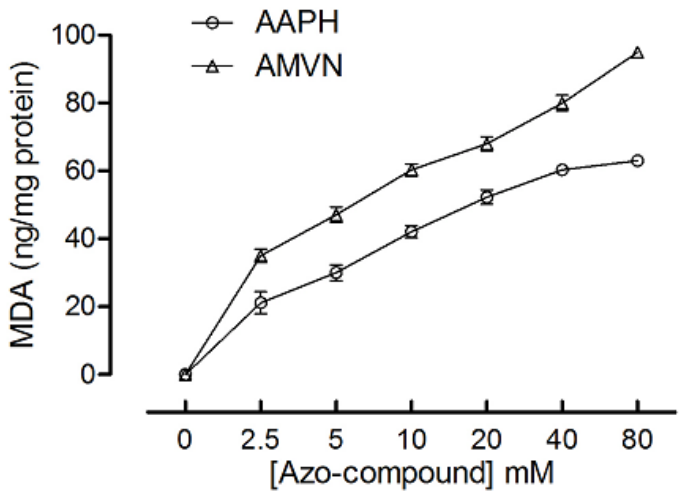

Figure 34: MDA formation as a function of incubation of LDL with varying concentrations of two different azo-compounds. LDL (1 mg cholesterol/ml) was incubated with different concentrations of AAPH and AMVN at 37°C for 90 min. Effect of 40 mM AAPH and 10 mM AMVN produced the same amount of MDA formation. Values represent mean ± SD, n=6.

3.2.2 Protection of ascorbic acid and α-tocopherol against lipid peroxidation induced by AAPH and AMVN

To compare the difference in antioxidant activity between L-FABP and ascorbic acid or α-tocopherol, LDL was incubated with 40 mM AAPH or 10 mM AMVN in the absence or presence of different concentrations of ascorbic acid or α-tocopherol (Figure 35 top and Figure 35 bottom). These two antioxidants inhibited the oxidation of LDL in a dose-dependent manner and were used as positive controls. In the AAPH generation system, 1 mM ascorbic acid was able to reduce MDA production by 60% (Figure 35 top). With AMVN, no significant protective effect against lipid peroxidation was observed in the 0 – 40 mM concentration range of ascorbic acid. At a concentration of 5 μM, α-tocopherol reduced more than 70% of MDA formation (Figure 35 top). The same concentration of α-tocopherol inhibited MDA production by less than 50% in the AMVN induced lipid peroxidation assay (Figure 35 bottom), indicating that α-tocopherol has a weaker effect in the inhibition of LDL oxidation by AMVN.

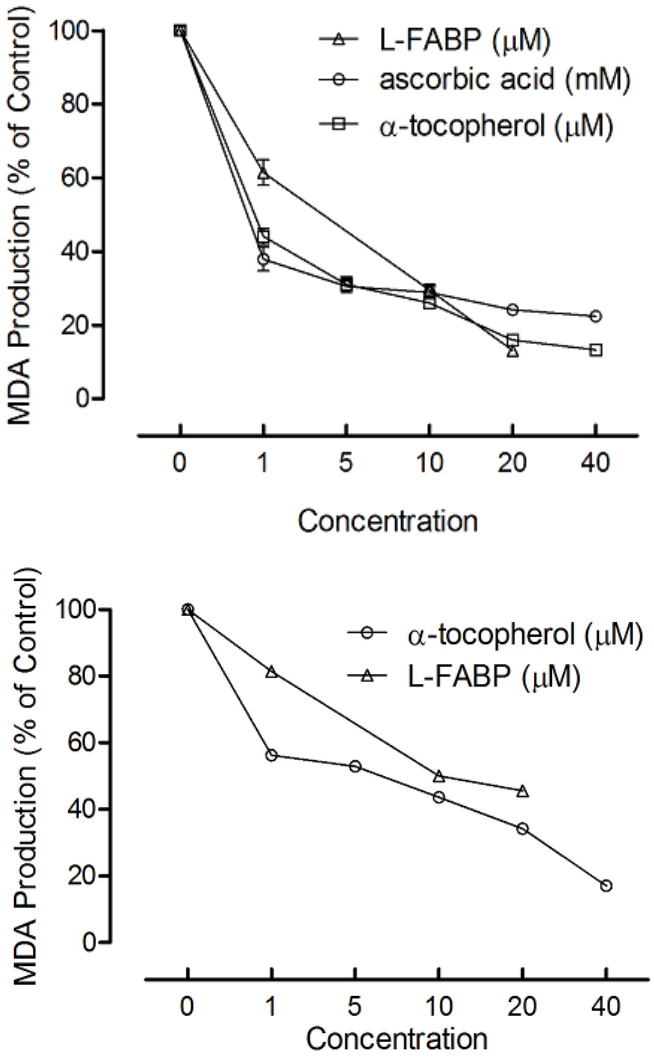

Figure 35: A comparison of the effect of ascorbic acid, α-tocopherol and L-FABP on AAPH and AMVN induced MDA production in LDL. Top: LDL (1 mg cholesterol/ml) was incubated with 40 mM AAPH ± different concentration of ascorbic acid, α-tocopherol and L-FABP for 90 min at 37°C. Bottom: LDL (1 mg cholesterol/ml) was incubated with 10 mM AMVN ± different concentration of α-tocopherol and L-FABP for 90 min at 37°C. Values represent mean ± SD, n=6.

3.2.3 Protection against lipid peroxidation by L-FABP in AAPH and AMVN

We were also interested in determining whether L-FABP is more effective as a hydrophilic or lipophilic free radical scavenger. Since L-FABP is water soluble it is predicted that most of the antioxidant properties may be directed in the cytosol. However, as a protein it also imparts some lipophilic properties and as such, some of the antioxidant property may occur within the lipophilic or cell membrane environment. Thus, we investigated the LDL oxidation levels mediated by 40 mM AAPH or 10 mM AMVN in the absence or presence of different L-FABP concentrations. As shown in Figure 36, there was a dose dependent inhibition in oxidized LDL with L-FABP on AAPH and AMVN induced MDA production. In the AAPH induced hydrophilic free radical generating system, a concentration of 1 μM L-FABP was able to reduce MDA formation by 40% and a 90% reduction in MDA formation was obtained when the concentration of L-FABP was increased to 20 μM. Figure 35 top shows that 10 μM L-FABP inhibited a similar amount of MDA production as 10 mM ascorbic acid and 10 μM α-tocopherol. At a concentration of 20 μM L-FABP, L-FABP protected against free radical damage much more so than either 20 μM α-tocopherol or 20 mM ascorbic acid.

L-FABP was less potent against MDA production when free radicals were induced by AMVN. Figure 36 shows that 20 μM of L-FABP provided greater antioxidant effect against lipid peroxidation induced by AAPH (90%) than that of AMVN (55%). Figure 35 bottom shows that 10 μM L-FABP inhibited 50% of MDA production and had a similar effect to that of 10 μM α-tocopherol in the AMVN induced lipophilic free radical generating system. Thus, the antioxidant activity of L-FABP is comparable to α-tocopherol but much greater than ascorbic acid at the same molar concentrations.

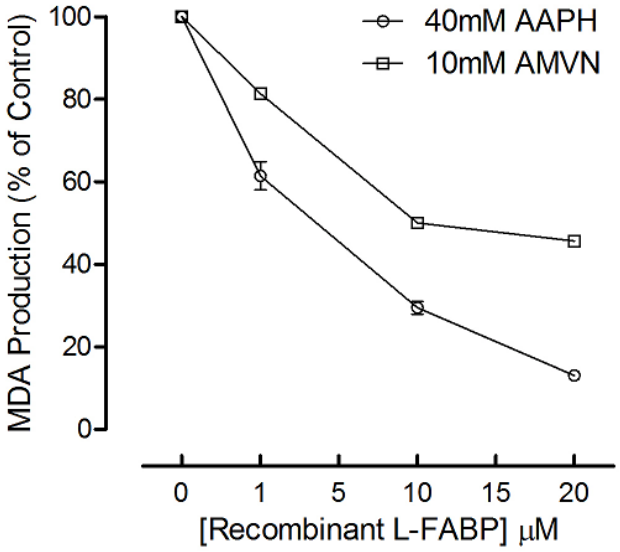

Figure 36: The effect of L-FABP on AAPH and AMVN induced MDA production in LDL. LDL (1 mg cholesterol/ml) was incubated with 40 mM AAPH or 10 mM AMVN ± different concentration of L-FABP for at 37°C 90 min. The graph shows the dose dependent manner of the lipid protective effect of L-FABP. Values represent mean ± SD, n=6.

3.2.4 Effect of ligand binding on the antioxidant activity of L-FABP

To determine whether long-chain fatty acid binding to L-FABP influences its antioxidant activity, LDL was incubated with either 40 mM AAPH or 10 mM AMVN in the absence or presence of 10 μM L-FABP which was preincubated with 30 μM α-bromo-palmitate (α-bromo-palmitate binds irreversible to L-FABP), or 30 μM palmitate (reversible binding). In the AAPH induced lipid peroxidation system, 10 μM L-FABP was able to significantly reduce MDA production by 70±2% ($p<0.001$) while α-bromo-palmitate and palmitate partially blocked the L-FABP antioxidative activity by 29±2% and 19±1%, respectively (Figure 37; compared to L-FABP no binding; $p<0.001$). In the AMVN induced lipid peroxidation system, 10 μM L-FABP was able to reduce MDA production by 50±1% while α-bromo-palmitate and palmitate blocked L-FABP antioxidative activity by 43±1% and 11±1%, respectively (Figure 37; compared to L-FABP no binding; $p<0.001$). These results indicate that blocking the L-FABP binding cavity attenuates some of the L-FABP antioxidant activity.

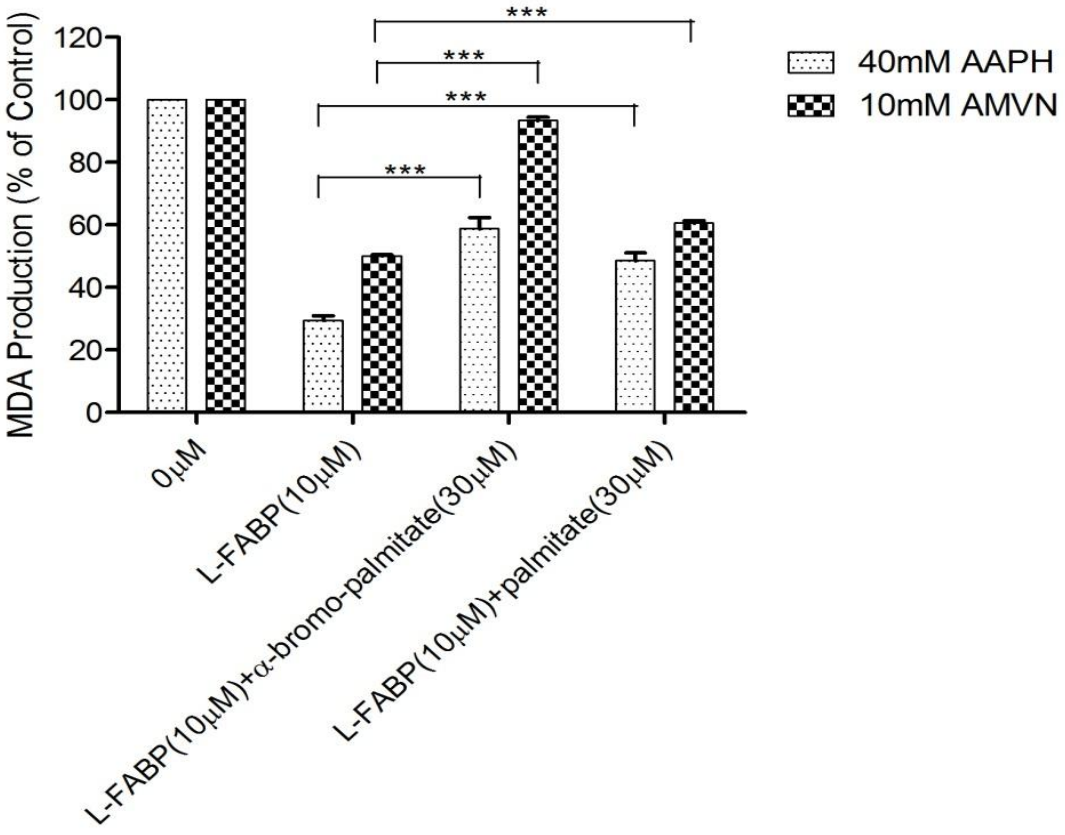

Figure 37: A comparison of the effect of recombinant L-FABP after binding with palmitate or α-bromo-palmitate on AAPH or AMVN induced MDA production in LDL. LDL (1 mg cholesterol/ml) was incubated with 40 mM AAPH or 10 mM AMVN for 90 min at 37°C ± L-FABP (10μM) ± palmitate or α-bromo-palmitate. Values represent mean ± SD, n=6.

3.2.5 The binding affinity of L-FABP to palmitate following oxidization by H_2O_2

Finally, to determine whether L-FABP oxidation influences its binding activity, L-FABP (50 µM) was incubated with 200 µM H_2O_2 and the binding affinity measured by calculating the unbound [^{3}H]-palmitate fraction (α). Albumin (BSA, 50 µM) was used as a positive control. Using the heptane:water partitioning method, the calculated α values in the presence of 50 µM L-FABP, 50 µM oxidized L-FABP or 50 µM BSA were $(7.48\pm0.77)\times10^{-6}$, $(1.40\pm0.19)\times10^{-5}$, and $(2.18\pm0.40)\times10^{-4}$, respectively. In the presence of H_2O_2, the binding affinity of 50 µM L-FABP with [^{3}H]-palmitate was significantly decreased compared to non-oxidized L-FABP (Table 15; $p<0.001$).

Table 15: [^{3}H]-palmitate heptane: buffer partition ratio and calculated the unbound [^{3}H]-palmitate fraction (α).

Group	Protein	Heptane:buffer partition ratio	α
1	50 µM L-FABP	0.0103±0.0011 (N=6)	$(7.48\pm0.77)\times10^{-6}$
2	50 µM L-FABP-H_2O_2	0.0193±0.0026 (N=6)	$(1.40\pm0.19)\times10^{-5}$
3	50 µM BSA	0.2998±0.0543 (N=6)	$(2.18\pm0.40)\times10^{-4}$

The binding affinity of L-FABP was calculated as the unbound [^{3}H]-palmitate fraction (α) BSA was used as a positive control. Values are mean±SD (n=6).

3.2.6 MALDI QqTOF mass to identify the modified recombinant L-FABP by AAPH or AMPH

To identify potential L-FABP oxidation products, 100 μM L-FABP was incubated with 40 mM AAPH or 10 mM AMVN and analyzed following separation using chromatography by MALDI-TOF MS. Analysis showed the major mass peak shift from *m*/*z* of 15,275.9 (L-FABP, Figure 38A) to 15,291.0 (L-FABP+AMVN, Figure 38B) or 15,352.0 (L-FABP+AAPH, Figure 38C). The mass shift of *m*/*z* 15,275.9 corresponded to ~80 Da oxidation product induced by AAPH. The mass shift of *m*/*z* 15,291.0 corresponded to a 16 Da oxidation product induced by AMVN.

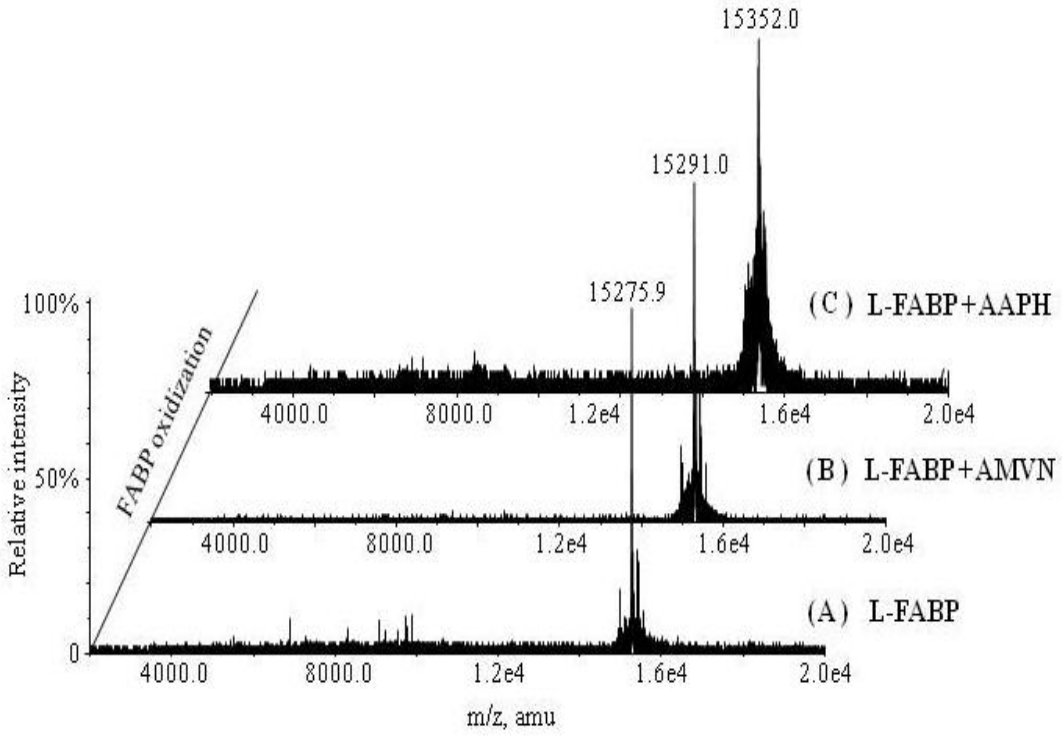

Figure 38: MALDI-TOF MS spectrum of recombinant L-FABP and L-FABP incubated with AAPH or AMVN. Samples were separated from impurities by column chromatography, desalted, and subjected to MALDI-TOF MS analysis. A: The high intensity peak at *m*/*z* 15,275.9 corresponds to the molecular mass of purified recombinant L-FABP. B: The high intensity peak at *m*/*z* 15,352.0 corresponds to the molecular mass of the recombinant L-FABP incubated with 40 mM AAPH. C: The high intensity peak at *m*/*z* 15,291.0 corresponds to the molecular mass of the recombinant L-FABP incubated with 10 mM AMVN.

3.2.7 MALDI QqTOF analyzed methionine and cysteine oxidized L-FABP groups

To identify the L-FABP oxidative peptides after incubation with AAPH or AMVN, 100 μM of L-FABP was incubated with 40 mM AAPH or 10 mM AMVN and the modified peptides mass fingerprint of the samples was carried out by in-solution digestion with endoproteinase Glu-C and analyzed by MALDI-TOF MS (L-FABP, Figure 39A; L-FABP+AMVN, Figure 39B; L-FABP+AAPH, Figure 39C). The methionine-containing peptides in the Glu-C digest of FABPs are shown in Table 16. In the MALDI MS spectrum of AAPH modified L-FABP (Figure 39C), the observed product 1-13+OX (*m*/*z* 2258.080), 14-26+OX/2OX (m/z 1526.705, 1542.706), 14-40+OX/2OX (m/z 3037.522, 3053.555), 87-103+OX (*m*/*z* 1870.946), 104-127+OX (*m*/*z* 2758.464) (OX=oxidized) corresponds to five oxidized methionine (Met^{1}, Met^{19}, Met^{22}, Met^{91} and Met^{113}) containing fragments, each provide evidence for oxidant modification of methionine by AAPH induced free radicals. In the MALDI MS spectrum of AMVN modified L-FABP (Figure 39B), the observed product 104-127+OX (*m*/*z* 2758.468) (OX=oxidized) corresponded to one oxidized methionine (Met^{113}) containing fragment, which provides evidence for oxidant modification of methionine by AMVN induced free radicals.

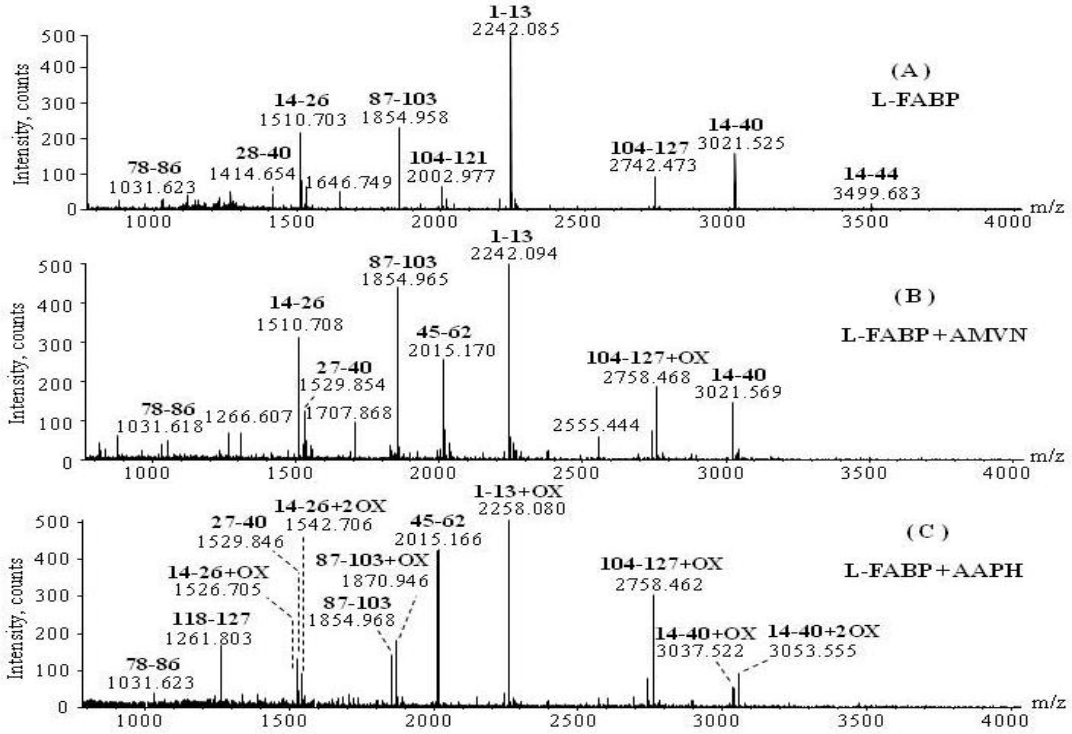

Figure 39: MALDI-TOF MS spectrum of the Glu-C digest of recombinant L-FABP containing peptide. A: purified recombinant L-FABP; B: recombinant L-FABP incubated with 40 mM AAPH; C: recombinant L-FABP incubated with 10 mM AMVN.

Table 16: MALDI MS analyses of the methionine-containing peptides in the Glu-C digests of FABPs

Calc. [MH]+	Peptide fragment	Peptide sequence	Oxidized residue	Observed relative intensity ratios between the unmodified peptide and its oxidized peptide counterparts **			
				L-FABP	L-FABP 10mM AMVN	L-FABP 10mM AMVN	L-FABP $-H_2O_2$
1031.628 1047.623	78-86 78-86 + OX	KVKAVVKME	Met85	100% 0%	- -	100% -	100% 0%
1510.707 1526.702 1542.697	14-26 14-26+OX* 14-26+2OX	NFEPFMKAMGLPE	Met19 Met22	91% 9% 0%	10% 41% 49%	91% 9% -	91% 9% 0%
1854.963 1870.958	87-103 87-103+OX	GDNKMVTTFKGIKSVTE	Met91	100% 0%	44% 56%	100% -	100% 0%
2242.084 2258.080	…1-13 …1-13+OX	….MNFSGKYQVQSQE	Met1	94% 6%	9% 91%	88% 12%	94% 6%
2742.461 2758.456	104-127 104-127+OX	FNGDTITNTMTLGDIVYKRVSKRI	Met113	91% 9%	21% 79%	17% 83%	91% 9%

* Met22 was the first oxidization site in this peptide as confirmed by MS/MS measurements.

** Percentage of the observed peptide peaks: the peak intensity / ∑ (the unmodified peptide intensity + its oxidized peptide intensity)

"-" denotes unobserved peak

3.2.8 MALDI QqTOF mass identity of H_2O_2 induced oxidized methionine

To identify the L-FABP oxidative peptides after incubation with H_2O_2, 50 μM of L-FABP was incubated with 200 μM H_2O_2 and the modified peptides mass fingerprinting of samples was carried out by in-solution digestion with endoproteinase Glu-C and analyzed by MALDI-TOF MS (L-FABP+H_2O_2, Figure 40). In the MALDI MS spectrum of H_2O_2 modified L-FABP, the observed product 1-13+OX (*m*/*z* 2258.083), 14-26+OX/2OX (m/z 1542.700), 14-40/44+OX/2OX (m/z 3053.541, 3531.753), 87-103+OX (*m*/*z* 1870.958), 104-127+OX (*m*/*z* 2758.464) (OX=oxidized) corresponded to five oxidized methionine (Met^1, Met^{19}, Met^{22}, Met^{91} and Met^{113}) containing fragments, each providing evidence for oxidant modification of methionine by H_2O_2 induced free radicals.

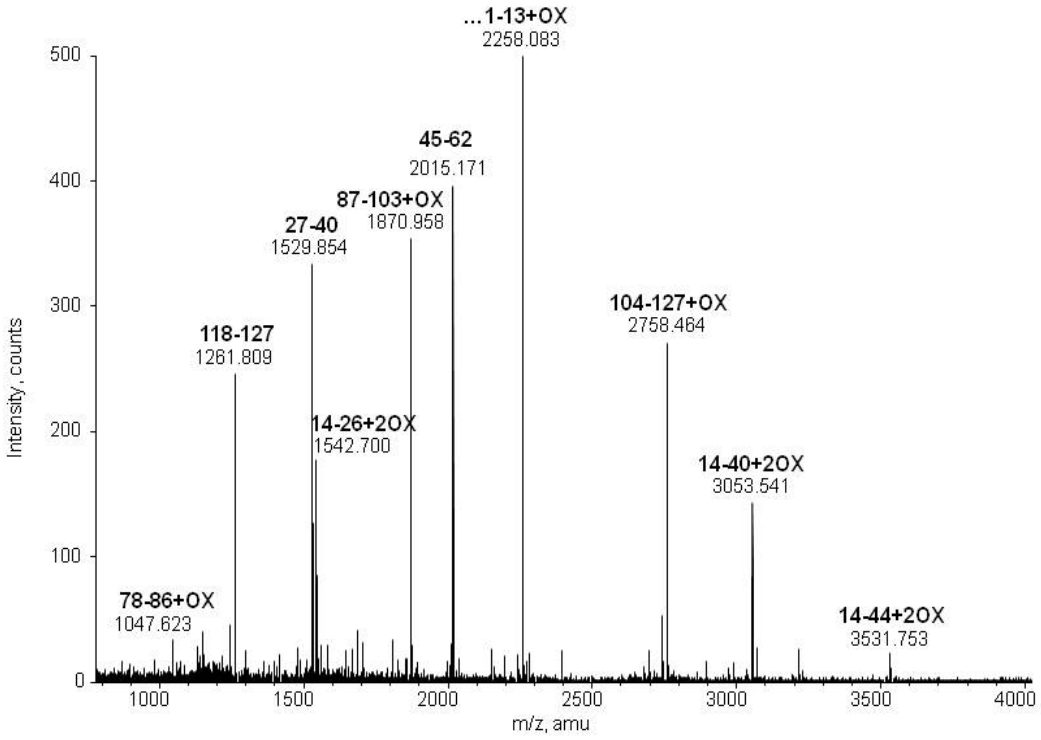

Figure 40: MALDI-TOF MS spectrum of the endoproteinase Glu-C digests of recombinant L-FABP incubated with H_2O_2.

3.3 Discussion

Damage by free radicals of lipophilic structures such as cell membranes or intracellular membranes may result in severe forms of cell damage and/or ultimately cell death. Lipid peroxidation products are especially important because they are highly reactive and able to form adducts with many cellular lipophilic macromolecules including cell membrane constituents, intracellular proteins, and nucleic acids (Moller and Wallin 1998). These adducts modify the structure and function of these cellular components and are involved in the pathogenesis of various degenerative diseases including heart disease (Savchenkova, Dudnik et al. 2003), diabetes (Stadler, Bonini et al. 2008), inflammation (Pang, Zhou et al. 2007), and neurodegenerative disorders (Hall 1992). Although cells contain specific antioxidant enzymes such as SOD, catalase, glutathione peroxidase, and compounds such as beta-carotene and tocopherols, the levels of these antioxidants may be too low to combat high concentrations of released free radicals. Moreover, many of these antioxidants direct their activity toward the aqueous milieu. α-Tocopherol, however, is a fat-soluble vitamin that may have some of its activity directed toward lipophilic structures (Massey, She et al. 1982).

Recent work by our research team has shown that in addition to being the intracellular counterpart to extracellular albumin, L-FABP also possesses strong antioxidant properties. Indeed, when clofibrate was used to increase L-FABP levels in animals subjected to bile-duct ligation, clofibrate treated animals had reduced levels of hepatic lipid peroxidation products and improved hepatic function (Wang, Shen et al. 2007). Clofibrate treated animals also had lower mortality rates (unpublished data). We speculated that L-FABP functions as an antioxidant during periods of cellular oxidative stress. Moreover, in a cell

transfection model, hepatocytes containing L-FABP had significantly lower ROS levels than those devoid of L-FABP (Wang, Gong et al. 2005). The mechanism whereby L-FABP inactivated ROS, however, was not elucidated.

Free radicals such as $O_2^{\cdot}$ and $OH^{\cdot}$ were initially thought to penetrate lipid bilayers with ease (Wagner, Buettner et al. 2000). More recent evidence, however, suggests that superoxides do not penetrate deeply into lipid bilayers but rather react at the surface or just below the surface of membranes (Gamliel, Afri et al. 2008). AMVN and AAPH are azo initiators that produce a slow and steady source of free radicals by known chemical decomposition mechanisms. AAPH is a water-soluble azo compound. Decomposition produces molecular nitrogen and 2 carbon radicals. The carbon radicals may combine to produce stable products or react with molecular oxygen to generate hydrophilic peroxyl radicals (Culbertson and Porter 2000). In the presence of LDL, AAPH released free radicals first oxidize the aqueous compartment of LDL (LDL has a hydrophobic core consisting of polyunsaturated fatty acids and esterified cholesterol molecules, which are surrounded by a shell of phospholipids and unesterified cholesterol) (Scanu and Wisdom 1972). AMVN, on the other hand, is a synthetic azo compound that dissociates spontaneously to form carbon-centered free radicals. Generation of carbon-centered radicals is directed at the lipophilic environment of membranes where its activity is sufficient to cause membrane phospholipid peroxidation (Niki 1990).

Using the free radical generators AAPH and AMVN together along with the positive control,ascorbic acid (hydrophilic antioxidant) and α-tocopherol (lipophilic antioxidant), we assessed the effectiveness of L-FABP as an antioxidant. Both α-tocopherol and ascorbic acid were effective in protecting LDL from free radicals generated by AAPH.

Using AMVN, however, ascorbic acid had no effect on inactivating free radicals while not surprisingly α-tocopherol was very effective. L-FABP was effective in inactivating free radicals released by both AAPH and AMVN. L-FABP is known to coat the surface of anionic phospholipid membranes (Davies, Thumser et al. 1999) and can prevent propagation of phospholipid oxidation reactions by reacting with the ROS in this environment. Where this becomes of particular importance is in the protection of cellular membranes during episodes of oxidative stress as is the case in fatty liver disease (Botella-Carretero, Balsa et al. 2008), coronary heart disease (Tornwall, Virtamo et al. 2004) and aging (Guarnieri, Giordano et al. 1996).

MALDI-TOF analysis was used to identify the mechanism of L-FABP's antioxidant activity. Sequence identification showed that in the AAPH hydrophilic system five of the seven methionine amino acids were oxidized. These included Met^{19}, Met^{22}, Met^{91}, Met^{1}, and $Met^{113.}$ Of these 5 amino acids Met^{1} was almost totally oxidized followed by Met^{113}, Met^{91}, Met^{22}, and Met^{19}. Met^{85} and Met^{74} were unavailable for reaction with free radicals. These findings likely reflect the positioning of these amino acids within the protein itself. Met^{74} is located at the L-FABP binding cavity side chain located on the $\beta E \beta F$ hairpin turn. This is an area of low solvent accessibility making it difficult to be accessible to free radicals (Thompson, Winter et al. 1997). Therefore, it is not surprising to observe that Met^{74} was not easily oxidized in either the AAPH or AMVN free radical systems. Similarly, the single cysteine group (Cys^{69}) of L-FABP in the presence of free radicals can form a sulfonic acid intermediate (Cys-SOH) that is subsequently reduced back by forming a disulfide bond through the action of thioredoxin (Pan and Bardwell 2006). Reactivity of

various amino acids was also investigated and showed that cysteine and methionine were the most reactive of all the amino acids (Sharp and Tomer 2007).

Binding of free radicals to one amino acid may also cause a conformational change in protein structure. This change could make other amino acids available or unavailable for reaction (Xu and Chance 2005). Using the lipophilic free radical generator AMVN, three of the seven methionines in L-FABP were available for reaction with Met^{74} and Met^{85} being unreactive in both systems and Met^{91} unreactive in the lipophilic system. Met^{113} was the only methionine residue with the highest degree of availability to free radicals (83%) in the AMVN system. Thus, MALDI-TOF MS analysis showed that several of the methionine groups in L-FABP do indeed react with free radicals. The cysteine group in our recombinant L-FABP was unavailable for reaction with free radicals because it was S-glutathionylated during the GST/L-FABP elution process by reduced glutathione. However, cysteine is well known to be highly effective in scavenging free radicals (Badaloo, Reid et al. 2002).

To understand the contribution of L-FABP's binding pocket to its antioxidant activity in both the hydrophilic and lipophilic free radical generating systems, we incubated L-FABP with palmitate or α-bromo-palmitate. Palmitate binding to L-FABP is a reversible process with distinct association and dissociation rate constants (Hung, Burczynski et al. 2003). α-Bromo-palmitate does not undergo esterification to form triglycerides. This property allows it to accumulate in the cytoplasm making it relatively more effective than palmitate at binding to L-FABP (Luxon 1996). Binding of palmitate to L-FABP decreased L-FABP's ability to inactivate free radicals, i.e., binding of long-chain fatty acids to L-FABP increased the amount of free radicals within the hydrophilic and lipophilic

environments. The amount of ROS when generated by AMVN was slightly higher than that generated by AAPH, suggesting that when palmitate is bound to the protein some methionine group(s) may be inaccessible for reaction with free radicals. This is especially evident in the lipophilic environment. Binding of α-bromo palmitate to L-FABP resulted in a more dramatic increase in ROS levels using the AMVN generator. While both systems resulted in higher ROS levels, these levels were higher in the lipophilic system. Met^{113} is known to be located in the binding cavity of L-FABP (Thompson, Winter et al. 1997). Since α-bromo palmitate is not metabolized it would be expected to bind to a larger extent than palmitate and block the accessibility of ROS to this amino acid. Similarly, binding of polyunsaturated long-chain fatty acids, that have binding constants much higher than that of palmitate, would be expected to have higher binding occupancy rates. In such cases Met^{113} would not be available for interaction with ROS. The methionine group within the L-FABP binding cavity is, therefore, of more importance when scavenging free radicals within a lipophilic environment. Met^{1} and Met^{22} are the only other two methionine groups that have the ability to react with ROS but to a lesser extent than Met^{113}. This is likely the reason why binding of α-bromo palmitate to L-FABP in the AMVN system did not totally abolish the antioxidant effect of L-FABP. It is conceivable that as L-FABP comes in close proximity to the membrane surface, the protein orientates itself such that the ligand binding pocket face is open to the membrane. This could occur by electrostatic interactions between the cell surface and protein. Such interactions have been shown to occur for heart-FABP and membranes (Herr, Aronson et al. 1996). In this manner L-FABP could interact with ROS at lipophilic interfaces. The fact that only 10% of the released free radicals were scavenged by L-FABP in the presence of α-bromo palmitate indicated that Met^{113} in L-

FABP binding cavity is likely the key amino acid that is largely responsible for L-FABP antioxidant activity in AMVN induced lipid peroxidation. On the other hand, by calculating the unbound [^{3}H]-palmitate fraction (α), we compared the differences of binding affinity between L-FABP and oxidized-L-FABP. We found that the binding affinity of L-FABP with [^{3}H]-palmitate was significantly decreased after L-FABP was oxidized by H_2O_2. The results suggest that when L-FABP is exposed to free radicals, the binding pockets of L-FABP are less accessible for the ligands. Further studies are required to determine the exact role of the binding cavity of L-FABP in relation to its antioxidant activity. As the positive control, the binding affinity of BSA with [^{3}H]-palmitate was lower than published values (Elmadhoun, Wang et al. 1998) and may likely be due to radiolabeled [^{3}H]-palmitate impurities and/or the volatilization of the heptane phase.

In summary, the TBARS assay showed that L-FABP protected LDL from oxidation with a similar potency to α-tocopherol but much greater potency than ascorbic acid. MALDI-TOF MS analysis showed that the methionine groups of L-FABP were responsible for the majority of its antioxidant activity in both lipophilic and hydrophilic systems. Met^{113} located in the L-FABP binding cavity appeared to be the most important amino acid for reacting with ROS in the lipophilic free radical generating system. Overall, these results demonstrate that rat L-FABP can act as a potent cellular antioxidant and therefore its role in disease states should be elucidated.

IV CONCLUSION

From the first discovery of L-FABP in the late 1960's, we have learnt that L-FABP plays an important role in cellular homeostasis, lipid metabolism and fatty acid binding and transport. Although cell culture and whole animal studies have revealed that L-FABP expression protects cells from oxidative stress, however, the molecular mechanism of this activity has yet to be determined. In the present study, we documented the cellular regulation mechanisms and molecular characteristics of L-FABP in the setting of oxidative stress.

Pharmacological agents such as PPAR agonists (statin and fibrate drugs) work through the PPAR:RXR system in the nucleus to increase L-FABP mRNA and protein levels. However, the precise mechanism, i.e. enhanced transcription, enhanced translation, and/or suppressed degradation was not clear. In the current study, clofibrate was observed to enhance transcription and suppress degradation of L-FABP mRNA. Further studies are required to delineate how clofibrate induced stabilization of L-FABP mRNA. The current studies also revealed that MK-886 (PPARα antagonist) reverses the clofibrate induced increases in L-FABP levels. Somewhat surprising was the finding that GW-9662 (PPARγ antagonist) had an inhibitory effect on clofibrate enhanced L-FABP levels as clofibrate is not thought to act through PPARγ receptors (Nanji, Dannenberg et al. 2004).

By regulating L-FABP expression, intracellular free radical levels shown by DCF fluorescence assay were inhibited in the setting of oxidative stress. Moreover, knockdown of L-FABP protein levels by RNA interference (siRNA) revealed that the reduction in

DCF fluorescence was due to the presence of L-FABP. Therefore, by virtue of its high intracellular levels, L-FABP represents an important protein in hepatocellular antioxidant system. By extension, treatment with pharmacological agents aimed at increasing L-FABP levels would be expected to improve the outcomes of some forms of liver diseases such as NAFLD and NASH where oxidative stress levels are increased.

Another novel feature of this work was in defining the molecular mechanism of L-FABP's antioxidant activity. By employing recombinant technology, we achieved the successful extraction of sufficient quantities of rat L-FABP to complete *in vitro* studies. Using the GST fusion system to produce and later extract L-FABP from *E. coli* was pivotal in defining the molecular mechanism of action. In vitro studies were then explored to elucidate the type of free radical (lipophilic or hydrophilic) was inactivated by L-FABP. Our results indicate that the susceptibility of L-FABP to AAPH or AMVN induced free radicals positively correlated with methionine groups within L-FABP. Moreover, MALDI-TOF results demonstrated the contribution of each methionine group within L-FABP in its ability to inactivate free radicals. The L-FABP binding site was also shown to be pivotal in inactivating free radicals released within the lipophilic milieu of membranes. These studies allow us to postulate a potential mechanism for inactivation of free radicals within the vicinity of membranes.

Because L-FABP coats the surface of anionic phospholipids membranes (Davies, Thumser et al. 1999), it may prevent the propagation of phospholipids oxidation reactions by inactivating ROS within this environment. Thus, the trajectory of the L-FABP binding site to the membrane structure is important. L-FABP would have to approach the membrane with its binding site open to the membrane. In this manner the methionine

group within the protein (Met^{113}) is available to inactivate free radicals in the vicinity. Generating mutants in methionine residues, particularly in several residues that are critical (e.g. Met^{113}), would further enhance our understanding of this process. It is known that methionine sulfoxide reductases reduces methionine sulfoxide residues *in vitro* (Xiong, Chen et al. 2006), and further studies are required to elucidate which class of methionine sulfoxide reductases act on L-FABP to reduce methionine sulfoxide *in vivo.*

In conclusion, oxidative stress plays an important role in the pathogenesis of various liver diseases. Our findings indicate that L-FABP is a potent antioxidant and intracellular L-FABP levels can be increased through pharmacological activation of PPARα without interfere with its antioxidant properties. Our findings also help to elucidate the mechanisms, whereby, L-FABP serves as an antioxidant. Together, these findings enhance our understanding and may serve as the bases for a novel approach to the treatment of patients with chronic liver diseases.

VI REFERENCES

Abd El Mohsen, M. M., M. M. Iravani, et al. (2005). "Age-associated changes in protein oxidation and proteasome activities in rat brain: modulation by antioxidants." Biochem Biophys Res Commun **336**(2): 386-91.

Ahmed, N., P. J. Thornalley, et al. (2004). "Processing of protein glycation, oxidation and nitrosation adducts in the liver and the effect of cirrhosis." J Hepatol **41**(6): 913-9.

Akhilender Naidu, K. A., K. A. Abhinender Naidu, et al. (1994). "Lipoxygenase: a non-specific oxidative pathway for xenobiotic metabolism." Prostaglandins Leukot Essent Fatty Acids **50**(4): 155-9.

Albano, E., E. Mottaran, et al. (2005). "Immune response towards lipid peroxidation products as a predictor of progression of non-alcoholic fatty liver disease to advanced fibrosis." Gut **54**(7): 987-93.

Amann, E., J. Brosius, et al. (1983). "Vectors bearing a hybrid trp-lac promoter useful for regulated expression of cloned genes in Escherichia coli." Gene **25**(2-3): 167-78.

Ames, B. N., M. K. Shigenaga, et al. (1993). "DNA lesions, inducible DNA repair, and cell division: three key factors in mutagenesis and carcinogenesis." Environ Health Perspect **101 Suppl 5**: 35-44.

Antonenkov, V. D., R. T. Sormunen, et al. (2006). "Localization of a portion of the liver isoform of fatty-acid-binding protein (L-FABP) to peroxisomes." Biochem J **394**(Pt 2): 475-84.

Arteel, G. E., J. A. Raleigh, et al. (1996). "Acute alcohol produces hypoxia directly in rat liver tissue in vivo: role of Kupffer cells." Am J Physiol **271**(3 Pt 1): G494-500.

Aygen, B., H. Celiker, et al. (2008). "The effects of trimetazidine on lipid peroxidation in patients with end-stage renal disease." Methods Find Exp Clin Pharmacol **30**(10): 757-60.

Badaloo, A., M. Reid, et al. (2002). "Cysteine supplementation improves the erythrocyte glutathione synthesis rate in children with severe edematous malnutrition." Am J Clin Nutr **76**(3): 646-52.

Bae, Y. S., S. W. Kang, et al. (1997). "Epidermal growth factor (EGF)-induced generation of hydrogen peroxide. Role in EGF receptor-mediated tyrosine phosphorylation." J Biol Chem **272**(1): 217-21.

Baldwin, A. S., Jr. (1996). "The NF-kappa B and I kappa B proteins: new discoveries and insights." Annu Rev Immunol **14**: 649-83.

Balendiran, G. K., F. Schnutgen, et al. (2000). "Crystal structure and thermodynamic analysis of human brain fatty acid-binding protein." J Biol Chem **275**(35): 27045-54.

Ballif, B. A. and J. Blenis (2001). "Molecular mechanisms mediating mammalian mitogen-activated protein kinase (MAPK) kinase (MEK)-MAPK cell survival signals." Cell Growth Differ **12**(8): 397-408.

Banaszak, L., N. Winter, et al. (1994). "Lipid-binding proteins: a family of fatty acid and retinoid transport proteins." Adv Protein Chem **45**: 89-151.

Bando, N., H. Hayashi, et al. (2004). "Participation of singlet oxygen in ultraviolet-a-induced lipid peroxidation in mouse skin and its inhibition by dietary beta-carotene: an ex vivo study." Free Radic Biol Med **37**(11): 1854-63.

Baneyx, F. and M. Mujacic (2004). "Recombinant protein folding and misfolding in Escherichia coli." Nat Biotechnol **22**(11): 1399-408.

Barzilai, A. and K. Yamamoto (2004). "DNA damage responses to oxidative stress." DNA Repair (Amst) **3**(8-9): 1109-15.

Bass, N. M. (1985). "Function and regulation of hepatic and intestinal fatty acid binding proteins." Chem Phys Lipids **38**(1-2): 95-114.

Bass, N. M. (1988). "The cellular fatty acid binding proteins: aspects of structure, regulation, and function." Int Rev Cytol **111**: 143-84.

Bass, N. M., J. A. Manning, et al. (1985). "Regulation of the biosynthesis of two distinct fatty acid-binding proteins in rat liver and intestine. Influences of sex difference and of clofibrate." J Biol Chem **260**(3): 1432-6.

Baumgardner, J. N., K. Shankar, et al. (2008). "A new model for nonalcoholic steatohepatitis in the rat utilizing total enteral nutrition to overfeed a high-polyunsaturated fat diet." Am J Physiol Gastrointest Liver Physiol **294**(1): G27-38.

Berlett, B. S. and E. R. Stadtman (1997). "Protein oxidation in aging, disease, and oxidative stress." J Biol Chem **272**(33): 20313-6.

Bernlohr, D. A., M. A. Simpson, et al. (1997). "Intracellular lipid-binding proteins and their genes." Annu Rev Nutr **17**: 277-303.

Berry, S. A., J. B. Yoon, et al. (1993). "Hepatic fatty acid-binding protein mRNA is regulated by growth hormone." J Am Coll Nutr **12**(6): 638-42.

Bilzer, M., H. Jaeschke, et al. (1999). "Prevention of Kupffer cell-induced oxidant injury in rat liver by atrial natriuretic peptide." Am J Physiol **276**(5 Pt 1): G1137-44.

Bishop-Bailey, D. (2000). "Peroxisome proliferator-activated receptors in the cardiovascular system." Br J Pharmacol **129**(5): 823-34.

Border, W. A. and N. A. Noble (1994). "Transforming growth factor beta in tissue fibrosis." N Engl J Med **331**(19): 1286-92.

Bordewick, U., M. Heese, et al. (1989). "Compartmentation of hepatic fatty-acid-binding protein in liver cells and its effect on microsomal phosphatidic acid biosynthesis." Biol Chem Hoppe Seyler **370**(3): 229-38.

Botella-Carretero, J. I., J. A. Balsa, et al. (2008). "Retinol and alpha-Tocopherol in Morbid Obesity and Nonalcoholic Fatty Liver Disease." Obes Surg.

Brosius, S., F. Grosse, et al. (1983). "Subspecies of DNA polymerase alpha from calf thymus with different fidelity in copying synthetic template-primers." Nucleic Acids Res **11**(1): 193-202.

Brown, J. R., E. Nigh, et al. (1998). "Fos family members induce cell cycle entry by activating cyclin D1." Mol Cell Biol **18**(9): 5609-19.

Brown, K. E., J. E. Poulos, et al. (1997). "Effect of vitamin E supplementation on hepatic fibrogenesis in chronic dietary iron overload." Am J Physiol **272**(1 Pt 1): G116-23.

Buege, J. A. and S. D. Aust (1978). "Microsomal lipid peroxidation." Methods Enzymol **52**: 302-10.

Bujanda, L., E. Hijona, et al. (2008). "Resveratrol inhibits nonalcoholic fatty liver disease in rats." BMC Gastroenterol **8**: 40.

Burczynski, F. J., S. M. Pond, et al. (1993). "Calibration of albumin-fatty acid binding constants measured by heptane-water partition." Am J Physiol **265**(3 Pt 1): G555-63.

Burnett, D. A., N. Lysenko, et al. (1979). "Utilization of long chain fatty acids by rat liver: studies of the role of fatty acid binding protein." Gastroenterology **77**(2): 241-9.

Carr, S., J. Miller, et al. (1999). "Expression of a recombinant form of the V antigen of Yersinia pestis, using three different expression systems." Vaccine **18**(1-2): 153-9.

Castelao, J. E. and M. Gago-Dominguez (2008). "Risk factors for cardiovascular disease in women: relationship to lipid peroxidation and oxidative stress." Med Hypotheses **71**(1): 39-44.

Catala, M., A. Anton, et al. (1999). "Characterization of the simultaneous binding of Escherichia coli endotoxin to Kupffer and endothelial liver cells by flow cytometry." Cytometry **36**(2): 123-30.

Catarzi, S., D. Degl'Innocenti, et al. (2002). "The role of H2O2 in the platelet-derived growth factor-induced transcription of the gamma-glutamylcysteine synthetase heavy subunit." Cell Mol Life Sci **59**(8): 1388-94.

Chan, L., C. F. Wei, et al. (1985). "Human liver fatty acid binding protein cDNA and amino acid sequence. Functional and evolutionary implications." J Biol Chem **260**(5): 2629-32.

Chen, L., R. Na, et al. (2008). "Lipid peroxidation up-regulates BACE1 expression in vivo: a possible early event of amyloidogenesis in Alzheimer's disease." J Neurochem **107**(1): 197-207.

Chen, S. H., P. Van Tuinen, et al. (1986). "Human liver fatty acid binding protein gene is located on chromosome 2." Somat Cell Mol Genet **12**(3): 303-6.

Chevion, M., E. Berenshtein, et al. (2000). "Human studies related to protein oxidation: protein carbonyl content as a marker of damage." Free Radic Res **33 Suppl**: S99-108.

Chmurzynska, A. (2006). "The multigene family of fatty acid-binding proteins (FABPs): function, structure and polymorphism." J Appl Genet **47**(1): 39-48.

Choi, S. I., H. W. Song, et al. (2001). "Recombinant enterokinase light chain with affinity tag: expression from Saccharomyces cerevisiae and its utilities in fusion protein technology." Biotechnol Bioeng **75**(6): 718-24.

Chong, S., F. B. Mersha, et al. (1997). "Single-column purification of free recombinant proteins using a self-cleavable affinity tag derived from a protein splicing element." Gene **192**(2): 271-81.

Chung, S. W., A. Toriba, et al. (2008). "Activation of 5-lipoxygenase and NF-kappa B in the action of acenaphthenequinone by modulation of oxidative stress." Toxicol Sci **101**(1): 152-8.

Cistola, D. P., J. C. Sacchettini, et al. (1989). "Fatty acid interactions with rat intestinal and liver fatty acid-binding proteins expressed in Escherichia coli. A comparative 13C NMR study." J Biol Chem **264**(5): 2700-10.

Cochrane, C. G. (1991). "Mechanisms of oxidant injury of cells." Mol Aspects Med **12**(2): 137-47.

Colbert, D., A. Anilionis, et al. (1984). "Molecular organization of the protein A gene and its expression in recombinant host organisms." J Biol Response Mod **3**(3): 255-9.

Corton, J. C., P. J. Lapinskas, et al. (2000). "Central role of PPARalpha in the mechanism of action of hepatocarcinogenic peroxisome proliferators." Mutat Res **448**(2): 139-51.

Cowan, S. W., M. E. Newcomer, et al. (1993). "Crystallographic studies on a family of cellular lipophilic transport proteins. Refinement of P2 myelin protein and the structure determination and refinement of cellular retinol-binding protein in complex with all-trans-retinol." J Mol Biol **230**(4): 1225-46.

Cubero, F. J. and N. Nieto (2008). "Ethanol and arachidonic acid synergize to activate Kupffer cells and modulate the fibrogenic response via tumor necrosis factor alpha, reduced glutathione, and transforming growth factor beta-dependent mechanisms." Hepatology **48**(6): 2027-39.

Culbertson, S. M. and N. A. Porter (2000). "Design of unsymmetrical azo initiators to increase radical generation efficiency in low-density lipoproteins." Free Radic Res **33**(6): 705-18.

Czaja, M. J., H. Liu, et al. (2003). "Oxidant-induced hepatocyte injury from menadione is regulated by ERK and AP-1 signaling." Hepatology **37**(6): 1405-13.

D'Odorico, A., A. Melis, et al. (1999). "Oxygen-derived free radical production by peripheral blood neutrophils in chronic cholestatic liver diseases." Hepatogastroenterology **46**(27): 1831-5.

Davies, J. K., A. E. Thumser, et al. (1999). "Binding of recombinant rat liver fatty acid-binding protein to small anionic phospholipid vesicles results in ligand release: a model for interfacial binding and fatty acid targeting." Biochemistry **38**(51): 16932-40.

de Boer, H. A., L. J. Comstock, et al. (1983). "The tac promoter: a functional hybrid derived from the trp and lac promoters." Proc Natl Acad Sci U S A **80**(1): 21-5.

De Cabo, R., R. Cabello, et al. (2004). "Calorie restriction attenuates age-related alterations in the plasma membrane antioxidant system in rat liver." Exp Gerontol **39**(3): 297-304.

de Gruijl, F. R., H. J. van Kranen, et al. (2001). "UV-induced DNA damage, repair, mutations and oncogenic pathways in skin cancer." J Photochem Photobiol B **63**(1-3): 19-27.

Delimaris, I., S. Georgopoulos, et al. (2008). "Serum oxidizability, total antioxidant status and albumin serum levels in patients with aneurysmal or arterial occlusive disease." Clin Biochem **41**(9): 706-11.

Di Pietro, S. M. and J. A. Santome (2000). "Isolation, characterization and binding properties of two rat liver fatty acid-binding protein isoforms." Biochim Biophys Acta **1478**(2): 186-200.

Divine, J. K., L. J. Staloch, et al. (2004). "GATA-4, GATA-5, and GATA-6 activate the rat liver fatty acid binding protein gene in concert with HNF-1alpha." Am J Physiol Gastrointest Liver Physiol **287**(5): G1086-99.

Dixon, Z. R., F. S. Shie, et al. (1998). "The effect of a low carotenoid diet on malondialdehyde-thiobarbituric acid (MDA-TBA) concentrations in women: a placebo-controlled double-blind study." J Am Coll Nutr **17**(1): 54-8.

Dormann, P., T. Borchers, et al. (1993). "Amino acid exchange and covalent modification by cysteine and glutathione explain isoforms of fatty acid-binding protein occurring in bovine liver." J Biol Chem **268**(22): 16286-92.

Dreyer, C., G. Krey, et al. (1992). "Control of the peroxisomal beta-oxidation pathway by a novel family of nuclear hormone receptors." Cell **68**(5): 879-87.

Drueke, T., V. Witko-Sarsat, et al. (2002). "Iron therapy, advanced oxidation protein products, and carotid artery intima-media thickness in end-stage renal disease." Circulation **106**(17): 2212-7.

Egelhofer, V., K. Bussow, et al. (2000). "Improvements in protein identification by MALDI-TOF-MS peptide mapping." Anal Chem **72**(13): 2741-50.

Ek, B. A., D. P. Cistola, et al. (1997). "Fatty acid binding proteins reduce 15-lipoxygenase-induced oxygenation of linoleic acid and arachidonic acid." Biochim Biophys Acta **1346**(1): 75-85.

El Khattabi, M., M. L. van Roosmalen, et al. (2008). "Lactococcus lactis as expression host for the biosynthetic incorporation of tryptophan analogues into recombinant proteins." Biochem J **409**(1): 193-8.

Elmadhoun, B. M., G. Q. Wang, et al. (1998). "Binding of [3H]palmitate to BSA." Am J Physiol **275**(4 Pt 1): G638-44.

Erlejman, A. G., S. V. Verstraeten, et al. (2004). "The interaction of flavonoids with membranes: potential determinant of flavonoid antioxidant effects." Free Radic Res **38**(12): 1311-20.

Ersoz, G., F. Gunsar, et al. (2005). "Management of fatty liver disease with vitamin E and C compared to ursodeoxycholic acid treatment." Turk J Gastroenterol **16**(3): 124-8.

Esterbauer, H., R. J. Schaur, et al. (1991). "Chemistry and biochemistry of 4-hydroxynonenal, malonaldehyde and related aldehydes." Free Radic Biol Med **11**(1): 81-128.

Evans, M. D., M. Dizdaroglu, et al. (2004). "Oxidative DNA damage and disease: induction, repair and significance." Mutat Res **567**(1): 1-61.

Faure, P., L. Troncy, et al. (2005). "Albumin antioxidant capacity is modified by methylglyoxal." Diabetes Metab **31**(2): 169-77.

Feinberg, A. P. and B. Vogelstein (1983). "A technique for radiolabeling DNA restriction endonuclease fragments to high specific activity." Anal Biochem **132**(1): 6-13.

Fivaz, J., M. C. Chiarra Bassi, et al. (2000). "EBV-derived episomes to probe chromatin structure and gene expression in human cells." Methods Mol Biol **133**: 167-82.

Forthoffer, N., C. Gomez-Diaz, et al. (2002). "A novel plasma membrane quinone reductase and NAD(P)H:quinone oxidoreductase 1 are upregulated by serum withdrawal in human promyelocytic HL-60 cells." J Bioenerg Biomembr **34**(3): 209-19.

Frei, B. and J. V. Higdon (2003). "Antioxidant activity of tea polyphenols in vivo: evidence from animal studies." J Nutr **133**(10): 3275S-84S.

Frolov, A., T. H. Cho, et al. (1997). "Isoforms of rat liver fatty acid binding protein differ in structure and affinity for fatty acids and fatty acyl CoAs." Biochemistry **36**(21): 6545-55.

Furutani, M., J. Hata, et al. (2005). "An engineered chaperonin caging a guest protein: Structural insights and potential as a protein expression tool." Protein Sci **14**(2): 341-50.

Gamliel, A., M. Afri, et al. (2008). "Determining radical penetration of lipid bilayers with new lipophilic spin traps." Free Radic Biol Med **44**(7): 1394-405.

Gavazza, M. B. and A. Catala (2006). "The effect of alpha-tocopherol on lipid peroxidation of microsomes and mitochondria from rat testis." Prostaglandins Leukot Essent Fatty Acids **74**(4): 247-54.

Guarnieri, C., E. Giordano, et al. (1996). "Alpha-tocopherol pretreatment improves endothelium-dependent vasodilation in aortic strips of young and aging rats exposed to oxidative stress." Mol Cell Biochem **157**(1-2): 223-8.

Gupta, R. and S. Luan (2003). "Redox control of protein tyrosine phosphatases and mitogen-activated protein kinases in plants." Plant Physiol **132**(3): 1149-52.

Gyamfi, M. A., I. Damjanov, et al. (2008). "The pathogenesis of ethanol versus methionine and choline deficient diet-induced liver injury." Biochem Pharmacol **75**(4): 981-95.

Hall, E. D. (1992). "Novel inhibitors of iron-dependent lipid peroxidation for neurodegenerative disorders." Ann Neurol **32 Suppl**: S137-42.

Hallett, P., A. J. Grimshaw, et al. (1990). "Cloning of the DNA gyrase genes under tac promoter control: overproduction of the gyrase A and B proteins." Gene **93**(1): 139-42.

Hanhoff, T., C. Lucke, et al. (2002). "Insights into binding of fatty acids by fatty acid binding proteins." Mol Cell Biochem **239**(1-2): 45-54.

Harano, Y., K. Yasui, et al. (2006). "Fenofibrate, a peroxisome proliferator-activated receptor alpha agonist, reduces hepatic steatosis and lipid peroxidation in fatty liver Shionogi mice with hereditary fatty liver." Liver Int **26**(5): 613-20.

Hashimoto, F. and H. Hayashi (2002). "Presence and features of fatty acyl-CoA binding activity in rat hepatic peroxisomes." J Biochem **131**(3): 453-60.

Haunerland, N., G. Jagschies, et al. (1984). "Fatty-acid-binding proteins. Occurrence of two fatty-acid-binding proteins in bovine liver cytosol and their binding of fatty acids, cholesterol, and other lipophilic ligands." Hoppe Seylers Z Physiol Chem **365**(3): 365-76.

Helledie, T., L. Grontved, et al. (2002). "The gene encoding the Acyl-CoA-binding protein is activated by peroxisome proliferator-activated receptor gamma through an intronic response element functionally conserved between humans and rodents." J Biol Chem **277**(30): 26821-30.

Herr, F. M., J. Aronson, et al. (1996). "Role of portal region lysine residues in electrostatic interactions between heart fatty acid binding protein and phospholipid membranes." Biochemistry **35**(4): 1296-303.

Hodsdon, M. E., J. W. Ponder, et al. (1996). "The NMR solution structure of intestinal fatty acid-binding protein complexed with palmitate: application of a novel distance geometry algorithm." J Mol Biol **264**(3): 585-602.

Hohoff, C., T. Borchers, et al. (1999). "Expression, purification, and crystal structure determination of recombinant human epidermal-type fatty acid binding protein." Biochemistry **38**(38): 12229-39.

Hsu, K. T. and J. Storch (1996). "Fatty acid transfer from liver and intestinal fatty acid-binding proteins to membranes occurs by different mechanisms." J Biol Chem **271**(23): 13317-23.

Hsu, T. C., M. R. Young, et al. (2000). "Activator protein 1 (AP-1)- and nuclear factor kappaB (NF-kappaB)-dependent transcriptional events in carcinogenesis." Free Radic Biol Med **28**(9): 1338-48.

Huang, H., O. Starodub, et al. (2004). "Liver fatty acid-binding protein colocalizes with peroxisome proliferator activated receptor alpha and enhances ligand distribution to nuclei of living cells." Biochemistry **43**(9): 2484-500.

Huang, H., O. Starodub, et al. (2002). "Liver fatty acid-binding protein targets fatty acids to the nucleus. Real time confocal and multiphoton fluorescence imaging in living cells." J Biol Chem **277**(32): 29139-51.

Huang, J. and J. M. May (2003). "Ascorbic acid spares alpha-tocopherol and prevents lipid peroxidation in cultured H4IIE liver cells." Mol Cell Biochem **247**(1-2): 171-6.

Hubbell, T., W. D. Behnke, et al. (1994). "Recombinant liver fatty acid binding protein interacts with fatty acyl-coenzyme A." Biochemistry **33**(11): 3327-34.

Hung, D. Y., F. J. Burczynski, et al. (2003). "Fatty acid binding protein is a major determinant of hepatic pharmacokinetics of palmitate and its metabolites." Am J Physiol Gastrointest Liver Physiol **284**(3): G423-33.

Hyvonen, M. T., K. Oorni, et al. (2001). "Changes in a phospholipid bilayer induced by the hydrolysis of a phospholipase A2 enzyme: a molecular dynamics simulation study." Biophys J **80**(2): 565-78.

Iglesias, J., M. Pazos, et al. (2009). "Caffeic acid as antioxidant in fish muscle: mechanism of synergism with endogenous ascorbic acid and alpha-tocopherol." J Agric Food Chem **57**(2): 675-81.

Issemann, I., R. Prince, et al. (1992). "A role for fatty acids and liver fatty acid binding protein in peroxisome proliferation?" Biochem Soc Trans **20**(4): 824-7.

Jaeschke, H. and T. Hasegawa (2006). "Role of neutrophils in acute inflammatory liver injury." Liver Int **26**(8): 912-9.

Jana, S. and J. K. Deb (2005). "Strategies for efficient production of heterologous proteins in Escherichia coli." Appl Microbiol Biotechnol **67**(3): 289-98.

Jefferson, J. R., J. P. Slotte, et al. (1991). "Intracellular sterol distribution in transfected mouse L-cell fibroblasts expressing rat liver fatty acid-binding protein." J Biol Chem **266**(9): 5486-96.

Jenny, R. J., K. G. Mann, et al. (2003). "A critical review of the methods for cleavage of fusion proteins with thrombin and factor Xa." Protein Expr Purif **31**(1): 1-11.

Johnson, F. and C. Giulivi (2005). "Superoxide dismutases and their impact upon human health." Mol Aspects Med **26**(4-5): 340-52.

Jolly, C. A., E. J. Murphy, et al. (1998). "Differential influence of rat liver fatty acid binding protein isoforms on phospholipid fatty acid composition: phosphatidic acid biosynthesis and phospholipid fatty acid remodeling." Biochim Biophys Acta **1390**(3): 258-68.

Kaiser, S., P. Di Mascio, et al. (1990). "Physical and chemical scavenging of singlet molecular oxygen by tocopherols." Arch Biochem Biophys **277**(1): 101-8.

Kaplan, W., P. Husler, et al. (1997). "Conformational stability of pGEX-expressed Schistosoma japonicum glutathione S-transferase: a detoxification enzyme and fusion-protein affinity tag." Protein Sci **6**(2): 399-406.

Kehrer, J. P., S. S. Biswal, et al. (2001). "Inhibition of peroxisome-proliferator-activated receptor (PPAR)alpha by MK886." Biochem J **356**(Pt 3): 899-906.

Kenchappa, R. S. and V. Ravindranath (2003). "Gamma-glutamyl cysteine synthetase is up-regulated during recovery of brain mitochondrial complex I following neurotoxic insult in mice." Neurosci Lett **350**(1): 51-5.

Ketterer, B., E. Tipping, et al. (1976). "A low-molecular-weight protein from rat liver that resembles ligandin in its binding properties." Biochem J **155**(3): 511-21.

Khan, S. H. and S. Sorof (1994). "Liver fatty acid-binding protein: specific mediator of the mitogenesis induced by two classes of carcinogenic peroxisome proliferators." Proc Natl Acad Sci U S A **91**(3): 848-52.

Kitaguchi, H., K. Ohkubo, et al. (2005). "Direct ESR detection of pentadienyl radicals and peroxyl radicals in lipid peroxidation: mechanistic insight into regioselective oxygenation in lipoxygenases." J Am Chem Soc **127**(18): 6605-9.

Kliewer, S. A., B. M. Forman, et al. (1994). "Differential expression and activation of a family of murine peroxisome proliferator-activated receptors." Proc Natl Acad Sci U S A **91**(15): 7355-9.

Konishi, M., M. Iwasa, et al. (2006). "Increased lipid peroxidation in patients with non-alcoholic fatty liver disease and chronic hepatitis C as measured by the plasma level of 8-isoprostane." J Gastroenterol Hepatol **21**(12): 1821-5.

Korolainen, M. A. and T. Pirttila (2009). "Cerebrospinal fluid, serum and plasma protein oxidation in Alzheimer's disease." Acta Neurol Scand **119**(1): 32-8.

Kouoh, F., B. Gressier, et al. (1999). "Antioxidant properties of albumin: effect on oxidative metabolism of human neutrophil granulocytes." Farmaco **54**(10): 695-9.

Kowalik-Jankowska, T., A. Rajewska, et al. (2006). "Products of Cu(II)-catalyzed oxidation of the N-terminal fragments of alpha-synuclein in the presence of hydrogen peroxide." J Inorg Biochem **100**(10): 1623-31.

Kragh-Hansen, U., V. T. Chuang, et al. (2002). "Practical aspects of the ligand-binding and enzymatic properties of human serum albumin." Biol Pharm Bull **25**(6): 695-704.

Krautwald, S. and M. Baccarini (1993). "Bacterially expressed murine CSF-1 possesses agonistic activity in its monomeric form." Biochem Biophys Res Commun **192**(2): 720-7.

Krijgsman, B., J. A. Papadakis, et al. (2002). "The effect of peripheral vascular disease on the serum levels of natural anti-oxidants: bilirubin and albumin." Int Angiol **21**(1): 44-52.

Kyng, K. J., A. May, et al. (2005). "Gene expression responses to DNA damage are altered in human aging and in Werner Syndrome." Oncogene **24**(32): 5026-42.

Lassen, D., C. Lucke, et al. (1995). "Three-dimensional structure of bovine heart fatty-acid-binding protein with bound palmitic acid, determined by multidimensional NMR spectroscopy." Eur J Biochem **230**(1): 266-80.

Lawrence, J. W., D. J. Kroll, et al. (2000). "Ligand-dependent interaction of hepatic fatty acid-binding protein with the nucleus." J Lipid Res **41**(9): 1390-401.

Lawrie, L. C., S. R. Dundas, et al. (2004). "Liver fatty acid binding protein expression in colorectal neoplasia." Br J Cancer **90**(10): 1955-60.

LeBel, C. P., H. Ischiropoulos, et al. (1992). "Evaluation of the probe 2',7'-dichlorofluorescin as an indicator of reactive oxygen species formation and oxidative stress." Chem Res Toxicol **5**(2): 227-31.

Lee, D. H., T. R. O'Connor, et al. (2002). "Oxidative DNA damage induced by copper and hydrogen peroxide promotes CG-->TT tandem mutations at methylated CpG dinucleotides in nucleotide excision repair-deficient cells." Nucleic Acids Res **30**(16): 3566-73.

Leesnitzer, L. M., D. J. Parks, et al. (2002). "Functional consequences of cysteine modification in the ligand binding sites of peroxisome proliferator activated receptors by GW9662." Biochemistry **41**(21): 6640-50.

Levi, A. J., Z. Gatmaitan, et al. (1969). "Two hepatic cytoplasmic protein fractions, Y and Z, and their possible role in the hepatic uptake of bilirubin, sulfobromophthalein, and other anions." J Clin Invest **48**(11): 2156-67.

Levine, R. L., L. Mosoni, et al. (1996). "Methionine residues as endogenous antioxidants in proteins." Proc Natl Acad Sci U S A **93**(26): 15036-40.

Li, H., M. Hortmann, et al. (2008). "Cyclooxygenase 2-selective and nonselective nonsteroidal anti-inflammatory drugs induce oxidative stress by up-regulating vascular NADPH oxidases." J Pharmacol Exp Ther **326**(3): 745-53.

Liu, C., E. Flamoe, et al. (2004). "Expression and purification of immunologically reactive DPPD, a recombinant Mycobacterium tuberculosis skin test antigen, using Mycobacterium smegmatis and Escherichia coli host cells." Can J Microbiol **50**(2): 97-105.

Liu, W. and J. Y. Wang (2005). "Modifications of protein by polyunsaturated fatty acid ester peroxidation products." Biochim Biophys Acta **1752**(1): 93-8.

Lopez-Ilasaca, M., P. Crespo, et al. (1997). "Linkage of G protein-coupled receptors to the MAPK signaling pathway through PI 3-kinase gamma." Science **275**(5298): 394-7.

Loureiro, A. P., P. Di Mascio, et al. (2000). "trans,trans-2,4-decadienal-induced 1,N(2)-etheno-2'-deoxyguanosine adduct formation." Chem Res Toxicol **13**(7): 601-9.

Luceri, C., L. Giovannelli, et al. (2008). "Liver and colon DNA oxidative damage and gene expression profiles of rats fed Arabidopsis thaliana mutant seeds containing contrasted flavonoids." Food Chem Toxicol **46**(4): 1213-20.

Lucke, C., M. Rademacher, et al. (2001). "Spin-system heterogeneities indicate a selected-fit mechanism in fatty acid binding to heart-type fatty acid-binding protein (H-FABP)." Biochem J **354**(Pt 2): 259-66.

Lucke, C., F. Zhang, et al. (2000). "Solution structure of ileal lipid binding protein in complex with glycocholate." Eur J Biochem **267**(10): 2929-38.

Lucke, C., F. Zhang, et al. (1996). "Flexibility is a likely determinant of binding specificity in the case of ileal lipid binding protein." Structure **4**(7): 785-800.

Luxon, B. A. (1996). "Inhibition of binding to fatty acid binding protein reduces the intracellular transport of fatty acids." Am J Physiol **271**(1 Pt 1): G113-20.

Luxon, B. A., M. T. Milliano, et al. (2000). "Induction of hepatic cytosolic fatty acid binding protein with clofibrate accelerates both membrane and cytoplasmic transport of palmitate." Biochim Biophys Acta **1487**(2-3): 309-18.

Maatman, R. G., H. T. van Moerkerk, et al. (1994). "Expression of human liver fatty acid-binding protein in Escherichia coli and comparative analysis of its binding characteristics with muscle fatty acid-binding protein." Biochim Biophys Acta **1214**(1): 1-10.

Maliakel, D. M., T. V. Kagiya, et al. (2008). "Prevention of cisplatin-induced nephrotoxicity by glucosides of ascorbic acid and alpha-tocopherol." Exp Toxicol Pathol **60**(6): 521-7.

Marderstein, E. L., B. Bucher, et al. (2003). "Protection of rat hepatocytes from apoptosis by inhibition of c-Jun N-terminal kinase." Surgery **134**(2): 280-4.

Marnett, L. J. (2000). "Oxyradicals and DNA damage." Carcinogenesis **21**(3): 361-70.

Martin, G. G., B. P. Atshaves, et al. (2005). "Liver fatty-acid-binding protein (L-FABP) gene ablation alters liver bile acid metabolism in male mice." Biochem J **391**(Pt 3): 549-60.

Martinez-Torrecuadrada, J. L., S. Romero, et al. (2005). "An efficient expression system for the production of functionally active human LKB1." J Biotechnol **115**(1): 23-34.

Masalkar, P. D. and S. A. Abhang (2005). "Oxidative stress and antioxidant status in patients with alcoholic liver disease." Clin Chim Acta **355**(1-2): 61-5.

Massey, J. B., H. S. She, et al. (1982). "Interaction of vitamin E with saturated phospholipid bilayers." Biochem Biophys Res Commun **106**(3): 842-7.

Masutani, H. (2001). "Oxidative stress and redox imbalance in acetaminophen toxicity." Pharmacogenomics J **1**(3): 165-6.

Mates, J. M., C. Perez-Gomez, et al. (2002). "Glutamine and its relationship with intracellular redox status, oxidative stress and cell proliferation/death." Int J Biochem Cell Biol **34**(5): 439-58.

Mathur, M., T. Das, et al. (1996). "Expression of L protein of vesicular stomatitis virus Indiana serotype from recombinant baculovirus in insect cells: requirement of a host factor(s) for its biological activity in vitro." J Virol **70**(4): 2252-9.

Mikkelsen, J., P. Hojrup, et al. (1987). "Amino acid sequence of acyl-CoA-binding protein from cow liver." Biochem J **245**(3): 857-61.

Miyasaka, Y., E. Nagai, et al. (2007). "The role of the DNA damage checkpoint pathway in intraductal papillary mucinous neoplasms of the pancreas." Clin Cancer Res **13**(15 Pt 1): 4371-7.

Moller, P. and H. Wallin (1998). "Adduct formation, mutagenesis and nucleotide excision repair of DNA damage produced by reactive oxygen species and lipid peroxidation product." Mutat Res **410**(3): 271-90.

Moran, J. B., F. J. Burczynski, et al. (1987). "Protein binding of palmitate measured by transmembrane diffusion through polyethylene." Anal Biochem **167**(2): 394-9.

Muller-Hill, B., L. Crapo, et al. (1968). "Mutants that make more lac repressor." Proc Natl Acad Sci U S A **59**(4): 1259-64.

Muller, K. and D. Gurster (1993). "Hydroxyl radical damage to DNA sugar and model membranes induced by anthralin (dithranol)." Biochem Pharmacol **46**(10): 1695-704.

Murphy, E. J., R. D. Edmondson, et al. (1999). "Isolation and characterization of two distinct forms of liver fatty acid binding protein from the rat." Biochim Biophys Acta **1436**(3): 413-25.

Nanji, A. A., A. J. Dannenberg, et al. (2004). "Alcoholic liver injury in the rat is associated with reduced expression of peroxisome proliferator-alpha (PPARalpha)-regulated genes and is ameliorated by PPARalpha activation." J Pharmacol Exp Ther **310**(1): 417-24.

Nanji, A. A., E. K. Yang, et al. (1996). "Medium chain triglycerides and vitamin E reduce the severity of established experimental alcoholic liver disease." J Pharmacol Exp Ther **277**(3): 1694-700.

Neufeld, G., T. Cohen, et al. (1999). "Vascular endothelial growth factor (VEGF) and its receptors." Faseb J **13**(1): 9-22.

Niki, E. (1990). "Free radical initiators as source of water- or lipid-soluble peroxyl radicals." Methods Enzymol **186**: 100-8.

Norris, A. W. and A. A. Spector (2002). "Very long chain n-3 and n-6 polyunsaturated fatty acids bind strongly to liver fatty acid-binding protein." J Lipid Res **43**(4): 646-53.

Ockner, R. K., J. A. Manning, et al. (1972). "A binding protein for fatty acids in cytosol of intestinal mucosa, liver, myocardium, and other tissues." Science **177**(43): 56-8.

Ohshima, H., T. Sawa, et al. (2006). "8-nitroguanine, a product of nitrative DNA damage caused by reactive nitrogen species: formation, occurrence, and implications in inflammation and carcinogenesis." Antioxid Redox Signal **8**(5-6): 1033-45.

Ohta, Y., T. Matsura, et al. (2007). "Xanthine oxidase-derived reactive oxygen species contribute to the development of D-galactosamine-induced liver injury in rats." Free Radic Res **41**(2): 135-44.

Oikari, S., T. Ahtialansaari, et al. (2008). "Downregulation of PPARs and SREBP by acyl-CoA-binding protein overexpression in transgenic rats." Pflugers Arch **456**(2): 369-77.

Okuda, M., K. Li, et al. (2002). "Mitochondrial injury, oxidative stress, and antioxidant gene expression are induced by hepatitis C virus core protein." Gastroenterology **122**(2): 366-75.

Ounjaijean, S., C. Thephinlap, et al. (2008). "Effect of green tea on iron status and oxidative stress in iron-loaded rats." Med Chem **4**(4): 365-70.

Paez, P. L., M. C. Becerra, et al. (2008). "Chloramphenicol-induced oxidative stress in human neutrophils." Basic Clin Pharmacol Toxicol **103**(4): 349-53.

Palmer, H. J. and K. E. Paulson (1997). "Reactive oxygen species and antioxidants in signal transduction and gene expression." Nutr Rev **55**(10): 353-61.

Pan, J. L. and J. C. Bardwell (2006). "The origami of thioredoxin-like folds." Protein Sci **15**(10): 2217-27.

Pang, B., X. Zhou, et al. (2007). "Lipid peroxidation dominates the chemistry of DNA adduct formation in a mouse model of inflammation." Carcinogenesis **28**(8): 1807-13.

Parola, M. and G. Robino (2001). "Oxidative stress-related molecules and liver fibrosis." J Hepatol **35**(2): 297-306.

Paulussen, R. J. and J. H. Veerkamp (1990). "Intracellular fatty-acid-binding proteins. Characteristics and function." Subcell Biochem **16**: 175-226.

Perez de Obanos, M. P., M. J. Lopez-Zabalza, et al. (2007). "Reactive oxygen species (ROS) mediate the effects of leucine on translation regulation and type I collagen production in hepatic stellate cells." Biochim Biophys Acta **1773**(11): 1681-8.

Pinzani, M. and K. Rombouts (2004). "Liver fibrosis: from the bench to clinical targets." Dig Liver Dis **36**(4): 231-42.

Poli, G., R. J. Schaur, et al. (2008). "4-hydroxynonenal: a membrane lipid oxidation product of medicinal interest." Med Res Rev **28**(4): 569-631.

Polisky, B., R. J. Bishop, et al. (1976). "A plasmid cloning vehicle allowing regulated expression of eukaryotic DNA in bacteria." Proc Natl Acad Sci U S A **73**(11): 3900-4.

Porter, N. A., S. E. Caldwell, et al. (1995). "Mechanisms of free radical oxidation of unsaturated lipids." Lipids **30**(4): 277-90.

Prakash, M., G. Gunasekaran, et al. (2008). "Effect of earthworm powder on antioxidant enzymes in alcohol induced hepatotoxic rats." Eur Rev Med Pharmacol Sci **12**(4): 237-43.

Pushpavalli, G., C. Veeramani, et al. (2008). "Influence of Piper betle on hepatic marker enzymes and tissue antioxidant status in D-galactosamine-induced hepatotoxic rats." J Basic Clin Physiol Pharmacol **19**(2): 131-50.

Quiles, J. L., M. C. Ramirez-Tortosa, et al. (1999). "Olive oil supplemented with vitamin E affects mitochondrial coenzyme Q levels in liver of rats after an oxidative stress induced by adriamycin." Biofactors **9**(2-4): 331-6.

Rajaraman, G. and F. J. Burczynski (2004). "Effect of dexamethasone, 2-bromopalmitate and clofibrate on L-FABP mediated hepatoma proliferation." J Pharm Pharmacol **56**(9): 1155-61.

Rajaraman, G., G. Q. Wang, et al. (2007). "Role of cytosolic liver fatty acid binding protein in hepatocellular oxidative stress: effect of dexamethasone and clofibrate treatment." Mol Cell Biochem **295**(1-2): 27-34.

Rao, V. A., S. R. Klein, et al. (2009). "The iron chelator Dp44mT causes DNA damage and selective inhibition of topoisomerase IIalpha in breast cancer cells." Cancer Res **69**(3): 948-57.

Raza, H., J. R. Pongubala, et al. (1989). "Specific high affinity binding of lipoxygenase metabolites of arachidonic acid by liver fatty acid binding protein." Biochem Biophys Res Commun **161**(2): 448-55.

Robertson, J. A., Y. Farnell, et al. (2002). "Estradiol up-regulates estrogen receptor messenger ribonucleic acid in endometrial carcinoma (Ishikawa) cells by stabilizing the message." J Mol Endocrinol **29**(1): 125-35.

Roginsky, V. A., G. Bruchelt, et al. (1998). "Ubiquinone-0 (2,3-dimethoxy-5-methyl-1,4-benzoquinone) as effective catalyzer of ascorbate and epinephrine oxidation and damager of neuroblastoma cells." Biochem Pharmacol **55**(1): 85-91.

Rolf, B., E. Oudenampsen-Kruger, et al. (1995). "Analysis of the ligand binding properties of recombinant bovine liver-type fatty acid binding protein." Biochim Biophys Acta **1259**(3): 245-53.

Roopashree, S. D., C. Chai, et al. (1995). "Expression of Carcinoscorpius rotundicauda factor C cDNA." Biochem Mol Biol Int **35**(4): 841-9.

Sacchettini, J. C., J. I. Gordon, et al. (1989). "Crystal structure of rat intestinal fatty-acid-binding protein. Refinement and analysis of the Escherichia coli-derived protein with bound palmitate." J Mol Biol **208**(2): 327-39.

Santos, A. C., S. A. Uyemura, et al. (1998). "Effect of naturally occurring flavonoids on lipid peroxidation and membrane permeability transition in mitochondria." Free Radic Biol Med **24**(9): 1455-61.

Sato, T., K. Baba, et al. (1996). "Rat liver fatty acid-binding protein: identification of a molecular species having a mixed disulfide with cysteine at cysteine-69 and enhanced protease susceptibility." J Biochem **120**(5): 908-14.

Savchenkova, A. P., L. B. Dudnik, et al. (2003). "Effects of fibrinogen on lipid peroxidation in patients with coronary heart disease and in vitro." Bull Exp Biol Med **135**(1): 29-33.

Scanu, A. M. and C. Wisdom (1972). "Serum lipoproteins structure and function." Annu Rev Biochem **41**: 703-30.

Schlezinger, J. J., W. D. Struntz, et al. (2006). "Uncoupling of cytochrome P450 1A and stimulation of reactive oxygen species production by co-planar polychlorinated biphenyl congeners." Aquat Toxicol **77**(4): 422-32.

Schroeder, F., A. D. Petrescu, et al. (2008). "Role of fatty acid binding proteins and long chain fatty acids in modulating nuclear receptors and gene transcription." Lipids **43**(1): 1-17.

Seimandi, M., G. Lemaire, et al. (2005). "Differential responses of PPARalpha, PPARdelta, and PPARgamma reporter cell lines to selective PPAR synthetic ligands." Anal Biochem **344**(1): 8-15.

Semple, R. K., V. K. Chatterjee, et al. (2006). "PPAR gamma and human metabolic disease." J Clin Invest **116**(3): 581-9.

Serdar, Z., K. Aslan, et al. (2006). "Lipid and protein oxidation and antioxidant status in patients with angiographically proven coronary artery disease." Clin Biochem **39**(8): 794-803.

Sevanian, A., K. Nordenbrand, et al. (1990). "Microsomal lipid peroxidation: the role of NADPH--cytochrome P450 reductase and cytochrome P450." Free Radic Biol Med **8**(2): 145-52.

Sharp, J. S. and K. B. Tomer (2007). "Analysis of the oxidative damage-induced conformational changes of apo- and holocalmodulin by dose-dependent protein oxidative surface mapping." Biophys J **92**(5): 1682-92.

She, Y. M., G. Q. Wang, et al. (2002). "Sequencing of rat liver cytosolic proteins by matrix-assisted laser desorption ionization-quadrupole time-of-flight mass spectrometry following electrophoretic separation and extraction." Anal Biochem **310**(2): 137-47.

Shiotani, S., M. Shimada, et al. (2007). "Rho-kinase as a novel gene therapeutic target in treatment of cold ischemia/reperfusion-induced acute lethal liver injury: effect on hepatocellular NADPH oxidase system." Gene Ther **14**(19): 1425-33.

Simon, T. C., K. A. Roth, et al. (1993). "Use of transgenic mice to map cis-acting elements in the liver fatty acid-binding protein gene (Fabpl) that regulate its cell lineage-specific, differentiation-dependent, and spatial patterns of expression in the gut epithelium and in the liver acinus." J Biol Chem **268**(24): 18345-58.

Smith, D. B. and K. S. Johnson (1988). "Single-step purification of polypeptides expressed in Escherichia coli as fusions with glutathione S-transferase." Gene **67**(1): 31-40.

Smith, R. and C. Tanford (1973). "Hydrophobicity of Long Chain n-Alkyl Carboxylic Acids, as Measured by Their Distribution Between Heptane and Aqueous Solutions." Proc Natl Acad Sci U S A **70**(2): 289-293.

Sorof, S. (1994). "Modulation of mitogenesis by liver fatty acid binding protein." Cancer Metastasis Rev **13**(3-4): 317-36.

Spitsberg, V. L., E. Matitashvili, et al. (1995). "Association and coexpression of fatty-acid-binding protein and glycoprotein CD36 in the bovine mammary gland." Eur J Biochem **230**(3): 872-8.

Stadler, K., M. G. Bonini, et al. (2008). "Involvement of inducible nitric oxide synthase in hydroxyl radical-mediated lipid peroxidation in streptozotocin-induced diabetes." Free Radic Biol Med.

Stadtman, E. R. and R. L. Levine (2000). "Protein oxidation." Ann N Y Acad Sci **899**: 191-208.

Storch, J. and A. E. Thumser (2000). "The fatty acid transport function of fatty acid-binding proteins." Biochim Biophys Acta **1486**(1): 28-44.

Storz, P. (2005). "Reactive oxygen species in tumor progression." Front Biosci **10**: 1881-96.

Stratton, S. P. and D. C. Liebler (1997). "Determination of singlet oxygen-specific versus radical-mediated lipid peroxidation in photosensitized oxidation of lipid bilayers: effect of beta-carotene and alpha-tocopherol." Biochemistry **36**(42): 12911-20.

Sweetser, D. A., E. H. Birkenmeier, et al. (1987). "The human and rodent intestinal fatty acid binding protein genes. A comparative analysis of their structure, expression, and linkage relationships." J Biol Chem **262**(33): 16060-71.

Sweetser, D. A., J. B. Lowe, et al. (1986). "The nucleotide sequence of the rat liver fatty acid-binding protein gene. Evidence that exon 1 encodes an oligopeptide domain shared by a family of proteins which bind hydrophobic ligands." J Biol Chem **261**(12): 5553-61.

Szocs, K. (2004). "Endothelial dysfunction and reactive oxygen species production in ischemia/reperfusion and nitrate tolerance." Gen Physiol Biophys **23**(3): 265-95.

Tafur, J. and P. J. Mills (2008). "Low-intensity light therapy: exploring the role of redox mechanisms." Photomed Laser Surg **26**(4): 323-8.

Takahashi, K., S. Odani, et al. (1983). "Isolation and characterization of the three fractions (DE-I, DE-II and DE-III) of rat-liver Z-protein and the complete primary structure of DE-II." Eur J Biochem **136**(3): 589-601.

Tan, N. S., N. S. Shaw, et al. (2002). "Selective cooperation between fatty acid binding proteins and peroxisome proliferator-activated receptors in regulating transcription." Mol Cell Biol **22**(14): 5114-27.

Tang, M. K., P. M. Kindler, et al. (2004). "Heart-type fatty acid binding proteins are upregulated during terminal differentiation of mouse cardiomyocytes, as revealed by proteomic analysis." Cell Tissue Res **316**(3): 339-47.

Tang, Q. Q., M. S. Jiang, et al. (1999). "Repressive effect of Sp1 on the C/EBPalpha gene promoter: role in adipocyte differentiation." Mol Cell Biol **19**(7): 4855-65.

Tatulian, S. A. (2001). "Toward understanding interfacial activation of secretory phospholipase A2 (PLA2): membrane surface properties and membrane-induced structural changes in the enzyme contribute synergistically to PLA2 activation." Biophys J **80**(2): 789-800.

Thannickal, V. J. and B. L. Fanburg (2000). "Reactive oxygen species in cell signaling." Am J Physiol Lung Cell Mol Physiol **279**(6): L1005-28.

Thompson, J., N. Winter, et al. (1997). "The crystal structure of the liver fatty acid-binding protein. A complex with two bound oleates." J Biol Chem **272**(11): 7140-50.

Thumser, A. E. and J. Storch (2000). "Liver and intestinal fatty acid-binding proteins obtain fatty acids from phospholipid membranes by different mechanisms." J Lipid Res **41**(4): 647-56.

Tikare, S. N., A. Das Gupta, et al. (2008). "Effect of antioxidants L-ascorbic acid and alpha-tocopherol supplementation in nickel exposed hyperglycemic rats." J Basic Clin Physiol Pharmacol **19**(2): 89-101.

Tornwall, M. E., J. Virtamo, et al. (2004). "Effect of alpha-tocopherol and beta-carotene supplementation on coronary heart disease during the 6-year post-trial follow-up in the ATBC study." Eur Heart J **25**(13): 1171-8.

Torres, P., P. Galleguillos, et al. (2008). "Antioxidant capacity of human blood plasma and human urine: simultaneous evaluation of the ORAC index and ascorbic acid concentration employing pyrogallol red as probe." Bioorg Med Chem **16**(20): 9171-5.

Tsuchiya, M., M. Suematsu, et al. (1994). "In vivo visualization of oxygen radical-dependent photoemission." Methods Enzymol **233**: 128-40.

Valenzuela, A. (1991). "The biological significance of malondialdehyde determination in the assessment of tissue oxidative stress." Life Sci **48**(4): 301-9.

van Aken, D., W. E. Benckhuijsen, et al. (2006). "Expression, purification, and in vitro activity of an arterivirus main proteinase." Virus Res **120**(1-2): 97-106.

van de Poll, M. C., C. H. Dejong, et al. (2008). "Decreased hepatosplanchnic antioxidant uptake during hepatic ischaemia/reperfusion in patients undergoing liver resection." Clin Sci (Lond) **114**(8): 553-60.

van Raalte, D. H., M. Li, et al. (2004). "Peroxisome proliferator-activated receptor (PPAR)-alpha: a pharmacological target with a promising future." Pharm Res **21**(9): 1531-8.

Vanden Heuvel, J. P., P. F. Sterchele, et al. (1993). "Coordinate induction of acyl-CoA binding protein, fatty acid binding protein and peroxisomal beta-oxidation by peroxisome proliferators." Biochim Biophys Acta **1177**(2): 183-90.

Velkov, T., S. Chuang, et al. (2005). "An improved method for the purification of rat liver-type fatty acid binding protein from Escherichia coli." Protein Expr Purif **44**(1): 23-31.

Wagner, B. A., G. R. Buettner, et al. (2000). "Myeloperoxidase is involved in H2O2-induced apoptosis of HL-60 human leukemia cells." J Biol Chem **275**(29): 22461-9.

Wang, A. L., T. J. Lukas, et al. (2008). "Age-related increase in mitochondrial DNA damage and loss of DNA repair capacity in the neural retina." Neurobiol Aging.

Wang, G., Y. Gong, et al. (2005). "Antioxidative function of L-FABP in L-FABP stably transfected Chang liver cells." Hepatology **42**(4): 871-9.

Wang, G., H. Shen, et al. (2007). "Expression and antioxidant function of liver fatty acid binding protein in normal and bile-duct ligated rats." Eur J Pharmacol **560**(1): 61-8.

Warnakulasuriya, S., S. Parkkila, et al. (2008). "Demonstration of ethanol-induced protein adducts in oral leukoplakia (pre-cancer) and cancer." J Oral Pathol Med **37**(3): 157-65.

Wei, Q. Y., W. F. Chen, et al. (2006). "Inhibition of lipid peroxidation and protein oxidation in rat liver mitochondria by curcumin and its analogues." Biochim Biophys Acta **1760**(1): 70-7.

Wells, P. G., Y. Bhuller, et al. (2005). "Molecular and biochemical mechanisms in teratogenesis involving reactive oxygen species." Toxicol Appl Pharmacol **207**(2 Suppl): 354-66.

Wolfrum, C., C. M. Borrmann, et al. (2001). "Fatty acids and hypolipidemic drugs regulate peroxisome proliferator-activated receptors alpha - and gamma-mediated gene expression via liver fatty acid binding protein: a signaling path to the nucleus." Proc Natl Acad Sci U S A **98**(5): 2323-8.

Wood, Z. A., E. Schroder, et al. (2003). "Structure, mechanism and regulation of peroxiredoxins." Trends Biochem Sci **28**(1): 32-40.

Wu, D., Q. Zhai, et al. (2006). "Alcohol-induced oxidative stress and cell responses." J Gastroenterol Hepatol **21 Suppl 3**: S26-9.

Wu, J. D., D. W. Lin, et al. (2009). "Oxidative DNA damage in the prostate may predispose men to a higher risk of prostate cancer." Transl Oncol **2**(1): 39-45.

Xiong, Y., B. Chen, et al. (2006). "High-affinity and cooperative binding of oxidized calmodulin by methionine sulfoxide reductase." Biochemistry **45**(49): 14642-54.

Xu, A., L. J. Wu, et al. (1999). "Role of oxyradicals in mutagenicity and DNA damage induced by crocidolite asbestos in mammalian cells." Cancer Res **59**(23): 5922-6.

Xu, G. and M. R. Chance (2005). "Radiolytic modification and reactivity of amino acid residues serving as structural probes for protein footprinting." Anal Chem **77**(14): 4549-55.

Xu, Z., D. A. Bernlohr, et al. (1992). "Crystal structure of recombinant murine adipocyte lipid-binding protein." Biochemistry **31**(13): 3484-92.

Yang, K. L., W. T. Chang, et al. (2008). "Antagonizing TGF-beta induced liver fibrosis by a retinoic acid derivative through regulation of ROS and calcium influx." Biochem Biophys Res Commun **365**(3): 484-9.

Yuki, T., Y. Maniwa, et al. (2008). "DNA damage sensor protein hRad9, a novel molecular target for lung cancer treatment." Oncol Rep **20**(5): 1047-52.

Zanotti, G., G. Scapin, et al. (1992). "Three-dimensional structure of recombinant human muscle fatty acid-binding protein." J Biol Chem **267**(26): 18541-50.

Zapletal, C., S. Heyne, et al. (2008). "The influence of selenium substitution on microcirculation and glutathione metabolism after warm liver ischemia/reperfusion in a rat model." Microvasc Res **76**(2): 104-9.

Zhang, J., R. A. Stanley, et al. (2006). "Lipid peroxidation inhibition capacity assay for antioxidants based on liposomal membranes." Mol Nutr Food Res **50**(8): 714-24.

Zimmerman, A. W. and J. H. Veerkamp (2002). "New insights into the structure and function of fatty acid-binding proteins." Cell Mol Life Sci **59**(7): 1096-116.